The Pennsylvania State University

The Graduate School

Department of Bioengineering

CHARACTERIZATION OF PROTEIN FILMS USING NOVEL ATOMIC FORCE MICROSCOPY TECHNIQUES

A Dissertation in

Bioengineering

by

Pranav Soman

Submitted in Partial Fulfillment
of the Requirements
for the Degree of

Doctor of Philosophy

May 2009

The dissertation of Pranav Soman was reviewed and approved* by the following:

Christopher A. Siedlecki
Associate Professor of Surgery and Bioengineering
Dissertation Advisor
Chair of Committee

William J. Weiss
Howard E. Morgan Professor of Surgery and Bioengineering

Erwin A. Vogler
Professor of Materials Science and Engineering and Bioengineering

Jeffrey Catchmark
Assistant Professor of Engineering Science and Mechanics, Agricultural and Biological Engineering, and School of Forest Resources

Herbert H. Lipowsky
Professor of Bioengineering
Head of the Department of Bioengineering

*Signatures are on file in the Graduate School

ABSTRACT

The success of long-term blood-contacting implanted devices greatly depends upon the interaction of the blood components with the device material. The search for a perfect hemocompatible biomaterial has not yielded success yet, largely due to the incomplete understanding of blood-material interactions, especially at sub-cellular and molecular levels. In this work, critical aspects of blood-material interactions are probed at the molecular scale using Atomic Force Microscopy (AFM). Conventional AFM imaging techniques are not capable of detecting specific plasma proteins on clinically relevant polymeric biomaterials, mostly due to the surface roughness of the biomaterial. This work has developed AFM techniques which will not require the topographical features otherwise needed by conventional AFM methods to detect proteins. Fibrinogen, the third most abundant plasma protein, plays a crucial role in surface induced thrombosis in blood contacting devices. AFM is used to characterize fibrinogen, in terms of its spatial location, on ultrasmooth mica substrate and a clinically relevant polymer substrate, poly (dimethyl-siloxane). Gold labels are used as immunological tags to detect adsorbed fibrinogen from a two-protein layer at molecular resolution. Force spectroscopy is used to calculate the time dependent activity of the platelet binding dodecapeptide epitope of fibrinogen. These nanoscale results are corroborated with macroscale platelet adhesion experiments. The effects of concentration and co-adsorption of bovine serum albumin with fibrinogen are studied on hydrophilic mica substrates. Polyethylene glycol (PEG) is investigated as a potential tether to attach proteins to the AFM probe. Modified PEG-probes are more efficient in decreasing the non-specific recognition problems which is

the main problem with glutaraldehyde linkers especially in the case of hydrophobic substrates. Taken together, this work fills the gaps in the current understanding of the blood-material interactions at the molecular level and provides important tools for future studies.

TABLE OF CONTENTS

LIST OF FIGURES

ACKNOWLEDGEMENTS

Coming to Dr. Siedlecki's lab was a turning point in my life. I used to always wonder - Why do advisors take in fresh students especially when their tenure is on the line? Why not hire a post-doc instead who is productive from the word GO? – This baffled me until recently, when I realized what PhD is all about. I think for an advisor it's sort of like an act of social service. He plants a seed, nurtures it for 4-5 years and hopes that it will flourish into a tree. "Flourishing" does not ONLY imply being successful in academics or life for that matter, it means much more than that. I am really glad that I had this opportunity to be in an environment which fosters personal as well as professional growth. I guess this thanksgiving I have a lot to be thankful for!

I am grateful to my thesis advisor Dr. Christopher Siedlecki for his mentoring efforts during my graduate research. His patience has helped me develop confidence in my ability to be an independent researcher {at times over-confidence!} I would also like to express my sincere gratitude to my committee members: Dr. Vogler, Dr. Weiss and Dr. Catchmark and for their heated debates about protein adsorption, guidance and constructive criticism.

Without the support of my family, friends and colleagues I would not have completed my journey through graduate school. I cannot thank them enough for all that they have given to my life.

Chapter 1

Introduction

Biomaterials have had an enormous impact on health care with tremendous success in the medical devices. It is estimated that over a thousand left-ventricular-assist-devices, nearly four million stents, over two hundred thousand heart valves and about two hundred million catheters were implanted in US patients in the year 2007 alone with cost exceeding $300 billion US dollars per year(Lysaght and O'Loughlin 2000, Ratner 2007). Much of this success has been achieved through judicious selection of existing materials, without the understanding of the structure-function relationship. For blood-contacting devices, the interaction of blood with the synthetic surface of the devices presents a daunting challenge for their biocompatibility. These interactions trigger several adverse biological responses including: complement activation, activation of the immune response, blood coagulation, and thrombosis(Gorbet and Sefton 2004). Among these, surface-induced thrombosis has remained a major obstacle for the biocompatibility and eventual success of such devices(Lamba, et al. 1998). Thrombosis may lead to clinical complications such as detachment of a portion of the thrombus (embolization) that can obstruct a narrow blood vessel in the brain or other organs, compromising the health of the patient(Schmid, et al. 1998). These complications can be alleviated to some degree by administration of anticoagulants, but these drugs may cause serious systemic problems including increased bleeding times and hemorrhaging(Verheugt 2008). Therefore there is a pressing need for improved blood-compatible materials for use in devices that contact

blood. Towards this objective, we have been studying the molecular mechanism underlying hemocompatibility of biomaterials. The sections in this chapter will discuss (A) protein adsorption, (B) the use of atomic force microscopy to study different aspects of protein adsorption, (C) surface-induced thrombosis including the role of fibrinogen and platelets, and finally, (D) the significance of this research.

1.1 Protein Adsorption to Biomaterials

The influence of water wetting on biomaterials and biocompatibility is not well understood. Water and ions are perhaps the first components of the biological milieu to arrive at the biomaterial surface and are closely followed by proteins(Andrade and Hlady 1986, Vogler 1998). Proteins reacting with this hydrated layer mediate a wide range of macroscopic biological outcomes including blood coagulation (contact activation by blood factor XII and/or stimulation of platelets by adsorbed fibrinogen) (Vogler, et al. 1995; Grunkemeier, et al. 2000), cell adhesion (membrane-bound receptors to adsorbed adhesins)(Cameron, et al. 2005), and complement activation (contact activation of blood factor C3) (Andersson, et al. 2005)and surface-induced thrombosis(Gorbet and Sefton 2004). Thus, the study of protein adsorption has been a topic of deep interest in biomaterial surface science research.

Adsorption of proteins from aqueous solution onto a solid surface is the net result of various types of interactions that simultaneously occur among all the components of

the system, such as protein, surface, water and low molecular weight ions. To get a macroscale view of protein adsorption, Gibbs free energy is often used.

$\Delta G_{ads} = \Delta H_{ads} - T\,\Delta S_{ads}$, where G, H, S and T are Gibbs free energy, enthalpy, entropy and temperature in K

For spontaneous adsorption of proteins to the surfaces, the change in the Gibbs free energy of the system must be negative which can be achieved by decrease in the enthalpy and/or an increase in the entropy. The interactions that are involved in protein adsorption to solid surfaces are known to include van der Waals forces, electrostatic forces, solvation forces (surface dehydration) and entropic forces. (Norde and Haynes 1996, Malmsten 1998, Nakanishi, Sakiyama and Imamura 2001). The extent of protein adsorption is determined by competition between attractive and non-specific repulsive forces. If the solid substrate is made up of electrically neutral material like most biomaterials are, electrostatic interactions are not likely to play a significant role. In addition the Debye length is usually less than 10A in physiological fluids. (Lee et al. 2001) Since biomaterial surfaces do not generally possess structures that can be recognized by proteins, such as binding sites of antibodies, specific interactions with the biomaterials should also be absent. Regarding protein-surface interactions, Vogler and others have demonstrated that the apparent free-energy of protein adsorption (ΔG_{ads} ~5RT) is not large compared to thermal energy. (Noh and Vogler, 2006) Therefore, among all the interactive forces, water-water and water-surface interactions seem to play the most important part in determining protein adsorption process.

In bulk water, individual water molecules are linked to each other through hydrogen bonds to form the locally tetrahedral arrangement which get disrupted when a

protein is dissolved in water. Water structure is also affected by the energy (hydrophilicity) of the surface. Hydrophobic surfaces may be defined as surfaces exhibiting a water contact angle $\theta > 65°$ (or the pure water adhesion tension $\tau° = \gamma° \cos\theta < 30$ dyn/cm, where $\gamma°$ is water interfacial tension = 72.8 dyn/cm)(Vogler 1998, 2001). Water molecules facing hydrophobic surfaces do not form hydrogen bonds with the surface. Instead, they form a self-assembled structure with its own hydrogen-bonding network due to the strong self-association property of water molecules. Although the molecules on the hydrophobic surfaces are attracted to water by dispersion forces, they are not attracted strongly enough to overcome the self-cohesive properties of water.

Discussion on protein adsorption will be incomplete without mentioning an important classification based on the concept of a two-dimensional (2-D) monolayer adsorption verses a three-dimensional (3-D) "interphase" adsorption between the material surface and the bulk biological fluid. According to the 'Langmuirian' paradigm, formerly used for gas adsorption, one molecule will bind to a single binding site on the surface, essentially forming a monolayer of adsorbed molecules(Horbett 1993, 1996). The underlying assumptions, although not necessarily realistic in the case of protein adsorption are that all binding sites are equivalent and independent and cannot influence the adsorption of another molecule on neighbouring sites. The 2D model also stipulates a limited number of "binding sites" on the surface and therefore limiting the number of proteins adsorbed at the interface(Horbett 1993). The composition of the adsorbed protein layer is determined by the intrinsic surface activity of each protein, its bulk concentration in the solution, and the surface. This paradigm emphasizes the short-range effects

associated with molecular interactions of solute (proteins) with the surface and ignores the role of solvent.

In contrast to the monolayer model of protein adsorption to materials surfaces, the "Gibbsian" paradigm proposes a 3-D model. This interphase region separates the two phases (e.g. a biomaterial and the biological fluid) that is comprised of continuously changing component concentrations and a solute-enriched zone near to, but not necessarily bound to the surface(Vogler 1998). Vogler and co-workers used pendant-drop tensiometry of aqueous buffer solutions of purified human proteins spanning several orders of magnitude in molecular weight (MW) and proposed that protein adsorption follows a homology in size rather than biochemical composition/specificity(Krishnan, et al. 2003, Noh and Vogler 2006). Their work predicts that the thickness of the "interphase" region scales with the size of the adsorbing protein, such that smaller proteins fill a single layer whereas larger proteins form multi-layers. They proposed that adsorption into a 3-D interphase is driven by protein concentration in solution rather than the biochemical specificity.

A variety of techniques have been utilized to study protein adsorption on surfaces under both physiologic and non-physiologic environments. Most techniques which are typically used for analysis of protein structures, such as X-ray crystallography (Weisel, et al. 1981) and NMR spectroscopy(Mayo, et al. 1996), are able to provide very detailed information about protein conformation and structure. However, these techniques are not easily applicable to surface-adsorbed proteins. Rather, the analysis of adsorbed proteins

relies heavily on surface analysis and spectroscopic techniques such as infrared spectroscopy(Barbucci, et al. 2003, Yokoyama, et al. 2003), circular dichroism(Damodaran 2003, Hylton, et al. 2005), attenuated total reflection Fourier-transform infrared (ATR-FTIR) spectroscopy(Clarke, et al. 2005, Roach, et al. 2005, Tunc, et al. 2005, Wang, et al. 2006), vibrational sum frequency spectroscopy (VSFG)(Jung, et al. 2003, Evans-Nguyen, et al. 2006), quartz crystal microbalance (QCM)(Welle 2004, Hemmersam, et al. 2005, Roach, Farrar and Perry 2005), time of flight secondary ion mass spectrometry(Michel, et al. 2005), ellipsometry(Seitz, et al. 2005, Poksinski and Arwin 2007), surface plasmon resonance(Green, et al. 1997, Green, et al. 1999, Garcia, et al. 2007), radiolabeling(Nonckreman, et al. **2007**), electrophoretic depletion measurements(Noh and Vogler 2006, Barnthip, et al. 2008), X-ray photoemission electron microscopy(Morin, et al. 2004 , Li, et al. 2006), among a multitude of other techniques(Horbett and Brash 1995).

One of the approaches is by labeling the protein with radioisotopes or fluorescent probes, both methods based on quantification of a signal emitted by labeled adsorbed proteins. It is even possible to resolve the conformation of the protein on the surface by monitoring the shifts in fluorescence labels attached on the protein of interest with fluorescence life-time giving us a window into the molecular dynamics of the adsorbing protein(Karlsson and Carlsson 2005). However, labeling especially radiolabeling is not a trivial task and also involves artifacts. Other approaches for analysis of adsorbed proteins include depletion measurements and the use of surfactants to elute adsorbed fibrinogen off the substrates for analysis by electrophoresis(Chinn, et al. 1991, Chinn, et al. 1992,

Slack and Horbett 1992, Balasubramanian, et al. 1999, Noh and Vogler 2006). Elution studies are also used to assess changes in adsorbed proteins by indirectly correlating the amount of protein remaining following elution with adhesion strength, conformational changes in the protein and subsequent changes in protein activity(Chinn, Posso, Horbett and Ratner 1991, Shiba, et al. 1991, Chinn, Posso, Horbett and Ratner 1992). The use of monoclonal antibodies in conjunction with platelet adhesion studies have also been exploited to study adsorbed protein states(Balasubramanian, Grusin, Bucher, Turitto and Slack 1999, Hemmersam, Foss, Chevallier and Besenbacher 2005, Tunc, Maitz, Steiner, Vazquez, Pham and Salzer 2005). Although these techniques have provided information about the amount and the biological activity of proteins on surfaces, the field is still not well-understood.

Colorimetric assays such as the Bradford or Lowry assays, extensively used for protein quantification by comparing the supernatant concentration before and after adsorption (Noble, et al. 2007) produce only averaged values over a micro-scale possibly obscuring aspects of interaction at the molecular scale. Similarly, protein adsorption studies with differential scanning calorimetry uses a global parameter such as absorbed or released heat as an indicator for protein unfolding when compared with the control protein in solution(Welzel 2002). In situ protein adsorption and subsequent time-dependent reorientation of proteins at surfaces can be studied using total internal reflection fluorescence (TIRF). Evanescent waves are generated by waves totally reflecting off a substrate–solution interface and these waves illuminate specific

fluorophores with a penetration depth of ~100 nm(Sanders and Jennissen 1996, Daly, et al. 2003).

More information about the structure of proteins at interfaces can be extracted with Fourier transform infrared spectroscopy (FTIR). The secondary structure of adsorbed proteins as well as a reconstructed image of adsorbed proteins can be obtained using FTIR. It involves deconvolution of an amide I band (1600–1700 cm^{-1}) to estimate the ratio of α-helices, β-sheets, turns or random coils in the protein molecules(Chittur 1998, Steiner, et al. 2007).

In X-ray photoelectron spectroscopy, adsorbed protein on a sample are bombarded with X-rays and the binding energy of the emitted elements from the top few nanometers is recorded(Sally 2006). In practice, detection of proteins at interfaces involves the detection of nitrogen and attenuation of a substrate signal due to adsorbed protein. XPS is a challenging technique because it's an ultra-high vacuum technique and therefore freeze-drying is needed to preserve the natural conformation of adsorbed proteins. Wagner has reported the detection limit for XPS ranged from 10 ng/cm^2 of fibrinogen (on mica) to 200 ng/cm^2 on allyl amine plasma polymers(Wagner, et al. 2002). However, the sensitivity was shown to be dependent on substrate surface chemistry and the organization of the adsorbed protein film.

Similar drawbacks like the necessity for freeze-drying of biological samples, ultra-high vacuum conditions and dependence on properties of the adsorbed protein layer also exists for time of flight-secondary ions mass spectroscopy (ToF-SIMS). ToF-SIMS

measures and converts the flight time of secondary ions emitted from the sample surface to mass spectra. Complicated laborious techniques including principal components analysis (PCA) are used to extract information about specific amino acids for characterization of the adsorbed protein layer. Wagner has also identified detection limits for ToF-SIMS ranging from 0.1 ng/cm^2 of fibrinogen to 100 ng/cm^2, depending on the substrate and data analysis(Wagner, McArthur, Shen, Horbett and Castner 2002).

Surface plasmon resonance (SPR) uses an optical method to measure the refractive index near (~300nm) a sensor surface to monitor adsorption processes in real time providing information on the rate of adsorption and the thickness of the adsorbed layer. Green et al. have applied SPR to study the competitive adsorption of albumin, IgG and fibrinogen on polystyrene from plasma under flow by individually probing the three proteins with antibody binding(Green, Davies, Davies, Roberts and Tendler 1997, Green, Davies, Roberts and Tendler 1999).

Surface enhanced Raman spectroscopy (SERS) uses the enhancement of Raman Scattering signal either by excitation of localized surface plasmons or through the formation of charge-transfer complexes at the interface to detect single-molecule on noble-metal substrate(Stiles, et al. 2008). SERS is used in several applications including directly measuring glucose concentration over a clinically relevant range (0-25mM) in a biosensor application and detecting the molecular vibrations in a single hemoglobin protein molecule immobilized to silver nanoparticles(Xu, et al. 1999).

Ellipsometry is an optical surface-sensitive method and has been used for several aspects of proteins adsorption. It measures the change of polarization of a light beam upon reflection off a sample and correlates it to the sample's thickness and refractive index adsorption of biomolecules(Elwing 1998). Other variations of ellipsometry like the phase-modulated and the spectroscopic ellipsometry are also extensively used for protein adsorption studies(Lousinian and Logothetidis 2007).

Quartz crystal microbalance with Dissipation monitoring (QCM-D) is a very sensitive mass balance. It detects the decrease in resonance frequency of a quartz crystal upon protein adsorption and correlates it with the adsorbed mass within the nanogram range. Information such as the dissipation factor also reveals the viscoelastic properties of thin films of proteins, polymers and cells(Modin, et al. 2006, Nguyen and Elimelech 2007).

Surface Force Apparatus (SFA) can be used to gain useful information about protein-material interaction by measuring detachment or adhesive forces at the interface(Claesson, et al. 1995). The interaction force between two macroscopic molecularly smooth surfaces held by cantilevered springs is measured by optical techniques. The separation distance is controlled precisely by a piezoelectric crystal tube and the interaction forces are accurately calculated by applying Hooke’s law to the cantilever springs. However, SFA can only measure the interaction force between protein layers and surfaces, blurring the single molecule interaction energy into an averaged value.

More sensitive techniques such as the optical tweezers or Atomic force Microscopy are used for single-molecule force measurements. In optical tweezer technique, the force applied to a laser-trapped nanoparticle increases linearly with the distance from the center of the beam. The position of the trapped nanoparticle is very precisely controlled by an acousto-optic deflector (AOD)(Neuman and Block 2004).

Most of these techniques used in detecting the proteins measure the average properties of the biological events. The advent of atomic force microscopy (AFM) and related scanning probe microscopies (SPM) offers new opportunities to directly examine protein adsorption on surfaces in liquid environment without significant sample treatment(Gettens, et al. 2005, Muguruma, et al. 2007, Schon, et al. 2007). Utilizing a microprobe mounted on a flexible cantilever scanning across the surface, AFM can obtain topography images with molecular level resolution, and can also measure the interaction forces between proteins and surfaces or proteins and proteins at the picoNewton scale. Moreover, AFM can perform these measurements of proteins under physiological conditions, opening the door to direct measurements of time-dependent, dynamic, biological processes at a molecular scale.

1.2 Atomic Force Microscopy (AFM)

Since the late 1980s, atomic force microscopy (AFM) has evolved as a powerful technique in the fields of biological sciences and material sciences(Binnig, et al. 1986). AFM is now established as a versatile tool to address the structure, properties and

functions of biological samples principally due to its unprecedented nanometer scale resolution and its ability to image surfaces in an aqueous environment. In AFM, a sharp tip attached to a cantilever is scanned over a surface to construct an image using the interactions between the tip and the surface. A very good analogy is a blind man reading brail script using his fingertips. The image will be created using the feel of touch between the braille script and his fingertip, with the resolution equal to the radius of the fingertip. Apart from the advantage of nanoscale resolution of the AFM, it produces a 3D image of the underlying surface under physiologically relevant aqueous conditions with minimal surface treatment.

1.2.1 Mode of Operation

Figure **1-1** explains the principal components of an AFM. The specimen is mounted on a piezoelectric scanner, which allows 3 D positioning with sub-nanometer accuracy over a desired area in the x-y plane. AFM probe consists of a silicon nitride or silicon tip with radius of curvature at the tip apex in the range of 5-40nm integrated to the apex of a microfabricated cantilever of a known spring constant, k (N/m). The size and shape of the tip determines the lateral resolution of an AFM image; the duller the probe tip, the lower the resolution of surface features. AFM imaging can be carried out in aqueous conditions using a fluid chamber around the probe on the surface. The force is monitored with piconewton sensitivity by measuring the deflection of the cantilever by a laser-photodiode control system. The movement of the scanner in the z-direction

correlates to the height of surface features (e.g. proteins adsorbed on a smooth substrate) and is usually determined by the tip-surface interactions(Dupres, et al. 2006). Different AFM imaging modes are available which mainly differ in the way the tip interacts with the samples.

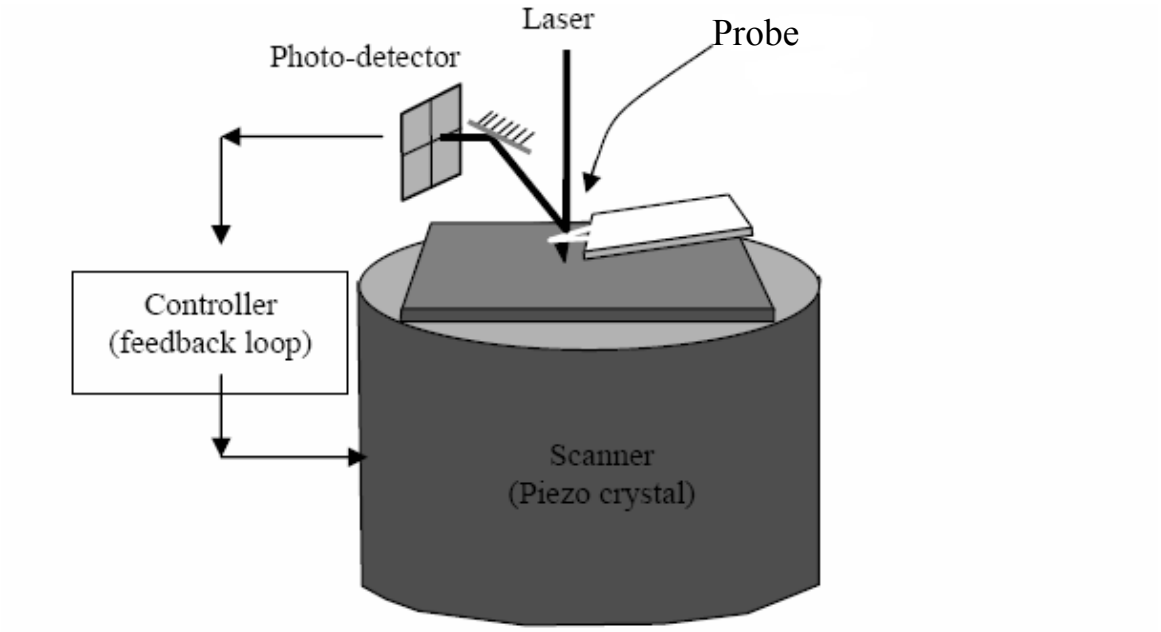

Figure **1-1**: Schematic of AFM showing the basic components: scanner where the piezoelectric transducer resider, cantilever-tip assembly, laser and the multi-segmented photodetector, and feedback loop between photodetector and scanner. Reprinted from (Agnihotri 2005)

Several imaging modes can be used to detect biomolecules on a variety of substrates. For high-resolution biomolecular imaging, contact mode and tapping imaging modes are extensively used.

1.2.1.1 Contact Mode

In contact mode, the tip is brought into physical contact with the surface and raster-scanned through the x-y plane. The surface features, in our case adsorbed proteins, induce a deflection in the cantilever which is monitored by an optical lever system, and the feedback loops maintain tip-sample contact under a constant force by moving the sample up or down, thereby generating a 3-D topographical image. In the optical lever system, a sharp laser is reflected off the back of the gold or aluminum-coated cantilever to a multi-segmented photo-detector. The small deflections of the cantilever (as small as 0.1A) is amplified and converted to voltage values by the photo-detector. Since the probe is in physical contact with the surface features, contact mode is more sensitive to small topographical changes. However, physical contact results in significant lateral forces experienced between the sample and the probe. This can cause deformation of sensitive biological surfaces or sweep the loosely-bound biomolecules.

1.2.1.2 Intermittent-Contact Mode

In tapping mode, also called intermittent or dynamic mode, an oscillating tip is scanned over the surface which significantly reduces the shear force applied by the tip and therefore is suited for loosely-bound biomolecules. The cantilever oscillation amplitude is maintained constant by a feedback loop. As the tip lightly taps the surface the amplitude decreases and this change in amplitude is used to measure the topographical variations in the sample. The tapping force can be controlled by setting up

an r_{sp} value, which is the ratio of set-point amplitude to free amplitude of oscillation. The feedback loops operate at a constant attenuation level of oscillation while scanning the surface to generate the surface image. This imaging mode retains the high-resolution capability from contact mode, but eliminates the significant lateral forces associated with contact mode, which might damage a sensitive sample or might sweep a biomolecule off the surface.

AFM has been used extensively to obtain nanometer scale images of biosystems including proteins, lipid membranes, DNA and cells, generally utilizing ultrasmooth surfaces such as muscovite mica, highly oriented pyrolytic graphite (HOPG) or self assembled monolayers (SAMs)(Argaman, et al. 1997, Radmacher 1997, Reviakine and Brisson 2000, Marchant, Kang, Sit, Zhou, Todd, Eppell and Lee 2002, Osada, et al. 2003, Touhami, et al. 2003, Hussain, et al. 2005, Toscano and Santore 2006). The low surface roughness (RMS~0.2nm) achieved with these model surfaces are ideal to characterize nanoscale protein features, including specific domains and conformational changes in these proteins upon adsorption. In this work, muscovite mica has been used extensively; since it can very easily produce clean atomically flat surfaces just by cleaving it with adhesive tape and are the most frequently used substrates for imaging biological samples. Adsorption of biomolecules on various substrates can be achieved by simple adsorption by either allowing a drop of protein to be dried using a stream of nitrogen gas or immersing the substrate in a protein solution for a given period of time. Protein sample can be also directly imaged under liquid conditions without any air-drying step by adsorption in the presence of electrolyte.

Over the years, several plasma proteins including fibrinogen(Cacciafesta, et al. 2001, Marchant, Kang, Sit, Zhou, Todd, Eppell and Lee 2002); fibronectin(Bergkvist, et al. 2003), vWF(Siedlecki, et al. 1996), and albumin (Dupont-Gillain, et al. 2003) are studied by AFM. Among the different proteins, fibrinogen adsorption on varied substrates remains of interest in the context of protein-biomaterial interactions. Sit and Marchant examined the interaction of fibrinogen with hydrophobic octadecyltrichlorosilane (OTS) SAM, positively-charged 3-aminopropyltriethoxysilane (APTES) SAM, and negatively-charged mica using AFM(Sit and Marchant 1999). However, AFM experiments can be quite limited in scope, particularly in complicated multi-protein adsorption experiments, because the proteins can be difficult to distinguish based on topography alone(Truong, et al. 1998, Cacciafesta, Hallam, Watkinson, Allen, Miles and Jandt 2001). Perhaps more importantly, clinically used biomaterials have rough topographies that dwarf the dimensions of the proteins of interest making detection of specific proteins on these surfaces even more difficult. Agnihotri et al. used tapping mode AFM to visualize fibrinogen adsorption on model hydrophobic HOPG and hydrophilic mica surfaces in an aqueous environment(Agnihotri and Siedlecki 2004). Different orientation states of adsorbed fibrinogen were distinguished by observing the differences in the relative heights of the D and the E domains in single molecules. The spreading kinetics of individual molecules was studied by measuring the heights of the D and E domains over a timescale of ~2 h. Both domains increase in height on hydrophilic mica substrate while they decrease in height on hydrophobic HOPG substrate. Agnihotri also used this mode to visualize the surface rearrangement of three poly(urethane urea)s

in an aqueous environment(Agnihotri, et al. 2006). The hydration process resulted in formation of 50-70 nm-sized raised features on the surface of the polymers and demonstrated hard domain enrichment near the surface.

1.2.1.3 Phase Imaging

Tapping mode imaging also has the ability to map simultaneously the topography and the compositional variations of the underlying specimen surface. In AFM 'tapping' mode, the phase lag of the vibrating probe with respect to external excitation can also be recorded to generate a second image, called a phase image or phase contrast image. Probe-surface interactions obtained from the amplitude of oscillation and the phase-shift recordings can be transformed into energy-dissipation measurements. This enables experimental data to be linked to material properties of the surface such as stiffness, viscoelasticity, adhesion energy as well as tip-sample interactions including electrostatic, van der Waals forces etc(Magonov and Reneker 1997, Garcia, Magerle and Perez 2007). Phase imaging has been employed to study the heterogeneous polymer surfaces as well as sensitive imaging of cell surfaces(Magonov and Reneker 1997). Lazzeri used phase imaging to characterize tribological properties like chemical degradation and wear of poly(methyl-methacrylate) (PMMA) and poly(L-lactic acid) (PLLA) polymers at micro and nanoscales(Lazzeri, et al. 2006). Garrett used AFM to visualize the phase-separated structure of poly(urethane urea) segmented block copolymer(Garrett, et al. 2001). Nagoa detected local variations in stiffness of COS-1 cell cytoplasm with a lateral resolution of

~30nm(Nagao and Dvorak 1999). Pesen showed that the contrast in AFM imaging of cell cortex of bovine pulmonary artery endothelial cells (BPAECs) is in effect because of differences in local mechanical properties(Pesen and Hoh 2005). Holland and Marchant used phase imaging for detecting fibrinogen on clinically relevant biomaterials: poly(dimethylsiloxane) (PDMS) and low density polyethylene (LDPE)(Holland and Marchant 2000). While fibrinogen could occasionally be observed in the phase images at submonolayer concentrations, the surface often proved too rough to clearly distinguish the adsorbed protein. Cassiafesta et al. was able to visualize human fibrinogen adsorbed onto only 2 out of 7 titanium oxide surfaces with different surface-roughness. These studies demonstrated the limitations of AFM in detecting proteins on rough surfaces(Cacciafesta, Hallam, Watkinson, Allen, Miles and Jandt 2001).

1.2.1.4 Force Mode

In force spectroscopy mode of the AFM, the deflection of cantilever is measured as a function of the vertical displacement of the piezoelectric scanner. The cantilever deflection can be translated into a force-distance curve using Hooke's law (F=-k x d, where k is the cantilever spring constant) shown in Figure **1-2** . As the probe approaches the surface from point A, the tip jumps into contact (point B) due to surface forces including van der Waals, electrostatic and hydration forces that overcome the stiffness of the cantilever. At point C, the probe and the surface are in contact. At point D, the direction of motion is reversed and the tip is pulled away from the surface. Due to the

adhesive force, the tip and the sample remain in contact and at point E, the contact breaks. This pull-off force gives a measure of the adhesion between the tip and the surface ($F_{adhesion}$ in Figure **1-2**) and can be used to detect proteins using specific ligand-receptor interactions. Adhesion force is plotted as a function of the sample position along the z-axis (perpendicular to the surface) to generate a force-distance curve.

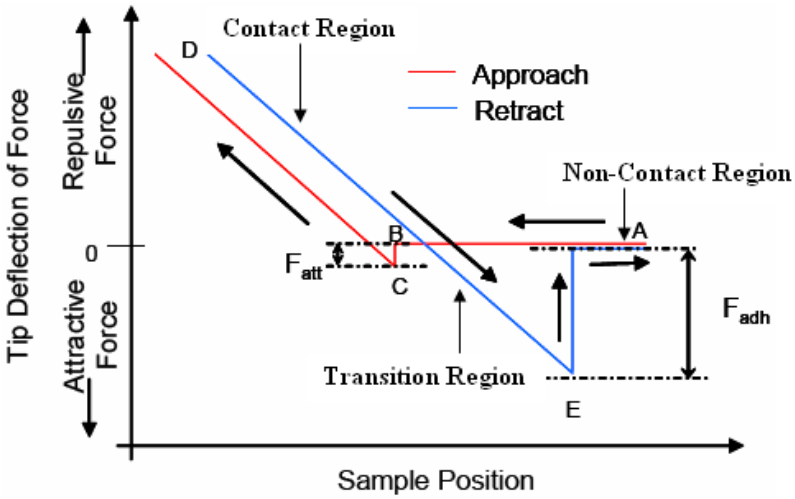

Figure **1-2**: Idealized force-distance curve: During force mode, the probe tip is first lowered into contact with the sample, then is indented into the surface, and finally is lifted off of the sample surface. Tip-surface interaction forces can be monitored by using this mode. (For clarity, the approach and retract part of the curve are shown displaced along the x-axis) Reprinted from (Agnihotri 2005)

The portion of the force-distance curve where the tip comes in contact with the surface (Refer to "contact region" in Figure **1-2**) provides information about the mechanical properties of the surface, whereas the non-contact region (Refer to "non-contact region" in Figure **1-2**) provides information about the pull-off force which is a measure of the adhesion between the tip and the surface. Radmacher used this region of the AFM force curve to determine the elastic properties of biological samples at a

submicrometer scale(Radmacher 1997). VanLandingham has used the contact-region of the force-distance curve to perform nanoindentation studies a number of polymer systems, including an elastomer, several polyurethane systems, thermally-cured epoxies, a thermoplastic polymer-thermosetting polymer adhesive system, and a thermoplastic matrix composite(Vanlandingham, et al. 1997). Several researchers have used this region to evaluate local mechanical characteristics of different cell types varying from muscle cells to osteoblasts with increased force sensitivity(Kuznetsova, et al. 2007).

Following pioneering work on the biotin/avidin interactions(Florin, et al. 1994), pull-off or debonding forces in the non-contact region has been used by many for (a) protein-material interactions (Kidoaki and Matsuda 2002) (b) protein-protein interactions including single molecule unfolding of large multidomain proteins (Best, et al. 2003) and thermodynamic parameters such as bond energies and (c) immunodetection of specific cell population(Dupres, Verbelen and Dufrene 2006). Of particular interest in implanted biomaterials is the measurement of the specific forces associated with cell adhesion proteins, such as integrins and plasma proteins like fibrinongen which play a central role in biomaterial-associated thrombosis.

1.2.1.4.1 Protein-material interactions

Force spectroscopy mode has been used to measure forces between plasma proteins (albumin, immunoglobulin(IgG) and fibrinogen) covalently immobilized to

AFM probes and well-defined model surfaces of self-assembled monolayers (SAMs) of alkanethiolates terminated with different functional groups (CH_3, NH_2, OH, and COOH)(Kidoaki and Matsuda 1999). The results showed that among the three proteins, fibrinogen exhibited the highest adhesion strength on all three surfaces. Sethuraman also used the pull-off forces between a set of seven globular proteins and a series of eight well-defined model surfaces (SAMs). The results demonstrated that all seven proteins behave similarly with respect to adhesion exhibiting a step increase in adhesion as wettability of the solid substrate decreases(Sethuraman, et al. 2004). Similar step increase in adhesive forces was studied by Xu and Siedlecki using protein-modified AFM probes and glow discharge plasma-modified LDPE surfaces(Xu and Siedlecki 2007). BSA, fibrinogen and FXII all exhibited a step dependence in adhesion force as water contact angles transitioned across the region of contact angle ~60–65°. Protein adhesion forces were found to increase with contact time on all surfaces, consistent with surface-induced conformational changes in the proteins. Remarkably, the protein adhesion forces showed similar trends over time, suggesting that the protein either can refold after separation or that these early unfolding processes are largely independent of the original state of the protein.

1.2.1.4.2 Protein-Protein Interactions

Force spectroscopy allows direct measurements of the strength of the biomolecular interactions at a single molecule level provide a powerful way of

quantifying these complex interactions(Hinterdorfer, et al. 1996). To probe the specific interactions, ligands are attached to the probe and the complementary receptors are immobilized on the surface. Lee and Marchant used this mode to measure the debonding forces between RGD and AGD ligands and human platelet receptor alpha(IIb)beta(3)(Lee and Marchant 2003). Lehenkari used AFM to study the characteristics of osteoclast integrin-ligand mechanics in the context of possible cell specific features. The integrin ($\alpha v\beta 3$) binding force, ranging from 32 to 97 picoNewtons (pN), was found to be cell and amino acid sequence-specific, and sensitive to the pH and divalent cation composition dependent of the cellular composition medium(Lehenkari and Horton 1999). Kokkoli studied collective and single-molecule interactions of the $\alpha v\beta 1$ receptor-GRGDSP ligand system by constructing a bioartificial membrane mimicing specific peptides(Kokkoli, et al. 2004).

Our laboratory has also used this mode to study antigen-antibody interactions by coupling the AFM probe with antibodies. Agnihotri et al. used AFM probe modified with polyclonal antibodies against fibrinogen and adhesion mapping to obtain both height and adhesion data simultaneously(Agnihotri and Siedlecki 2005). Adhesion mapping over a surface patterned with BSA by micro-contact printing (μCP) and backfilled with fibrinogen verified the protein sensitivity of the modified probe. A dual-component protein film containing fibrinogen and BSA was imaged with the modified probe and adhesion images were used to generate a recognition image with a lateral resolution of ~16 nm. Our laboratory also used model hydrophobic and hydrophilic surfaces to study specific interactions of integrins with adsorbed fibrinogen(Agnihotri and Siedlecki Under Review). Debonding strengths were observed in the range of 50-80 pN for loading rates

varying from 10-100 nN/s on both hydrophobic and hydrophilic surfaces. An important physiological implication of these results is that the surface properties appear to influence platelet adhesion only by modulating the expression of critical epitopes in the adsorbed fibrinogen. Once the receptor-binding epitope is available, then binding of the platelet membrane receptor will follow the same kinetics regardless of the surface properties.

Thermodynamic properties of various protein-protein/antibody interactions such as free energy changes and kinetic rates of dissociation can also be calculated using this mode. The pull-off forces measured in these experiments may correspond to the breaking of several bonds which is primarily based on the protein density on the tip and the surface. However, when many such bonds are linking two cells or a platelet with adsorbed fibrinogen, there is a very small probability for all the receptors to be simultaneously unbound, resulting in a strong adhesion force. If a force is applied to separate the molecules, the free energy minimum at the equilibrium binding position will diminish and, for a sufficiently strong force, disappear. An increased rate of bond dissociation under external force was first emphasized by Bell using a model for the offrate kinetics (Bell 1978) . Kokkoli used AFM to measure single and collective interactions with immobilized αvβ1 integrins and GRGDSP peptide-mimicing membranes. Under loading rates of 1-305 nN/s, the study revealed the presence of two activation energy barriers in the unbinding process, an outer barrier at a distance of 0.09 nm in the high strength regime and an outer barrier at 2.77 nm for loading rates below 59 nN/s(Kokkoli, Ochsenhirt and Tirrell 2004). Lee and Marchant used a modified cantilever tips with covalently grafted peptides (RGD and AGD) to measure debonding

forces of platelet receptor GP2b3a. The single receptor interaction revealed a logarithmic dependence of the rate of loading(Lee and Marchant 2003). The study found that differences in the zero off-kinetic rates can be attributed to the relative effectiveness of ligands during the initial and subsequent binding interaction of fibrinogen to αIIbβ3 in the process of platelet aggregation. Xu and Siedlecki used modified colloid probe to analyze the effects of surface wettability, loading force, loading rate and contact time on fibrinogen adhesion on model surfaces(Xu and Siediecki Under Review). This paper explored the energy profile of fibrinogen-surface interactions using modified Bell's model using the relationship of adhesion force and the logarithm of loading rate to predict the energy landscape profile of fibrinogen-surface bonds. Multiple energy barriers were found in the dissociation of proteins from poorly wettable surface while single energy barrier was found on hydrophilic surfaces.

1.2.1.4.3 Immunodetection with AFM

This mode gives the AFM the unique ability to map the distribution of individual binding sites with nanoscale resolution. An array of force curves can be recorded in the x, y plane on a given area/size essentially creating a 'Force-Volume' or 'Adhesion' spatially resolved maps of molecular interaction forces. The spring constants for the silicon nitride probes used for sensitive force measurements are in the range of 0.01 – 0.1N/m, which translate to high force sensitivity (picoNewton (pN) range). The force spectroscopy mode of the AFM uses the rupture force between the tip and the surface to detect interactions.

Grandbois et al. used the adhesion mapping mode to generate an image of a mixed layer of group A and O red blood cells with a contrast based only on the measured strength of a specific receptor–ligand pair(Grandbois, et al. 2000). The image was obtained by measuring and plotting for each image pixel the adhesion force between the mixed RBC layer and the functionalized AFM tip and was able to clearly discriminate between the two cell populations and to produce an image based on affinity contrast.

Agnihotri extended molecular recognition imaging by AFM to detect artificially patterned proteins on mica substrate(Agnihotri and Siedlecki 2005). Functionalized AFM probes were used to generate binary recognition images where the specific and non-specific interactions were differentiated based on a statistically derived cut-off value.

1.3 Surface Induced Thrombosis

Blood is a mixture of cells (erythrocytes, leukocytes) and cell-fragments (thrombocytes) suspended in a complex solution (plasma) of gases, salts, proteins, carbohydrates, and lipids in water. Under normal physiological conditions, a complicated hemostatic system maintains blood in a fluid state. In the event of vascular injury, the system reacts in a self-amplifying manner to stem bleeding. The endothelial cell lining is also actively involved producing inhibitors of blood coagulation and platelet aggregation including Nitric Oxide (NO), Prostaglandin (PGI2), thrombomodulin and fibrinolytic activators(Colman, et al. 2001). However, a biomaterial surface in contact with blood, acts as a stimulus for the hemostatic response that leads to surface-induced thrombosis.

The interaction of blood components with a biomaterial surface can initiate thrombosis via two mechanisms: one, by activation of the intrinsic coagulation cascade (also known as contact phase activation); and two, by direct interaction of the circulating platelets with the adsorbed fibrinogen (Figure **1-3**).

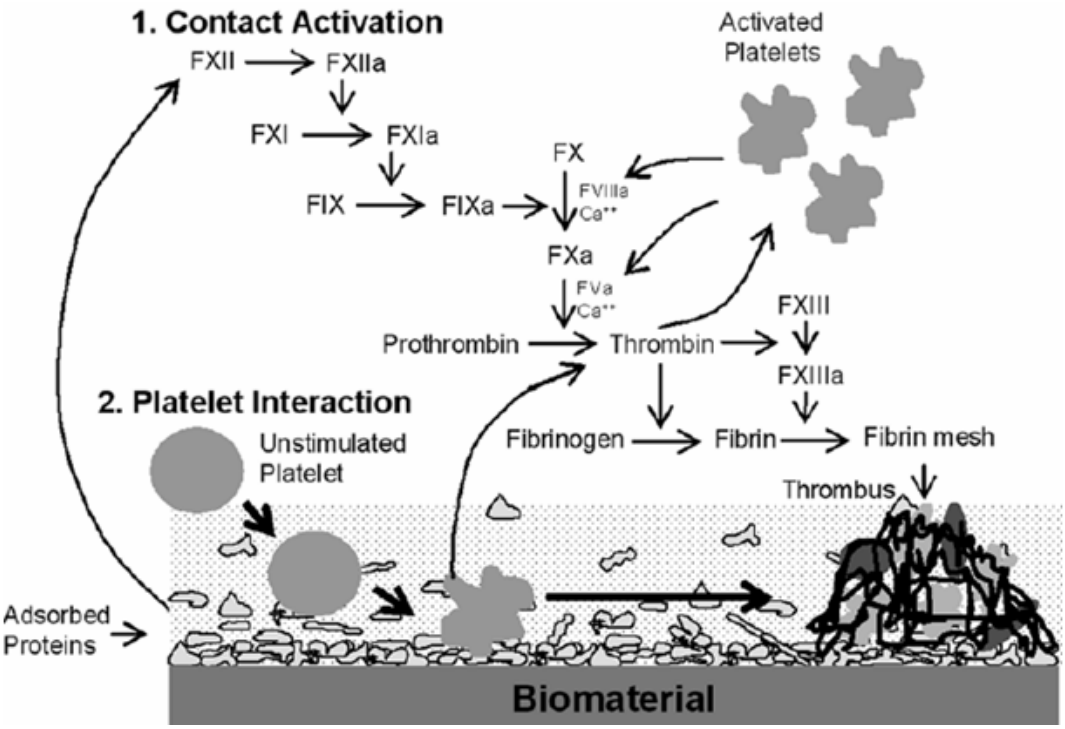

Figure **1-3**: Schematic showing the main components of the two mechanisms of surface-induced thrombosis. Contact activation of factor XII initiates the intrinsic coagulation cascade. Direct interaction of circulating platelets with the adsorbed fibrinogen also leads to thrombus formation Reprinted from (Agnihotri 2005)

Contact phase activation involves activation of the zymogen factor XII (FXII or Hageman factor) to its active form FXIIa by the surface. Each cascade step involves a limited proteolytic cleavage of a factor to an activated enzyme. These blood coagulation reactions are classically grouped in two major pathways— the extrinsic and intrinsic

cascades that converge into the common pathway to ultimately generate thrombin. Once thrombin is generated in this cascade, it converts fibrinogen to fibrin monomers by cleaving fibrinopeptides A and B, eventually forming an insoluble fibrin mesh. The second mechanism of surface-induced thrombosis involves interaction of circulating blood platelets with the biomaterial surface, which is mediated by the adsorbed protein layer. Platelet membrane has two primary adhesive proteins: GPIb-IXV and GPIIbIIIa. The principal ligand for GPIb-IX-V complex is von Willebrand Factor (vWF), while activated GPIIbIIIa binds to fibrinogen. The GPIIbIIIa on a non-stimulated platelet remains in a low affinity state for soluble fibrinogen. However, once fibrinogen is adsorbed to a surface, it attains the capability to interact with GPIIbIIIa on a circulating platelet, triggering what is called 'outside-in' signaling, which results in platelet activation(Savage and Ruggeri 1991, Plow and Shattil 2001). Once a platelet is activated, it spreads out on the surface, releasing the contents of cytoplasmic granules that start the coagulation cascade culminating in the formation of a fibrin mesh. The end product is a thrombus with platelets and blood cells trapped in the fibrin mesh.

1.3.1 Fibrinogen:

Fibrinogen, the third most prevalent protein in plasma with a circulating concentration of approximately 2.6-3.5 mg/mL plays a critical role in the hemostatic response. The fibrinogen molecule is a symmetric, dimeric molecule which consists of three pairs of intertwined polypeptide chains designated as Aα, Bβ and γ(Hantgan, et al.

2001). There are six putative sites in fibrinogen through which it can interact with the platelet membrane receptor protein (Figure **1-4**). There are two pairs of RGD sequences (RGDS at residues 95-98 and RGDF at residues 572-575) in each of the Aα chains, and a peptide sequence located at the C-terminus of each of the γ chains known as the γ-chain dodecapeptide (residues 400-411, HHLGGAKQAGDV). Adhesion of both stimulated and unstimulated platelets to immobilized fibrinogen is also mediated primarily through the γ-chain carboxyl terminus(Plow and Shattil 2001). It was shown that mutations in either of the α chain RGD sequences have no effect on platelet aggregation, whereas substitution of a variant γ-chain dodecapeptide results in significant reduction in platelet aggregation activity(Farrell, et al. 1992). Soluble fibrinogen does not bind to an unstimulated platelet, but the unique ability of surface-adsorbed fibrinogen to cause direct platelet adhesion and activation of unstimulated platelets suggests conformational changes in fibrinogen molecule upon adsorption.

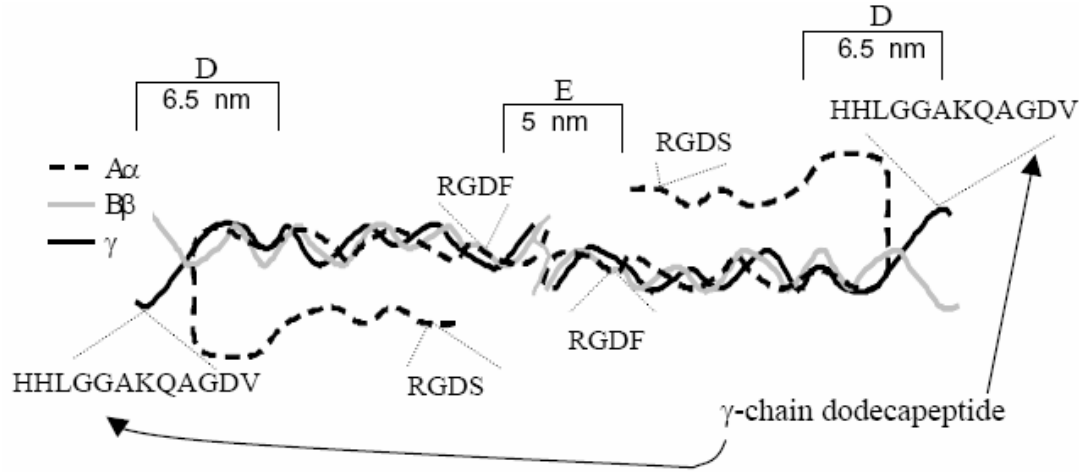

Figure **1-4**: Fibrinogen is a symmetric molecule with two sets of three intertwined polypeptide chains termed as Aα, Bβ and γ chains. Each fibrinogen molecule possesses three pairs of potential platelet binding peptide sequences, two RGD sequences in each of the Aα (RDGF and RGDS) and a dodecapeptide sequence (HHLGGAKQAGDV) in each of the γ chains, with the γ chain dodecapeptide sequence being the primary ligand for platelet adhesion to adsorbed fibrinogen.

1.3.2 Platelet Membrane Receptor Protein, GPIIbIIIa

The platelet membrane receptor protein GPIIbIIIa (also called αIIbβ3) is the most abundant glycoprotein on the platelet membrane with approximately 40,000 to 80,000 copies per platelet. The platelet membrane GPIIbIIIa interacts with a variety of ligands including fibrinogen, fibronectin , von Willebrand factor, vitronectin and thrombospondin by recognizing the common adhesive amino acid sequence Arg-Gly-Asp (RGD) as well as the γ-chain dodecapeptide of fibrinogen(George and Colman 2001, Plow and Shattil 2001). There are a number of agonists such as thrombin, ADP, epinephrine, and thromboxane A2 that trigger platelet activation and inside-out signaling(Shattil 1999). This leads to conformational changes in the GPIIbIIIa heterodimer exposing the ligand-

binding sites. The affinity modulation is also accompanied by the lateral clustering of integrins and the translocation of additional GPIIbIIIa from within the platelets(Plow and Shattil 2001). On a biomaterial surface, binding of adsorbed fibrinogen to a GPIIbIIIa on an unstimulated platelet causes platelet adhesion and activation. This regulation of platelet function by ligand-binding is called *outside-in* signaling. Fibrinogen binding to a GPIIbIIIa receptor is followed by oligomerization of receptors, and the signal is propogated by direct and indirect interactions of the αIIb or β3 cytoplasmic tails, or both, with the intracellular proteins(Plow and Shattil 2001).

1.4 Significance of Research

Surface thrombosis remains a significant limitation in successful commercialization of blood-contacting medical devices such as catheters, vascular grafts, heart valves and cardiac assist devices like ventricular assist systems (VAS). The pediatric artificial heart project in the Hershey medical center was undertaken to provide cardiac support for patients ranging in age from new-born to teens. Juvenile goats and sheep were used as animal models for testing of pediatric ventricular assist devices (VADs). The Pediatric VAD is basically a mechanical pump that consists of a polymer blood sac which comes in contact with blood. Selection of a biomaterial for a specific medical application involves understanding the desired material properties and biological response to the biomaterial. In the last 30 years, polyurethane elastomers have emerged as one of the most widely used biomaterials in diverse applications such as catheters,

intra-aortic balloons, vascular prostheses, heart valves, lead insulations of pacemakers and blood sacs of ventricular assist devices(Lamba, Woodhouse and Cooper 1998). The pediactric VAD project also uses poly (urethane urea) biomaterial primarily due to its excellent mechanical properties as well as better hemocompatibility as compared to other polymers. However preliminary studies with polyurethane blood sac showed a tendency of forming thrombus in the blood sac despite anti-coagulation treatment. (Refer Figure 5A) (Bachmann, et al. 2000, Weiss 2004)

Several thrombus evaluation techniques have been tried over the year. Conventional examination of the explanted biomaterial surface includes gross and microscopic examination of heart, lung, kidneys, liver, spleen, and vascular connections, which involves visual examination with further histological and microscopic studies (Portner, et al. 1983)(Figure **1-5**). Yamanaka used scanning electron microscopy (SEM) to visualize the topography of the retrieved blood sacs by scanning images from different areas of the VAD(Yamanaka, et al. 2005). SEM analysis performed was unable to distinguish polymeric from biologic features and was also not able to distinguish between different biologic components. Low density of small proteinaceous structures were seen in all regions on surfaces of explanted PUU blood sacs. (Figure **1-5**) Immunofluoroscence microscopy was used for functional labeling of adsorbed molecules; however poly (urethane urea) contributes significant background fluorescence to the images thereby decreasing the contrast of the secondary tags considerably(Yamanaka, et al. 2006). Autofluorescence of the blood sac polyurethane (PU) material was found to cause difficulty in imaging of platelets and fibrin on the

surface (Figure **1-5**). SDS-PAGE (Sodium Dodecyl Sulfate-PolyAcrylamide Gel Electrophoresis) and Western blotting were also used to analyze adsorbed proteins on explanted surfaces(Cornelius, et al. 2002). In a recent paper, Maria has shown that the chloramine-T (CAT) labeling method for binding iodine to albumin and IgG molecules can result in enhanced aggregation and fragmentation of the proteins(Holmberg, et al. 2007). This change in protein stability may result in misinterpretation of results from radioactive labeling experiments often used to determine the amount of protein adsorbed on a surface. In view of the ever-increasing use of artificial materials in the body, better techniques and information are required to characterize the major events occurring at the blood-implant interface.

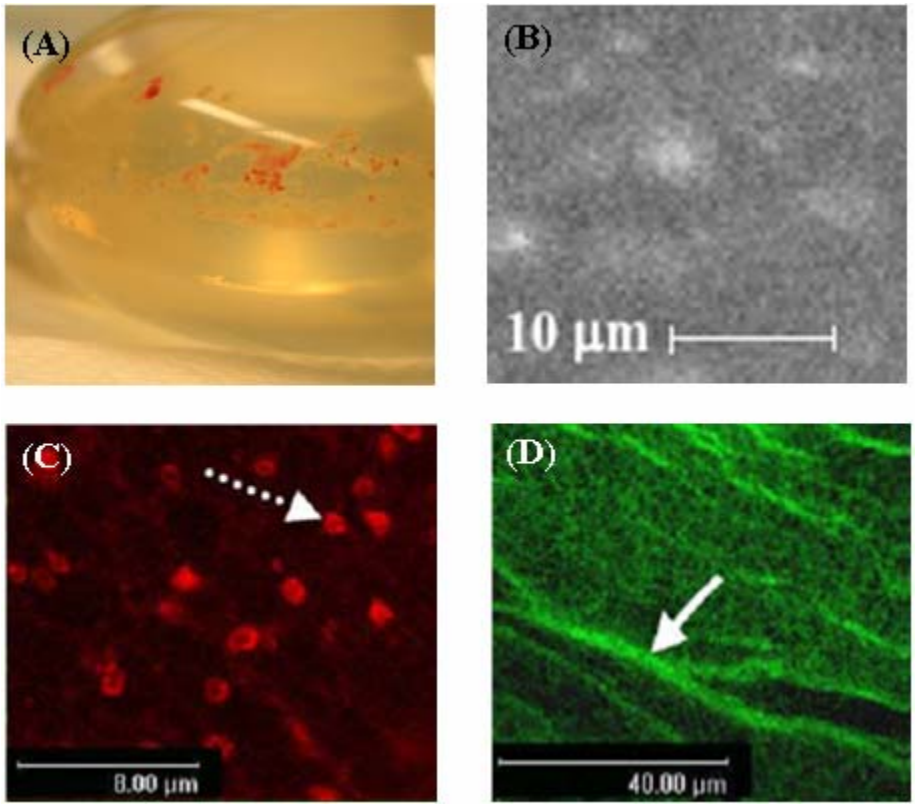

Figure **1-5**: Thrombus formation on a poly (urethane urea) blood sac from a left ventricular assist system implanted in a calf for 30 days. (A) Macroscopic blood clots on the poly (urethane urea) sac surface, (B) Scanning electron microscopy of an explanted PUU sac with features resembling a protein layer (C) Confocal microscopy of the bovine platelets in platelet rich plasma (PRP) clot on PUU sac. (Dotted arrow lines: platelets). Platelets can be identified by labeling for the αIIb chain on the αIIbβ3 integrin present on the platelet membrane. (D) Fibrin in a bovine platelet rich plasma clot on PUU (Solid arrows: fibrin). Fibrin can be labeled with a monoclonal antibody solution that recognizes bovine fibrinogen. (Courtesy: Hanako Yamanaka, Penn State College of Medicine).

Atomic force microscopy (AFM) was used to visualize the surface of a poly (urethane urea) (PUU) blood sac retrieved from a 30 day implanted device. It was realized that imaging specific proteins on a clinically relevant biomaterial like PUU requires more that the conventional AFM techniques. Conventional AFM techniques use ultrasmooth substrates for imaging. The low surface roughness (RMS roughness~0.2nm)

achieved with these model surfaces are ideal to characterize nanoscale protein features, including specific domains and conformational changes in these proteins. However AFM experiments can be quite limited in scope, particularly in complicated multi-protein adsorption experiments, because the proteins are difficult to distinguish based on topography alone. The PUU sac comes in contact with hundreds of plasma proteins and cannot be distinguished based on topography alone. Perhaps more importantly, polymeric biomaterials such as poly (urethane urea) (PUU) have rough topographies that dwarf the dimensions of the proteins of interest making AFM imaging of specific proteins on these surfaces difficult. Therefore, this work was initiated to develop novel AFM techniques that do not rely on topography to characterize specific proteins on in-vivo explants.

Polyurethanes have unique properties of micro-phase separated structure which affects proteins adsorption and subsequent cellular events. Polyurethane materials are block copolymers constructed from a mixture of "soft" and "hard" segments that form a microphase-separated structure as a result of thermodynamic immiscibility of the polar hard segments and the relatively non-polar soft segments {Xu , Manuscript in preparation #615}. The soft segment is composed of a polyol and the hard segment is composed of diisocyanate and a chain extender, usually low molecular weight diol (for polyurethanes) or diamine (for poly(urethane urea)s. Numerous studies have demonstrated that the degree of phase separation is of critical importance and influences both protein adsorption (Lamba, Woodhouse and Cooper 1998) and platelet interaction (Pitt, et al. 1993) and could very well be the reason for its superior blood-compatibility(Skarja and Brash 1997). Groth et al. investigated the relationship of hard to soft segment ratio with

protein adsorption, lymphocyte adhesion, and platelet adhesion and activation(Groth , et al. 1994). The study demonstrated an increase in fibrinogen adsorption and platelet activation and a decrease in detection of monoclonal antibody against fibrinogen with increase in hard segment content of polyurethanes.

Direct measurements of phase separated microstructures have been difficult to obtain. Prior to relatively recent advancements in atomic force microscopy (AFM), electron microscopy with difficult sample preparation techniques was the only method for directly observing surface microphase structures. It is widely believed that polyurethane materials undergo significant reorganization when placed in aqueous environments. Results from our laboratory also confirm reorientation and rearrangement of hard domains of polyurethane biomaterials resulting in enrichment of hard domains on surfaces(Agnihotri, Garrett, Runt and Siedlecki 2006). Xu et al. also observed decrease in activity of fibrinogen and platelet adhesion on polyurethane surfaces with hydration time {Xu , Manuscript in preparation #615}. Results suggested water-induced enrichment of polar hydrophilic hard domains in polyurethanes changed the local surface physical and chemical properties and influenced the conformational structures of fibrinogen, resulting in the different availability of platelet binding sites such as the fibrinogen γchain dodecapeptide. When the polyurethane sac is implanted in the model animal for testing the VAD, the sac comes in contact with blood and undergoes similar reorientation of hard and soft phases which subsequently affect fibrinogen adsorption and platelet adhesion and ultimately leading to thrombosis. Therefore, it is critical to characterize the surface of polyurethanes in aqueous conditions. Hsu et. al. demonstrated decreased platelet

activation with increased nanophase separation, which becomes even more significant because the sizes of these phases varying from 10-100nm are comparable to the size of adsorbing proteins(Hsu and Kao 2005). It would be very interesting to observe and study protein adsorption on these phase-separated polymers.

Conventional AFM techniques are not able to visualize or detect plasma proteins adsorbed on polyurethanes from low concentration single molecule solutions mostly because of the surface roughness of these polymers. In case of blood, there are about 500 different proteins which can potentially adsorb onto the rough polymer surface making detection even more complicated. Improved understanding of plasma protein interactions with biomedically relevant surfaces can provide the necessary framework for understanding subsequent responses and eventually designing improved biomaterials. This work has developed novel methods to detect both the location and biological activity of adsorbed proteins on model as well as clinically relevant polymeric substrates without the necessary topographical clues in conventional AFM techniques. Taken together, the different parts of this study fill the gaps in the current understanding of blood-material interactions at the molecular level. This project also provides solid groundwork and is an important tool for future studies with polyurethanes and other clinically relevant polymeric biomaterials.

1.5 References

1. Agnihotri, A. Molecular level interactions between blood components and model biomaterials studied by atomic force microscopy. The Pennsylvania State University, Hershey, PA, 2005.

2. Agnihotri, A.; Garrett, J.; Runt, J.; Siedlecki, C., Atomic force microscopy visualization of poly(urethane urea) microphase rearrangements under aqueous environment. *Journal of Biomaterials Science Polymer Edition* **2006,** 17, (1-2), 227-238.

3. Agnihotri, A.; Siedlecki, C., Adhesion mode atomic force microscopy study of dual component protein films. *Ultramicroscopy* **2005,** 102, (4), 257-268.

4. Agnihotri, A.; Siedlecki, C., Interactions of the Platelets Integrin Receptor GP IIb-IIIa with Surface-Adsorbed Fibrinogen. **Under Review**.

5. Agnihotri, A.; Siedlecki, C., Time-dependent conformational changes in fibrinogen measured by Atomic Force Microscopy. *Langmuir* **2004,** 20, 8846-8852.

6. Andersson, J.; Ekdahl, K.; Lambris, J.; Nilsson, B., Binding of C3 fragments on top of adsorbed plasma proteins during complement activation on a model biomaterial surface. *Biomaterials* **2005,** 26, (13), 1477-1485.

7. Andrade, J.; Hlady, V., Protein adsorption and materials biocompatibility: A tutorial review and suggested hypotheses. In *Advances in Polymer Science*, Springer:: Berlin / Heidelberg, 1986; Vol. 79, pp 1-63.

8. Argaman, M.; Golan, R.; Thomson, N.; Hansma, H., Phase imaging of moving DNA molecules and DNA molecules replicated in the atomic force microscope. *Nucl. Acids Res.* **1997,** 25, (21), 4379-4384.

9. Bachmann, C.; Hugo, G.; Rosenberg, G.; Deutsch, S.; Fontaine, A.; Tarbell, J., Fluid dynamics of a pediatric ventricular assist device. *Artificial Organs* **2000,** 24, (5), 362-372.

10. Balasubramanian, V.; Grusin, N.; Bucher, R.; Turitto, V.; Slack, S., Residence-time dependent changes in fibrinogen adsorbed to polymeric biomaterials. *J Biomed Mater Res A* **1999,** 44, 253-260.

11. Barbucci, R.; Lamponi, S.; Magnani, A., Fibrinogen conformation and platelet reactivity in relation to material-blood interaction: Effect of stress hormones. *Biomacromolecules* **2003,** 4, (6), 1506-1513.

12. Barnthip, N.; Noh, H.; Leibner, E.; Vogler, E., Volumetric interpretation of protein adsorption: Kinetic consequences of a slowly-concentrating interphase. *Biomaterials* **2008,** 29, (21), 3062-3074.

13. Bell, G., Models for the specific adhesion of cells to cells. *Science* **1978,** 200, 618-627.

14. Bergkvist, M.; Carlsson, J.; Oscarsson, S., Surface-dependent conformations of human plasma fibronectin adsorbed to silica, mica, and hydrophobic surfaces, studied with use of Atomic Force Microscopy. *J. Biomed. Mater. Res. Part A* **2003,** 64A, 349-356.

15. Best, R.; Brockwell, D.; Toca-Herrera, J.; Blake, A.; Smith, D.; Radford, S.; Clarke, J., Force mode atomic force microscopy as a tool for protein folding studies. *Analytica Chimica Acta* **2003,** 479, (1), 87-105.

16. Binnig, G.; Quate, C.; Gerber, C., Atomic force microscope. *Physical Review Letters* **1986,** 56, 930-933.

17. Cacciafesta, P.; Hallam, K.; Watkinson, A.; Allen, G.; Miles, M.; Jandt, K., Visualisation of human plasma fibrinogen adsorbed on titanium implant surfaces with different roughness *Surf. Sci.* **2001,** 491, 405-420.

18. Cameron, J.; Wilson, R.; Leavesley, D.; Pearcy, M., Mediation of Biomaterial-Cell Interactions by Adsorbed Proteins: A Review. *Tissue Engineering* **2005,** 11, (1-2), 1-18.

19. Chinn, J.; Posso, S.; Horbett, T.; Ratner, B., Postadsorptive transition in fibrinogen adsorbed to polyurethanes: Changes in antibody binding and sodium dodecy1 sulfate elutability. *Journal of Biomedical Materials Research* **1992,** 26, (6), 757-778.

20. Chinn, J.; Posso, S.; Horbett, T.; Ratner, B., Postadsorptive transitions in fibrinogen adsorbed to Biomer: Changes in baboon platelet adhesion, antibody binding, and sodium dodecyl sulfate elutability. *Journal of Biomedical Materials Research* **1991,** 25, (4), 535-555.

21. Chittur, K., FTIR/ATR for protein adsorption to biomaterial surfaces. *Biomaterials* **1998,** 19, (4-5), 357-369.

22. Claesson, P.; Blomberg, E.; Fröberg, J.; Nylander, T.; Arnebrant, T., Protein interactions at solid surfaces. *Advances in Colloid and Interface Science* **1995,** 57, 161-227.

23. Clarke, M.; Wang, J.; Chen, Z., Conformational changes of fibrinogen after adsorption. *J. Phys. Chem. B* **2005,** 109, (46), 22027-22035.

24. Colman, R.; Hirsh, J.; Marder, V.; Clowes, A.; George, J., Overview of Hemostasis. In *Hemostasis and Thrombosis*, Colman, R.; Hirsh, J.; Marder, V.; Clowes, A.; George, J., Eds. Lippincott Williams and Wilkins: Philadelphia, 2001.

25. Cornelius, R.; Archambault, J.; Berry, L.; Chan, A.; Brash, J., Adsorption of proteins from infant and adult plasma to biomaterial surfaces. *Journal of Biomedical Materials Research* **2002,** 60, (4), 622-632.

26. Daly, S.; Przybycien, T.; Tilton, R., Coverage-Dependent Orientation of Lysozyme Adsorbed on Silica. *Langmuir* **2003,** 19, (9), 3848-3857.

27. Damodaran, S., In situ measurement of conformational changes in proteins at liquid interfaces by circular dichroism spectroscopy. *Analytical and Bioanalytical Chemistry* **2003,** 376, (2), 182-188.

28. Dupont-Gillain, C.; Fauroux, C.; Gardner, D.; Leggett, G., Use of AFM to probe the adsorption strength and time-dependent changes of albumin on self-assembled monolayers. *J. Biomed. Mater. Res. Part A* **2003,** 67A, 548-558.

29. Dupres, V.; Verbelen, C.; Dufrene, Y., Probing molecular recognition sites on biosurfaces using AFM. *Biomaterials* **2006**.

30. Elwing, H., Protein adsorption and ellipsometry in biomaterial research. *Biomaterials* **1998,** 19, 397-406.

31. Evans-Nguyen, K.; Fuierer, R.; Fitchett, B.; Tolles, L.; Conboy, J.; Schoenfisch, M., Changes in adsorbed fibrinogen upon conversion to fibrin. *Langmuir* **2006,** 22, (11), 5115-5121.

32. Farrell, D.; Thiagarajan, P.; Chung, D.; Davie, E., Role of Fibrinogen Alpha-Chain and Gamma-Chain Sites in Platelet-Aggregation. *Proc. Natl. Acad. Sci. USA* **1992,** 89, 10729-10732.

33. Florin, E.; Moy, V.; Gaub, H., Adhesion forces between individual ligand-receptor pairs. *Science* **1994,** 264, (5157), 415-417.

34. Garcia, R.; Magerle, R.; Perez, R., Nanoscale compositional mapping with gentle forces. *Nat Mater* **2007,** 6, (6), 405-411.

35. Garrett, J.; Siedlecki, C.; Runt, J., Microdomain morphology of poly(urethane urea) multiblock copolymers. *Macromolecules* **2001,** 34, (20), 7066-7070.

36. George, J.; Colman, R., Overview of platelet structure and function. In *Hemostasis and Thrombosis*, Colman, R.; Hirsh, J.; Marder, V.; Clowes, A.; George, J., Eds. Lippincott Williams and Wilkins: Philadelphia, 2001.

37. Gettens, R.; Bai, Z.; Gilbert, J., Quantification of the kinetics and thermodynamics of protein adsorption using atomic force microscopy. *Journal of Biomedical Materials Research Part A* **2005,** 72A, (3), 246-257.

38. Gorbet, M.; Sefton, M., Biomaterial-associated thrombosis: roles of coagulation factors, complement, platelets and leukocytes. *Biomaterials* **2004,** 25, (26), 5681-5703.

39. Grandbois, M.; Dettmann, W.; Benoit, M.; Gaub, H., Affinity imaging of red blood cells using an atomic force microscope. *J. Histochem. Cytochem.* **2000,** 48, (5), 719-724.

40. Green, R.; Davies, J.; Davies, M.; Roberts, C.; Tendler, S., Surface plasmon resonance for real time in situ analysis of protein adsorption to polymer surfaces. *Biomaterials* **1997,** 18, (5), 405-413.

41. Green, R.; Davies, M.; Roberts, C.; Tendler, S., Competitive protein adsorption as observed by surface plasmon resonance. *Biomaterials* **1999,** 20, 385–391.

42. Groth , T.; Klosz , K.; Campbell , E.; New , R.; Hall , B.; Goering , H., Protein adsorption, lymphocyte adhesion and platelet adhesion/activation on polyurethane ureas

is related to hard segment content and composition. *J Biomater Sci Polym Ed* **1994,** 6, 497-510.

43. Hantgan, R.; Simpson-Haidaris, P.; Francis, C.; Marder, V., Fibrinogen Structure and Physiology. In *Hemostasis and Thrombosis*, Colman, R.; Hirsh, J.; Marder, V.; Clowes, A.; George, J., Eds. Lippincott Williams and Wilkins: Philadelphia, 2001.

44. Hemmersam, A.; Foss, M.; Chevallier, J.; Besenbacher, F., Adsorption of fibrinogen on tantalum oxide, titanium oxide and gold studied by the QCM-D technique. *Colloids and Surfaces B: Biointerfaces* **2005,** 43, (3-4), 208-215.

45. Hinterdorfer, P.; Baumgartner, W.; Gruber, H.; Schilcher, K.; Schindler, H., Detection and localization of individual antibody-antigen recognition events by atomic force microscopy. *PNAS* **1996,** 93, (8), 3477-3481.

46. Holland, N.; Marchant, R., Individual plasma proteins detected on rough biomaterials by phase imaging AFM. *Journal of Biomedical Materials Research* **2000,** 51, (3), 307-315.

47. Holmberg, M.; Stibius, K.; Ndoni, S.; Larsen, N.; Kingshott, P.; Hou, X., Protein Aggregation and Degradation during Iodine Labeling and its Consequences for Protein Adsorption to Biomaterials. *Analytical Biochemistry* **2007,** 361, (1), 120-125.

48. Horbett, T., Principles underlying the role of adsorbed plasma proteins in blood proteins in blood interactions with foreign materials. . *Cardiovascular Pathology* **1993,** 2, 137s-148s.

49. Horbett, T., Proteins: Structure, Properties, and Adsorption to Surfaces. In *Biomaterial Science: An Introduction to Materials in Medicine*, Ratner, B.; Hoffman, A.; Schoen, F.; Lemons, J., Eds. Academic Press: San Diego, 1996.

50. Horbett, T.; Brash, J., *Proteins at Interfaces II : Fundamentals and Applications*. American Chemical Society, 1995: Washington, DC, 1995.

51. Hsu, S.; Kao, Y., Biocompatibility of poly(carbonate urethane)s with various degrees of nanophase separation. *Macromol Biosci* **2005,** 5, 246-253.

52. Hussain, M.; Agnihotri, A.; Siedlecki, C., AFM imaging of ligand binding to platelets integrin alpha IIb ß3 receptors reconstituted into planar lipid bilayers. *Langmuir* **2005,** 21, 6979-6986.

53. Hylton, D.; Shalaby, S.; Latour Jr., R., Direct correlation between adsorption-induced changes in protein structure and platelet adhesion. *Journal of Biomedical Materials Research Part A* **2005,** 73A, (3), 349-358.

54. Jung, S.; Lim, S.; Albertorio, F.; Kim, G.; Gurau, M.; Yang, R.; Holden, M.; Cremer, P., The vroman effect: A molecular level description of fibrinogen displacement. *J. Am. Chem. Soc.* **2003,** 125, (42), 12782-12786.

55. Karlsson, M.; Carlsson, U., Protein Adsorption Orientation in the Light of Fluorescent Probes: Mapping of the Interaction between Site-Directly Labeled Human Carbonic Anhydrase II and Silica Nanoparticles. *Biophys. J.* **2005,** 88, (5), 3536-3544.

56. Kidoaki, S.; Matsuda, T., Adhesion Forces of the Blood Plasma Proteins on Self-Assembled Monolayer Surfaces of Alkanethiolates with Different Functional Groups Measured by an Atomic Force Microscope. *Langmuir* **1999,** 15, (22), 7639-7646.

57. Kidoaki, S.; Matsuda, T., Mechanistic aspects of protein/material interactions probed by atomic force microscopy. *Colloids and Surfaces B: Biointerfaces* **2002,** 23, (2-3), 153-163.

58. Kokkoli, E.; Ochsenhirt, S.; Tirrell, M., Collective and single-molecule interactions of alpha5beta1 integrins. *Langmuir* **2004,** 20, 2397-2404.

59. Koopal, L.; Avena, M., A simple model for adsorption kinetics at charged solid-liquid interfaces. *Colloids and Surfaces A: Physicochemical and Engineering Aspects* **2001,** 192, (1-3), 93-107.

60. Krishnan, A.; Siedlecki, C.; Vogler, E., Traube-Rule Interpretation of Protein Adsorption at the Liquid-Vapor Interface. *Langmuir* **2003,** 19, (24), 10342-10352.

61. Kuznetsova, T.; Starodubtseva, M.; Yegorenkov, N.; Chizhik, S.; Zhdanov, R., Atomic force microscopy probing of cell elasticity. *Micron* **2007,** 38, (8), 824-833.

62. Lamba, N.; Woodhouse, K.; Cooper, S., *Polyurethanes in Biomedical Applications*. CRC Press: Boca Raton, 1998; p 5-23.

63. Lazzeri, L.; Cascone, M.; Narducci, P.; Vitiello, N.; D'Acunto, M.; Giusti, P., Atomic force microscopy wear characterization of biomedical polymer coatings. *Tribotest* **2006,** 12, (3), 257-265.

64. Lee, I.; Marchant, R. E., Molecular interaction studies of hemostasis: fibrinogen ligand-human platelet receptor interactions. *Ultramicroscopy*

Proceedings of the Fourth International Conference on Scanning Probe Microscopy, Sensors and Nanostructures **2003,** 97, (1-4), 341-352.

65. Lehenkari, P.; Horton, M., Single integrin molecule adhesion forces in intact cells measured by atomic force microscopy. *Biochemical and Biophysical Research Communications* **1999,** 259, (3), 645-650.

66. Li, L.; Hitchcock, A.; Robar, N.; Cornelius, R.; Brash, J.; Scholl, A.; Doran, A., X-ray Microscopy Studies of Protein Adsorption on a Phase-Segregated

Polystyrene/Polymethyl Methacrylate Surface. Concentration and Exposure-Time Dependence for Albumin Adsorption. . *J. Phys. Chem. B* **2006,** 110, (33), 16763-16773.

67. Lousinian, S.; Logothetidis, S., Optical properties of proteins and protein adsorption study. *Microelectronic Engineering* **2007,** 84, (3), 479-485.

68. Lysaght, M.; O'Loughlin, J., Demographic scope and economic magnitude of contemporary organ replacement therapies. *ASAIO Journal* **2000,** 46, (5), 515-521.

69. Magonov, S.; Reneker, D., Characterization of polymer surfaces with atomic force microscopy. *Annual Review of Materials Science* **1997,** 27, (1), 175-222.

70. Malmsten, M., Formation of adsorbed protein layers. *Journal of Colloid and Interface Science* **1998,** 207, (2), 186-199.

71. Marchant, R.; Kang, I.; Sit, P.; Zhou, Y.; Todd, B.; Eppell, S.; Lee, I., Molecular views and measurements of hemostatic processes using atomic force microscopy. *Curr Protein Pept Sci* **2002,** 3, (3), 249-74.

72. Mayo, K.; Fan, F.; Beavers, M.; Eckardt, A.; Keane, P.; Hoekstra, W.; Andrade-Gordon, P., Integrin receptor GPIIb/IIIa bound state conformation of the fibrinogen gamma-Chain C-Terminal Peptide 400-411: NMR and Transfer NOE Studies. *Biochemistry* **1996,** 35, (14), 4434-4444.

73. Michel, R.; Pasche, S.; Textor, M.; Castner, D., Influence of PEG architecture on protein adsorption and conformation. *Langmuir* **2005,** 21, (26), 12327-12332.

74. Modin, C.; Stranne, A.; Foss, M.; Duch, M.; Justesen, J.; Chevallier, J.; Andersen, L.; Hemmersam, A.; Pedersen, F.; Besenbacher, F., QCM-D studies of attachment and differential spreading of pre-osteoblastic cells on Ta and Cr surfaces. *Biomaterials* **2006,** 27, (8), 1346-1354.

75. Morin, C.; Hitchcock, A.; Cornelius, R.; Brash, J.; Urquhart, S.; Scholl, A.; Doran, A., Selective adsorption of protein on polymer surfaces studied by soft X-ray photoemission electron microscopy. *Journal of Electron Spectroscopy and Related Phenomena* **2004** 137, 785-794.

76. Muguruma, H.; Miura, S.; Murata, N., Adsorption of antibody protein onto plasma-polymerized film characterized by atomic force microscopy and quartz crystal microbalance. *IEICE Transactions on Electronics* **2007,** E90C, (3), 649-651.

77. Nagao, E.; Dvorak, J., Phase Imaging by Atomic Force Microscopy: Analysis of Living Homoiothermic Vertebrate Cells. *Biophys. J.* **1999,** 76, (6), 3289-3297.

78. Nakanishi, K.; Sakiyama, T.; Imamura, K., On the adsorption of proteins on solid surfaces, a common but very complicated phenomenon. *Journal of Bioscience and Bioengineering* **2001,** 91, (3), 233-244.

79. Neuman, K.; Block, S., Optical trapping. *Review of Scientific Instruments* **2004,** 75, (9), 2787-2809.

80. Nguyen, T.; Elimelech, M., Adsorption of Plasmid DNA to a Natural Organic Matter-Coated Silica Surface: Kinetics, Conformation, and Reversibility. *Langmuir* **2007,** 23, (6), 3273-3279.

81. Noble, J.; Knight, A.; Reason, A.; Di Matola, A.; Bailey, M.; 99-111., A comparison of protein quantitation assays for biopharmaceutical applications. *Molecular Biotechnology* **2007,** 32, (2), 99-111.

82. Noh, H.; Vogler, E., Volumetric interpretation of protein adsorption: Mass and energy balance for albumin adsorption to particulate adsorbents with incrementally increasing hydrophilicity. *Biomaterials* **2006,** 27, (34), 5801-5812.

83. Nonckreman, C.; Rouxhet, P.; Dupont-Gillain, C., Dual radiolabeling to study protein adsorption competition in relation with hemocompatibility. *Journal of Biomedical Materials Research Part A* **2007,** 81A, (4), 791-802.

84. Norde, W.; Haynes, C., Thermodynamics of Protein Adsorption. In Interfacial Phenomena and Bioproducts. In Brash, J. L., Ed. Marcel Dekker: 1996.

85. Osada, T.; Itoh, A.; Ikai, A., Mapping of the receptor-associated protein (RAP) binding proteins on living fibroblast cells using an atomic force microscope. *Ultramicroscopy* **2003,** 97, (1-4), 353-357.

86. Parida, S.; Dash, S.; Patel, S.; Mishra, B., Adsorption of organic molecules on silica surface. *Advances in Colloid and Interface Science* **2006,** 121, (1-3), 77-110.

87. Pesen, D.; Hoh, J., Micromechanical Architecture of the Endothelial Cell Cortex. *Biophys. J.* **2005,** 88, (1), 670-679.

88. Pitt, W.; Weaver, D.; Cooper, S., Fibronectin adsorption kinetics on phase segragated polyurethaneureas. *Journal of Biomaterials Science Polymer Edition* **1993,** 4, 337-346.

89. Plow, E.; Shattil, S., Integrin Alpha IIb beta 3 and Platelet Aggregation. In *Hemostasis and Thrombosis*, Colman, R.; Hirsh, J.; Marder, V.; Clowes, A.; George, J., Eds. Lippincott Williams and Wilkins: Philadelphia, 2001.

90. Poksinski, M.; Arwin, H., Total internal reflection ellipsometry: ultrahigh sensitivity for protein adsorption on metal surfaces. *Optics Letters* **2007** 32, (10), 1308-1310.

91. Portner, P.; Green, G.; Ramasamy, N., The Blood Interface at Artificial Surfaces within a Left Ventricular Assist System. *Annals New York Academy of Sciences* **1983**.

92. Radmacher, M., Measuring the elastic properties of biological samples with the AFM. *Engineering in Medicine and Biology Magazine, IEEE* **1997,** 16, (2), 47-57.

93. Ratner, B., The catastrophe revisited: Blood compatibility in the 21st Century. *Biomaterials* **2007,** 28, (34), 5144-5147.

94. Reviakine, I.; Brisson, A., Formation of supported phospholipid bilayers from unilamellar vesicles investigated by atomic force microscopy. *Langmuir* **2000,** 16, 1806-1815.

95. Roach, P.; Farrar, D.; Perry, C., Interpretation of protein adsorption: Surface-induced conformational changes. *J. Am. Chem. Soc.* **2005,** 127, (22), 8168-8173.

96. Sally, L., Applications of XPS in bioengineering. *Surface and Interface Analysis* **2006,** 38, (11), 1380-1385.

97. Sanders, A.; Jennissen, H., Monitoring fibrinogen adsorption kinetics by interfacial TIRF rheometry. *Journal of Molecular Recognition*

1996, 9, (5-6), 503-508.

98. Savage, B.; Ruggeri, Z., Selective recognition of adhesive sites in surface-bound fibrinogen by glycoprotein IIb-IIIa on nonactivated platelets. *J. Biol. Chem.* **1991,** 266, (17), 11227-11233.

99. Schmid, C.; Weyand, M.; Nabavi, D.; Hammel, D.; Deng, M.; Ringelstein, E.; Scheld, H., Cerebral and systemic embolization during left ventricular support with the novacor N100 device. The annals of thoracic surgery. *65* **1998,** 6, 1703-1710.

100. Schon, P.; Gorlich, M.; Coenen, M.; Heus, H.; Speller, S., Nonspecific protein adsorption at the single molecule level studied by atomic force microscopy. *Langmuir* **2007,** 23, 9921-9923.

101. Seitz, R.; Brings, R.; Geiger, R., Protein adsorption on solid-liquid interfaces monitored by laser-ellipsometry. *Applied Surface Science* **2005,** 252, (1), 154-157.

102. Sethuraman, A.; Han, M.; Kane, R.; Belfort, G., Effect of Surface Wettability on the Adhesion of Proteins. *Langmuir* **2004,** 20, (18), 7779-7788.

103. Shattil, S., Signaling through platelet integrin alpha IIb beta 3: inside-out, outside-in, and sideways. *Thromb Haemost.* **1999,** 82(2), (Aug), 318-25.

104. Shiba, E.; Lindon, J. N.; Kushner, L.; Matsueda, G. R.; Hawiger, J.; Kloczewiak, M.; Kudryk, B.; Salzman, E. W., Antibody-detectable changes in fibrinogen adsorption affecting platelet activation on polymer surfaces. *Am J Physiol Cell Physiol* **1991,** 260, (5), C965-974.

105. Siedlecki, C.; Eppell, S.; Marchant, R., Interactions of human von Willebrand Factor with a hydrophobic self-assembled monolayer studied by atomic force microscopy. *Journal of Biomedical Materials Research* **1994,** 28, (9), 971-980.

106. Siedlecki, C.; Lestini, B.; KottkeMarchant, K.; Eppell, S.; Wilson, D.; Marchant, R., Shear-dependent changes in the three-dimensional structure of human von Willebrand factor. *Blood* **1996,** 88, 2939-2950.

107. Sit, P.; Marchant, R., Surface-dependent conformations of human fibrinogen observed by atomic force microscopy under aqueous conditions. *Thromb Haemost* **1999,** 82, 1053–60.

108. Skarja, G.; Brash, J., Physicochemical properties and platelet interactions of segmented polyurethanes containing sulfonate groups in the hard segment. *Journal of Biomedical Materials Research* **1997,** 34, 439-455.

109. Slack, S.; Horbett, T., Changes in fibrinogen adsorbed to segmented polyurethanes and hydroxyethylmethacrylate-ethylmethacrylate copolymers. *Journal of Biomedical Materials Research* **1992,** 26, (12), 1633-1649.

110. Soman, P.; Rice, Z.; Siedlecki, C., Measuring the Time-Dependent Functional Activity of Adsorbed Fibrinogen by Atomic Force Microscopy. *Langmuir* **2008,** 24, (16), 8801-8806.

111. Steiner, G.; Tunc, S.; Maitz, M.; Salzer, R., Conformational Changes during Protein Adsorption. FT-IR Spectroscopic Imaging of Adsorbed Fibrinogen Layers. *Anal. Chem.* **2007,** 79, (4), 1311-1316.

112. Stiles, P.; Dieringer, J.; Shah, N.; Duyne , R., Surface-Enhanced Raman Spectroscopy. *Ann. Rev. Anal. Chem* **2008,** 1, 601-626.

113. Tassel, P., Protein Adsorption Kinetics: Influence of Substrate Electric Potential In Proteins at Solid-Liquid Interfaces. In *Proteins at Solid-Liquid Interfaces*, Déjardin, P., Ed. Springer: Berlin Heidelberg, 2006.

114. Toscano, A.; Santore, M., Fibrinogen adsorption on three silica-based surfaces: conformation and kinetics. *Langmuir* **2006,** 22, (6), 2588-2597.

115. Touhami, A.; Nysten, B.; Dufrene, Y., Nanoscale mapping of the elasticity of microbial cells by atomic force microscopy. *Langmuir* **2003,** 19, (11), 4539-4543.

116. Truong, C.; Sykes, M.; McDermott, M., Real-time observation of plasma protein film formation on well-defined surfaces with scanning force microscopy. *Langmuir* **1998,** 14, 2435-2443.

117. Tunc, S.; Maitz, M.; Steiner, G.; Vazquez, L.; Pham, M.; Salzer, R., In situ conformational analysis of fibrinogen adsorbed on Si surfaces. *Colloids and Surfaces B: Biointerfaces* **2005,** 42, (3-4), 219-225.

118. Vanlandingham, M.; McKnight, S.; Palmese, G.; Elings, J.; Huang, X.; Bogetti, T.; Eduljee, R. J., Nanoscale Indentation of Polymer Systems Using the Atomic Force Microscope. *The Journal of Adhesion* **1997,** 64, (1 - 4 August), 31 - 59.

119. Verheugt, F., How can the bleeding risk associated with warfarin therapy be reduced? *Nat Clin Pract Cardiovasc Med* **2008,** 5, (1), 14-15.

120. Vogler, E., Structure and reactivity of water at biomaterial surfaces. *Advances in Colloid and Interface Science* **1998,** 74, (1 February), 69-117.

121. Vogler, E.; Martin, D.; Montgomery, D.; Graper, J.; Sugg, H., A graphical method for predicting surfactant and protein adsorption properties. *Langmuir* **1993,** 9, 497-507.

122. Wagner, M.; Horbett, T.; Castner, D., Characterizing Multicomponent Adsorbed Protein Films using Electron Spectroscopy for Chemical Analysis, Time-Of-Flight Secondary Ion Mass Spectrometry, and Radiolabeling: Capabilities and Limitations. *Biomaterials* **2003,** 24, (11), 1897-1908.

123. Wagner, M.; McArthur, S.; Shen, M.; Horbett, T.; Castner, D., Limits of detection for time of flight secondary ion mass spectrometry (ToF-SIMS) and X-ray photoelectron spectroscopy (XPS): detection of low amounts of adsorbed protein. *Journal of Biomaterials Science Polymer Edition, Polymer Edition* **2002,** 13, (4), 407-428.

124. Wang, J.; Chen, X.; Clarke, M.; Chen, Z., Vibrational spectroscopic studies on fibrinogen adsorption at polystyrene/protein solution interfaces: Hydrophobic side chain and secondary structure changes. *J. Phys. Chem. B* **2006,** 110, (10), 5017-5024.

125. Weisel, J.; Phillips, G.; Cohen, C., A model from electron microscopy for the molecular structure of fibrinogen and fibrin. *Nature* **1981,** 289, (5795), 263-267.

126. Weiss, W., Technical Proposal: Pediatric Circulatory Support. In BAA NHLBI-HV-04-01: The Pennsylvania State University, 2004.

127. Welle, A., Competitive plasma protein adsorption on modified polymer surfaces monitored by quartz crystal microbalance technique. *Journal of Biomaterials Science-Polymer Edition* **2004,** 15, (3), 357-370.

128. Welzel, P., Investigation of adsorption-induced structural changes of proteins at solid/liquid interfaces by differential scanning calorimetry. *Thermochimica Acta* **2002,** 382, (1-2), 175-188.

129. Xu, H.; Bjerneld, E.; Käll, M.; Börjesson, L., Spectroscopy of Single Hemoglobin Molecules by Surface Enhanced Raman Scattering. *Physical Review Letters* **1999,** 83, (21), 43-57.

130. Xu, L.-C.; Siedlecki, C., Effects of surface wettability and contact time on protein adhesion to biomaterial surfaces. *Biomaterials* **2007,** 28, (22), 3273-3283.

131. Xu, L.; Siediecki, C., Surface Wettability, Loading Force, Loading Rate, and Contact Time Effects on Fibrinogen Adhesion on Surface Studied by Colliod AFM. **Under Review**.

132. Yamanaka, H.; Rosenberg, G.; Weiss, W.; Snyder, A.; Zapanta, C.; Siedlecki, C., Multiscale Analysis of Surface Thrombosis In Vivo in a Left Ventricular Assist System. *ASAIO journal* **2005,** 51, (5), 567-77.

133. Yamanaka, H.; Rosenberg, G.; Weiss, W.; Snyder, A.; Zapanta, C.; Siedlecki, C., Short-term In Vivo Studies of Surface Thrombosis in a Left Ventricular Assist System. *ASAIO Journal* **2006,** 52, (3), 257-265.

134. Yokoyama, Y.; Ishiguro, R.; Maeda, H.; Mukaiyama, M.; Kameyama, K.; Hiramatsu, K., Quantitative analysis of protein adsorption on a planar surface by Fourier transform infrared spectroscopy: lysozyme adsorbed on hydrophobic silicon-containing polymer. *Journal of Colloid and Interface Science* **2003,** 268, (1), 23-32.

135. Grunkemeier, J. M., W. B. Tsai, C. D. McFarland and T. A. Horbett (2000). "The effect of adsorbed fibrinogen, fibronectin, von Willebrand factor and vitronectin on the procoagulant state of adherent platelets." Biomaterials **21**(22): 2243-2252.

136. Lee JH, Li Tonglei and Park, K. Solvation interactions for protein adsorption to biomaterial surfaces. In *Water in Biomaterials Surface Science*, M Morra, John Wiley & Sons, Ltd. Chichester, New York, 2001.

137. Vogler, E., J. Graper, H. Sugg, L. Lander and W. Brittain (1995). "Contact activation of the plasma coagulation cascade. II. Protein adsorption to procoagulant surfaces." Journal of Biomedical Materials Research **29**(8): 1017-1028.

138. Vogler, EA. How water wets biomaterial surfaces. In *Water in Biomaterials Surface Science*, M Morra, John Wiley & Sons, Ltd. Chichester, New York, 2001.

Chapter 2

Immunological Identification of Fibrinogen in Dual-Component Protein Films by AFM Imaging

Abstract

The success of long-term blood-contacting implanted devices is largely dependent upon the interaction of the blood components with the device biomaterial surface. The ability to study these interactions has been hindered by a lack of methods to measure single-molecule interactions in complex multi-protein environments similar to the environment found in-vivo. In this chapter, we demonstrate the use of atomic force microscopy (AFM) in conjunction with gold nanolabels to detect the protein fibrinogen under aqueous conditions without the topographical clues usually necessary for high resolution visualization. BSA was patterned onto both muscovite mica and plasma-treated polydimethylsiloxane (PDMS) substrates and these test substrates were subsequently backfilled with fibrinogen to yield a featureless protein layer. The fibrinogen in this dual protein layer was detected using high resolution AFM imaging following infusion of anti-fibrinogen conjugated with nanogold particles. This AFM immuno-detection technique will potentially be applicable to complex multi-component protein films adsorbed on clinically-relevant polymers used in medical devices.

2.1 Introduction

The adsorption of plasma proteins is one of the first events to occur following blood biomaterial contact and this adsorbed protein influences subsequent biological events including platelet adhesion and thrombogenesis on the biomaterial surface (Gorbet and Sefton 2004). Protein adsorption in complex and competitive environments have been studied by a variety of techniques. Although these techniques have provided a wealth of macroscopic and microscopic information describing adsorption behaviors of fibrinogen and other proteins, the nature of protein surface activity is still not completely understood. The advent of atomic force microscopy (AFM) has provided a new tool for the study of individual plasma proteins at molecular scale with ultrahigh resolution and under physiologically relevant aqueous conditions (Binnig, et al. 1986, Marchant, et al. 2002).

AFM has been used extensively to obtain nanometer scale images of biosystems including proteins, lipid membranes, DNA and cells, generally utilizing ultrasmooth model surfaces such as muscovite mica, highly oriented pyrolytic graphite or self assembled monolayers (Argaman, et al. 1997, Radmacher 1997, Reviakine and Brisson 2000, Reviakine, et al. 2000, Marchant, Kang, Sit, Zhou, Todd, Eppell and Lee 2002, Osada, et al. 2003, Touhami, et al. 2003, Hussain, et al. 2005, Toscano and Santore 2006). The low surface roughness of these model surfaces is ideal to characterize nanoscale protein features, including specific domains and conformational changes in these proteins upon adsorption. However AFM experiments are still somewhat limited in

scope, particularly in complicated multi-protein adsorption experiments, because the proteins can be difficult to distinguish based on topography alone (Truong, et al. 1998). Perhaps more importantly, clinically used biomaterials have rough topographies that often dwarf the dimensions of the proteins of interest making detection of specific proteins on these surfaces even more difficult. Holland and Marchant successfully used phase imaging for detecting fibrinogen on two clinically relevant biomaterials: poly(dimethylsiloxane) (PDMS) and low density polyethylene (LDPE) (Holland and Marchant 2000). While fibrinogen could occasionally be observed in the phase images when present at submonolayer concentrations, the surface often proved too rough to clearly distinguish the adsorbed protein. Figure 2-1 illustrates an example of fibrinogen adsorbed onto a commonly used biomedical polymer, poly(urethane urea) and imaged by tapping mode AFM. Neither height nor phase images reveal any details sufficient to identify protein on this material. There remains a need to develop new techniques that do not rely heavily on topography to recognize specific proteins.

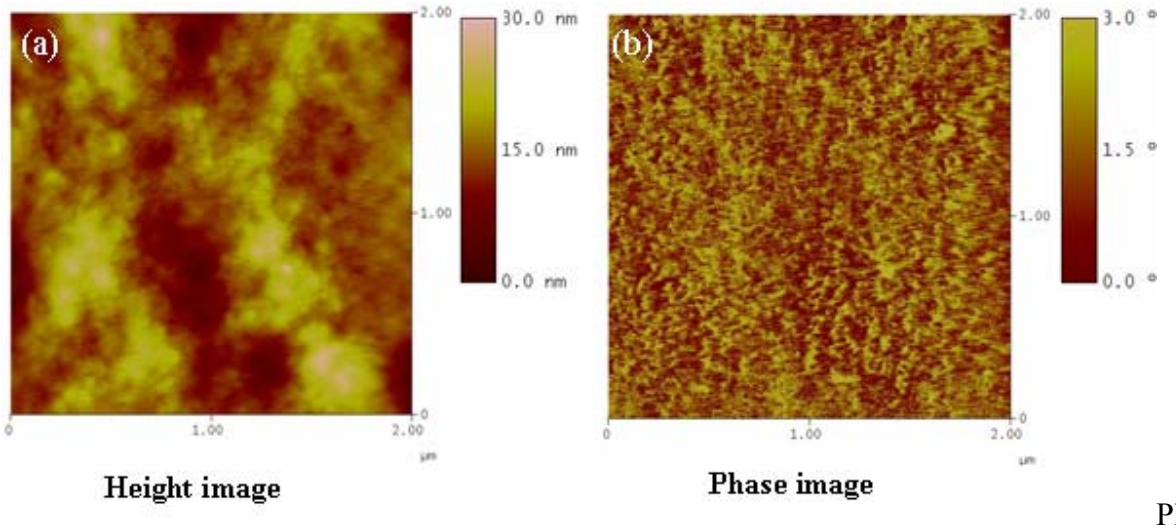

Place Figure Here

Figure **2-1**: AFM images of poly (urethane urea) (PUU)sample after incubation of phosphate buffer for 1 hour and fibrinogen (500 µg/ml) for 15 minutes: Height (a) and phase (b) images do not identify fibrinogen due to the inherent roughness of the biomaterial polymer surface.

Alternative non-conventional AFM techniques have been developed for detection of specific proteins without dependence on topography. The force spectroscopy techniques of AFM utilize molecular recognition events to detect artificially patterned areas, red blood cells and antibody-antigen interactions (Hinterdorfer, et al. 1996, Radmacher 1997). Our group has previously used an AFM probe modified with polyclonal antibodies to detect fibrinogen in a dual-protein environment. The dual protein layer containing bovine serum albumin (BSA) and fibrinogen dual protein layer was formed using microcontact printing techniques and adhesion mode AFM was used to detect the fibrinogen using the antibody-modified probe (Agnihotri and Siedlecki 2005). A limitation of this method was the amount of time required for generation of an adhesion map (~60 minutes). This limitation is particularly important when studying the post adsorptive transitions in the fibrinogen structure on different substrates (Balasubramanian, et al. 1999, Agnihotri and Siedlecki 2004). Moreover, this technique yields relatively low resolution images when used with standard AFM equipment and relies on complex statistical analysis to generate maps of protein distribution. Nanogold particles, commonly used in electron microscopy, (Hainfeld and Powell 1997, Yang, et al. 2000, Montesano-Roditis, et al. 2001) have been used in conjunction with AFM. Mikoshiba used 10 nm gold particles to visualize the inositol 1,4,5-trisphosphate receptor using AFM and Transmission Electron Microscopy (TEM) (Wakako, et al. 2006). Hussain and Siedlecki used nanogold particles to directly visualize individual ligand-receptor interactions in physiologically relevant environment (Hussain, Agnihotri and Siedlecki 2005), where the nanogold labels were conjugated to an RGD peptide and the presence of a peptide ligand bound to integrin receptors could be detected by the

differences in the mechanical properties measured by AFM phase imaging. Similar gold bead labeling techniques were used by Putnam et al. to label cells (Putnam, et al. 1993) and Eppell et al. (Eppell, et al. 1995) to perform correlative microscopy studies on platelets. These types of labels were used for protein analysis by Lin et al. to map the heparin binding site on fibronectin (Lin, et al. 2000) and by Raghavachari and Marchant to examine the exposure of functional domains in von Willebrand Factor following conformational changes induced by fluid shear (Raghavachari, et al. 2000). However, in each of these protein labeling studies, the protein was adsorbed in submonolayer amounts to visualize the binding events.

In this work we describe a novel application of nanogold labels conjugated to antibodies against human fibrinogen to determine the distribution of fibrinogen molecules in a dual protein layer that fully covers the surface. This study was carried out initially on the model substrate mica and then extended to a model polymer substrate, glow discharge plasma-treated poly (dimethylsiloxane) (PDMS). Furthermore, this technique can potentially be extended for detection of proteins on complex polymers used in biomedical applications.

2.2 Materials and Methods

2.2.1 General

Phosphate buffered saline (PBS, 0.01 M sodium phosphate buffer, 150mM NaCl, pH 7.4, Sigma Inc.) was prepared using filtered water from a Millipore Simplicity 185 system which utilizes two ultraviolet filters (185 and 254 nm) to reduce carbon contaminants. Human fibrinogen (90% clottable) and polyclonal rabbit anti-human fibrinogen (90% IgG) were used as received from Calbiochem, La Jolla, CA. Anti-fibrinogen antibody was dissolved in phosphate buffer to yield a concentration of 1mg/ml and aliquots were stored at -20°C until use. Bovine serum albumin (BSA) was obtained from Sigma Chemicals Co, St. Louis, MO.

2.2.2 Preparation of Nanogold conjugates

Sulfo-N-hydroxy-Succinimido Nanogold (Nanoprobes Inc., Yaphank, NY) are functionalized gold particles 1.4 nm in diameter. These functionalized particles have reactivity to primary amines and can be covalently linked to any protein. The Nanogold reagent was dissolved in 200 µl of deionized water. Polyclonal rabbit anti-human fibrinogen was conjugated to Nanogold using the protocol for labeling proteins with molecular weight greater than 15,000 Da specified by the company. The anti-fibrinogen solution (1mg/ml) was reacted with the activated Nanogold solution at pH 7.4 for 1 hour at room temperature while rotating on a hematology mixer to ensure optimal conjugation.

The reaction mixture was concentrated to a volume of 10µl using a centricon centrifugal filter (Millipore Inc.) with a 30,000 molecular weight cut-off. The retinate was brought to a volume of 100µl before purification by High Performance Liquid Chromatography (HPLC, Superose 200 column, Beckman Coulter Inc., Fullerton, CA). Conjugated nanogold was collected and stored at 4°C until use.

2.2.3 Dual protein layer formation using micro-contact printing

Proteins were patterned on mica and PDMS substrates using microcontact printing as described previously (Agnihotri and Siedlecki 2005). Briefly, a 15 mm diameter poly(dimethylsiloxane) (PDMS, Sylgard 184, Dow Corning) rubber stamp having ~700 nm diameter holes was prepared by replication molding of a photoresist pattern prepared using optical lithography techniques (Milner, et al. 2006). The PDMS stamp was incubated in 1 or 5mg/ml bovine serum albumin (BSA) for 1 hour; the stamp was then rinsed in PBS for 5 minutes and dried with nitrogen. Freshly cleaved, hydrophilic, muscovite mica (Ted Pella Inc., CA) or glow discharged plasma-cleaned PDMS was used as the substrate for stamping experiments. The PDMS substrate was rendered hydrophilic (water contact angle ~ 15°) by glow-discharge plasma cleaning in an ambient environment for 45 minutes at 100 W power. The protocol for sample preparation and labeling is shown schematically in Figure 2-2. A BSA-inked PDMS stamp was placed onto the mica or PDMS substrates under a 5 mg weight for 30 seconds to ensure proper stamping of proteins onto the substrate. The stamp was carefully peeled off and the

substrate surface was immediately imaged using tapping mode AFM under PBS. The sample was transferred to an external fluid cell similar in design and dimension to the AFM fluid cell used for imaging. Human fibrinogen solution (1mg/ml) was delivered through the fluid cell at a rate of 1 ml/hour for 1 hour to allow fibrinogen to adsorb in the protein-free holes created by printing. After the sample was rinsed with buffer solution in the external fluid cell for 5 minutes, Nanogold conjugated anti-fibrinogen (1:5 dilution) was delivered to the fluid cell at a rate of 1 ml/hr for 1 hour. The sample was again rinsed with PBS before being moved to the AFM imaging stage for analysis.

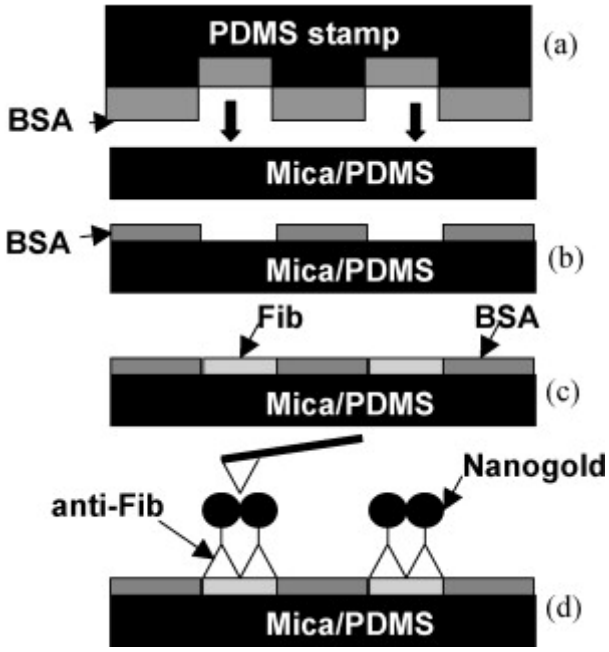

Figure **2-2**: Schematic representation showing the procedure for preparation of patterned samples and application of the nanogold conjugate. A microtextured PDMS stamp is inked with BSA and placed into contact with mica or glow-discharge plasma-cleaned PDMS substrates (a) yielding a BSA pattern (b). Fibrinogen is added to produce a topographically uniform dual protein layer of BSA and human fibrinogen (c), which is then labeled by a gold-conjugated antibody and imaged by tapping mode AFM (d).

2.2.4 AFM imaging

All images were acquired in tapping mode (intermittent contact mode) with a Nanoscope IIIa Multimode® AFM (Digital Instruments, CA) under both ambient and aqueous PBS buffer using short thick cantilever silicon nitride probes (NP – S; spring constant ~ 0.6 N/m^2, Digital Instruments, CA). Topographic images and phase images were captured at 512 x 512 pixels resolution with scan size of 5 x 5 μm^2. All imaging was carried out at a scan rate of 1 Hz with a resonant frequency of ~8 kHz. The tapping force can be controlled the r_{sp} value, which is the ratio of set-point amplitude to free amplitude of oscillation. The AFM probe free amplitude of oscillation and r_{sp} values were fixed at 20 nm and 0.75, respectively, for all images. AFM images were flattened using a first order line fit and low pass filtered to remove high frequency noise spikes from the images. Quantitative analysis of the dual protein layer thickness was made using the cross-section tool provided with the instrument software.

2.3 Results and Discussion

2.3.1 Dual protein layer formation on mica

Mica is frequently used as a substrate for high resolution AFM imaging because it is quite simple to produce clean, hydrophilic ultrasmooth surfaces by simply cleaving with adhesive tape. Figure 2-3 shows height and phase images of BSA micro-contact printed onto a freshly cleaved muscovite mica substrate and imaged under both ambient conditions and aqueous buffer conditions by tapping mode AFM. The dark regions are

mica substrate with diameter of ~800 nm, surrounded by BSA protein layer. Section analysis (not shown) calculates the height of the BSA pattern to be ~2.5 nm, approximately equal to a BSA monolayer(Green, et al. 1997b). The pattern can also be observed in the phase image which detects the mechanical property differences between the protein and the substrate.

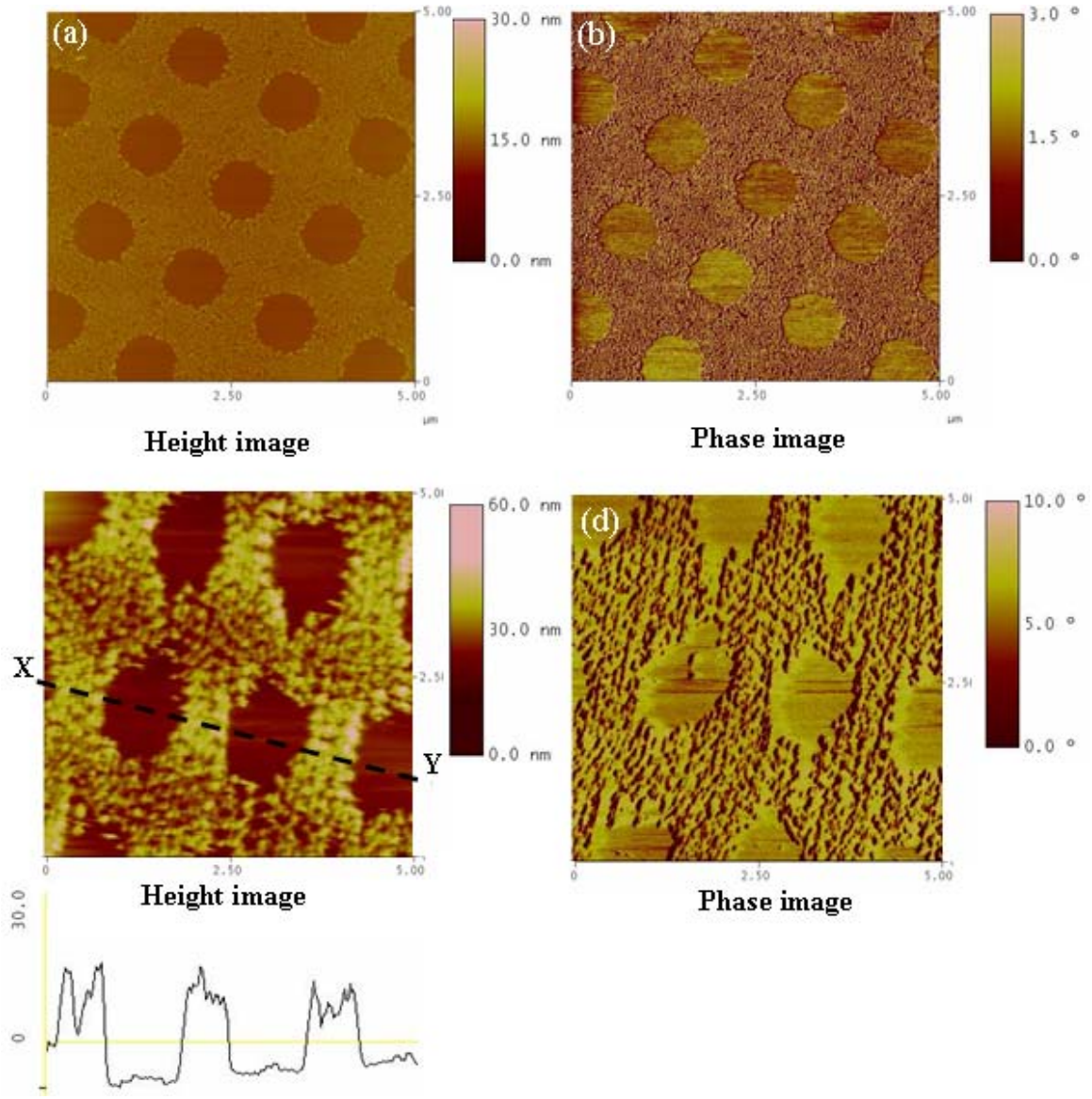

Figure **2-3**: AFM tapping mode images of a BSA pattern micro-contact printed onto mica: Height (a) and phase (b) images of a monolayer of BSA under ambient conditions. The circular holes seen in the images in ambient condition have a diameter of ~800 nm with the height of the protein layer ~2.5 nm; height (c) and phase (d) images of multilayer of stamped BSA in phosphate buffer saline. The BSA pattern is clearly visible. Enlargement of the pattern (diameter ~ 1100 nm) is from AFM imaging drift common in buffer conditions; section analysis (e) shows the height of the BSA multilayer to be ~12.5nm.

Given the large differences in size of BSA (4 nm x 8 nm) and fibrinogen (8 nm x 45 nm) (Green, et al. 1997a), there is only one scenario in which a uniform 2 - protein layer can be created using a monolayer of BSA and fibrinogen. After backfilling the BSA pattern with fibrinogen, if all BSA molecules are adsorbed in an end-on configuration and all fibrinogen molecules are adsorbed in a side-on configuration, it would produce an 8 nm thick uniform film.

Considering the difficulties in achieving a completely uniform dual protein layer when the proteins are segregated as they are here, the PDMS stamp was incubated with higher BSA concentration (5mg/ml) to create a multi-layer of BSA onto mica. When imaged in buffer, the holes in the patterned surface appear slightly enlarged which can be attributed to small AFM scanner drift which is common in AFM experiments in aqueous conditions(Agnihotri and Siedlecki 2005). Both the height and phase images illustrate that there is no protein in the patterned holes. Section analysis revealed that the BSA height was ~12.5 nm, which is approximately 5 times the height of a single monolayer of BSA (2.5 nm on mica surface).

2.3.2 Fibrinogen adsorption and identification

The sample was placed in an external fluid cell and fibrinogen was adsorbed onto the stamped BSA layer to form a uniform protein layer. We investigated various concentrations of fibrinogen (250 μg/ml, 500 μg/ml and 1 mg/ml) and adsorption times

(30 minutes and 1 hour) to determine parameters for reproducibly creating a smooth protein layer in which the protein patterns are not visible. This is critically important because the objective of the technique is to detect proteins without having topographical clues about the distribution of the different protein types. Figure 2-4 shows representative height and phase images obtained under aqueous buffer following fibrinogen adsorption for 1 hour from a 1mg/ml solution. We found this time and concentration combination suitable for reproducibly generating smooth protein layers and this protocol was used in all subsequent images. The distribution of the two protein types are not distinguishable in either the height or the phase image thereby demonstrating the formation of a uniform layer with fibrinogen presumably located within the holes produced by micro-contact printing and the BSA surrounding these fibrinogen regions. This situation can be considered analogous to imaging of proteins on polymer biomaterial samples where individual proteins cannot be identified due to the density of the adsorbed proteins and the inherent roughness of the underlying substrate.

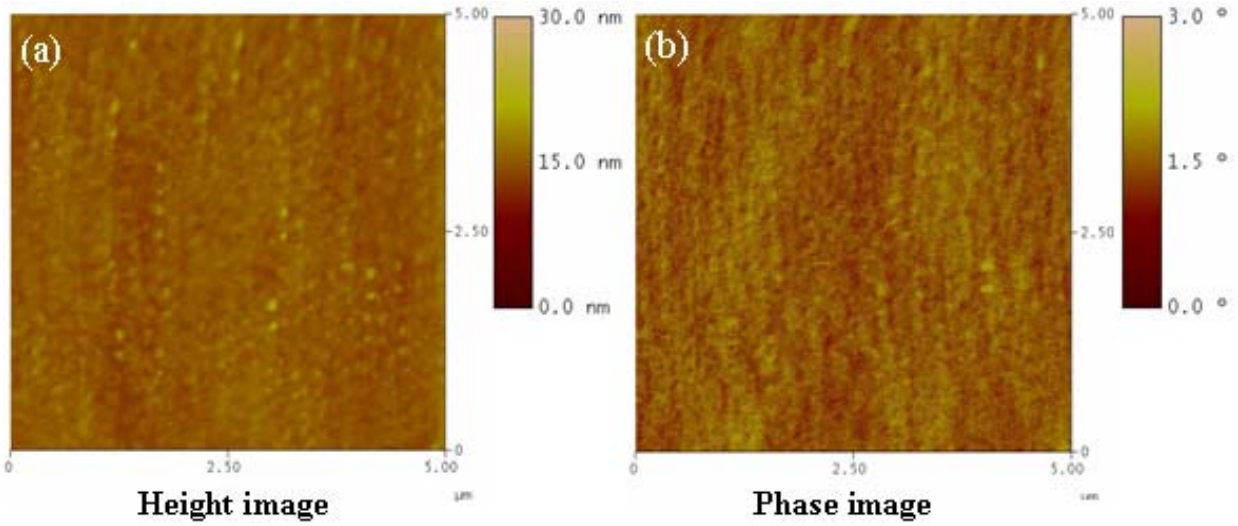

Figure **2-4**: AFM tapping mode images of BSA-patterned mica substrate after human fibrinogen adsorption (1 mg/ml delivered though the fluid cell at the rate of 1 ml/hr for 1 hour): Height (a) and phase (b) images show that the micro-contact printed pattern is not visible after backfilling of the holes with fibrinogen, demonstrating the formation of a uniform layer of the two proteins.

2.3.3 Nanogold labeling of fibrinogen

The Nanogold conjugate is functionalized with sulfo-N-hydroxysuccinimide ester having reactivity towards primary amines and therefore it can be covalently coupled to the antibodies against human fibrinogen by a simple protocol. In this study, we utilize the mechanical properties of the gold label to visualize binding of the antibody to the protein antigen of interest directly by AFM tapping mode phase imaging. The patterned protein substrates were washed thoroughly prior to addition of the nanogold conjugate to ensure that there is no free fibrinogen in solution that might react with the antibody and subsequently undergo nonspecific adsorption to the surface. Height and phase images

shown in Figure 2-5 illustrate that the protein patterns are visualized by tapping mode AFM after addition of conjugate. The nanogold-conjugated antibody binds to the surface-adsorbed fibrinogen and is identified from the phase angle shift induced by the presence of the hard nanogold particles. The data shows that the region containing fibrinogen and conjugated nanogold seems to present a lower phase angle than the BSA coated region. Generally, regions of increased hardness or modulus appear as bright spots in the phase image. However, it has been shown that phase images can be sensitive to the operating parameters including r_{sp} and the free amplitude of oscillation, particularly in a heterogeneous system having different compliances (Bar, et al. 1997). Phase images can even undergo contrast reversals as imaging parameters are changed, making it difficult to assign features in height and phase images to different components based on the direction of phase shift alone (Pickering and Vancso 1998).

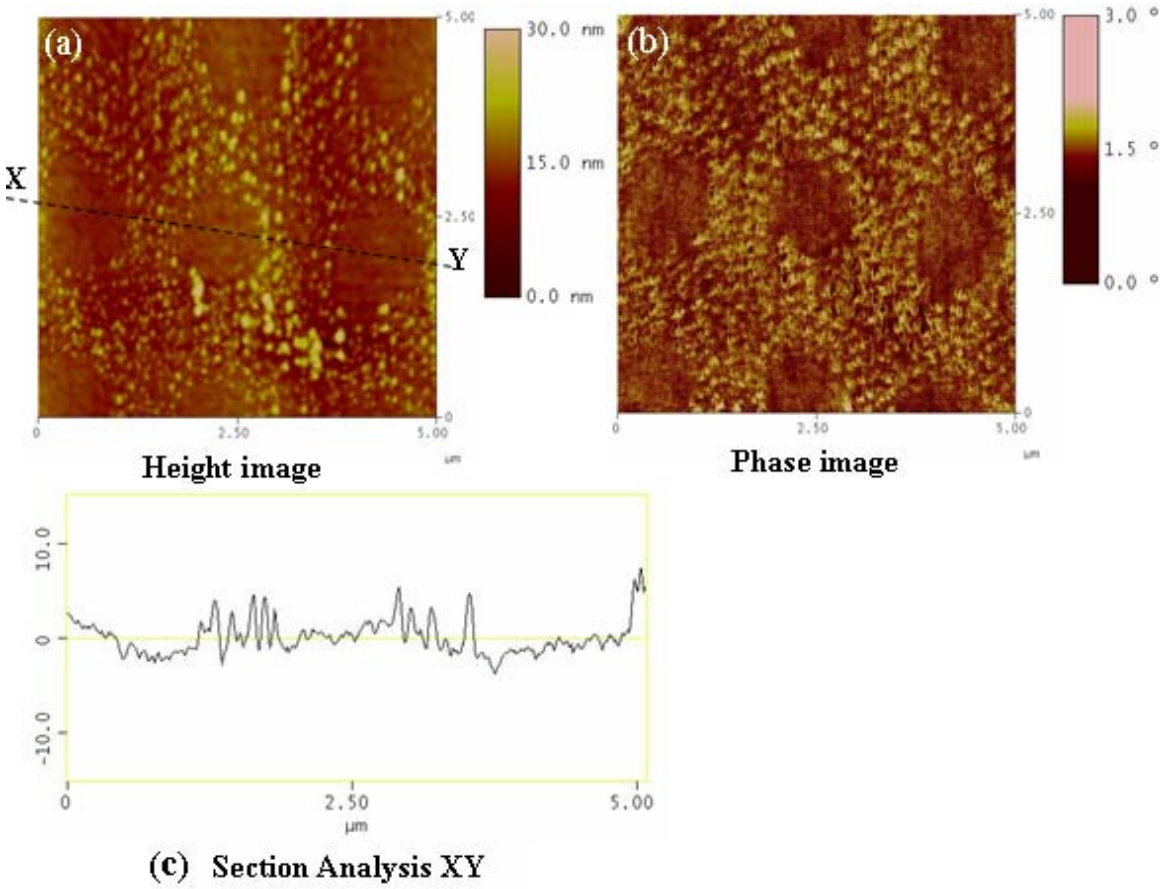

Figure **2-5**: Tapping mode images of patterned dual protein layer following Nanogold-antibody incubation (delivered to the fluid cell at a rate of 1ml/hr for 1hour): Height image (a) and phase image (b). The dark regions indicate the location of the conjugated Nanogold binding to fibrinogen while the bright regions indicate lack of binding to BSA.

Section analysis performed on the topography image (Fig. 5c) showed a small decrease in the apparent height following conjugate binding although the roughness of the sample makes it difficult to measure the exact height difference. As the nanogold conjugates should only interact with fibrinogen on the sample, an increase in height in the fibrinogen regions on the sample is expected, which is contrary to what we observed. However, we have previously observed a "shadowing effect" in height images, it is simply an image artifact that arises from differences in the interactions of the AFM tip with the underlying

substrate that changes the apparent height of the sample (see for example fig. 5 in (Agnihotri, et al. 2006)).

To confirm that this apparent loss of height in the fibrinogen regions was not a result of desorption of the fibrinogen during labeling, a dual protein layer was again prepared, washed with protein-free PBS for 1 hour at 1ml/hour flow rate and imaged by tapping mode AFM. Height and phase images from these experiments are shown in Figure 2-6 . No patterns were observed in either the height or phase images, demonstrating that there is no detectable desorption of fibrinogen from the sample surface. A second concern was that the anti-fibrinogen antibody was binding to the fibrinogen in the patterned regions and was somehow in itself responsible for the height and phase contrast. This would be expected to yield an increased height image, but nonetheless we tested the effects of adding unconjugated anti-fibrinogen antibodies to the images. Tapping mode imaging did not show evidence of the patterns thereby demonstrating that the contrast seen in figure 2-5 arises from the conjugated anti-fibrinogen and is not an artifact of the labeling procedures.

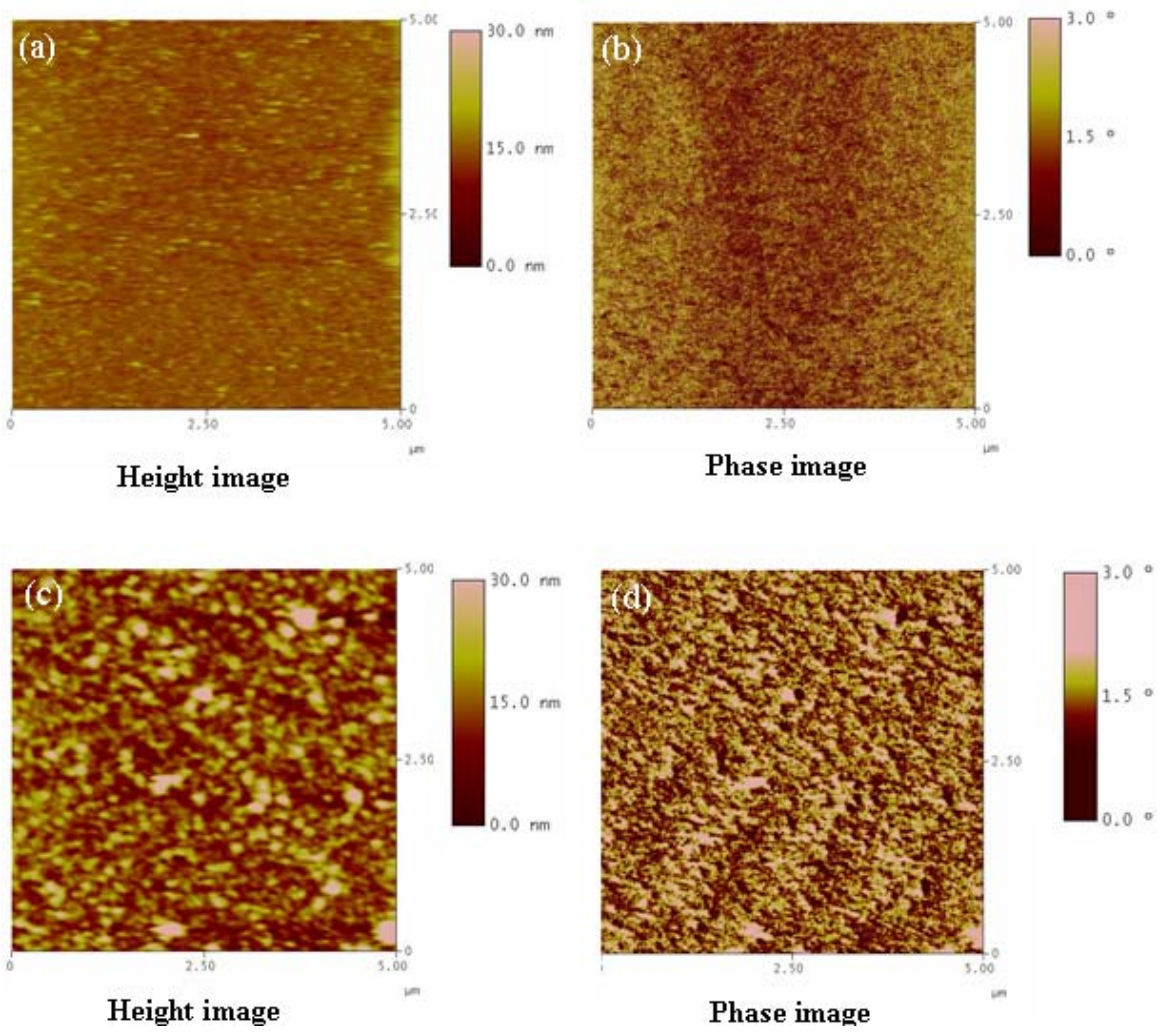

Figure **2-6**: AFM images of control experiments: Height (a) and phase (b) images after washing of the patterned dual protein layer with PBS buffer for 1 hour. Height (c) and phase images (d) of the patterned dual protein layer following labeling with unconjugated anti-fibrinogen. Tapping mode imaging reveals that the pattern was not detected in these experiments, demonstrating that the phase differences seen previously arise from binding of the nanogold-antibody conjugates.

Finally, control experiments were carried out to verify that there is no desorption or migration of BSA onto the regions where fibrinogen is expected to adsorb. A multilayer of BSA was stamped on mica and was monitored for 3 hours in a hydrated fluid cell. Figure 2-7 shows tapping mode images taken every hour and clearly shows an absence of marked migration of the BSA off the protein layer into the holes, thereby demonstrating the stability of the BSA multilayer on mica substrate.

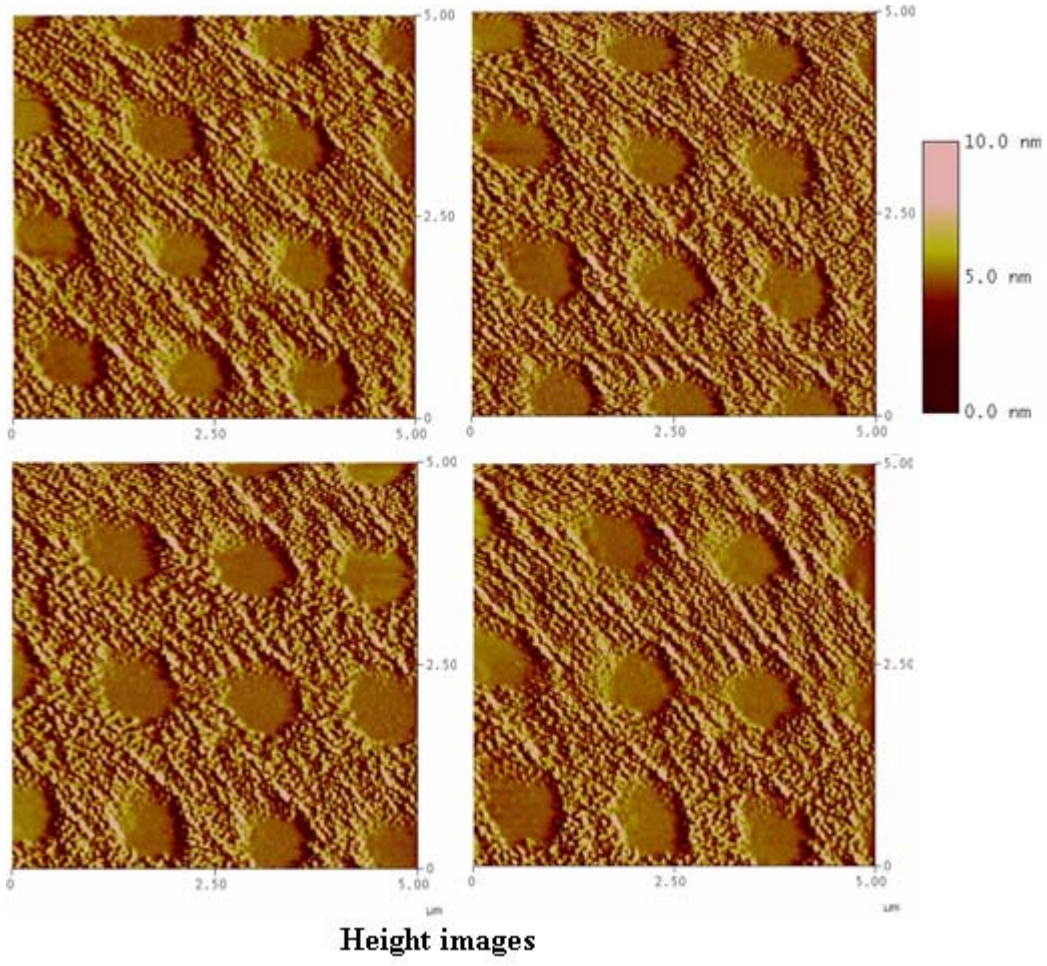

Figure **2-7**: Sequential AFM tapping mode images of stamped multilayer of BSA on a mica substrate under PBS: Immediately after stamping on mica substrate (a) and after 1 hour (b), 2 hours (c) and 3 hours (d) of hydration. Images show that there is no migration of BSA from the patterns.

2.3.4 Nanogold labeling of protein patterns on PDMS

The efficacy of the nanogold technique was tested on a clinically relevant polymer, PDMS. PDMS is a relatively smooth homopolymer generally lacking any significant topographical features which might cause difficulty in producing/imaging of protein patterns. Moreover, glow discharge plasma cleaning can change the PDMS surface from hydrophobic to hydrophilic, which has been shown to be essential for proper stamping of proteins (Thibault, et al. 2005). The PDMS stamp was incubated with 0.1 and 1mg/ml of BSA for 1 hour (similar conditions for data shown in figs. 2.3a and 2.3b) and then stamped onto hydrophilic PDMS substrate. Tapping mode images in ambient conditions were not able to detect any pattern, most likely due to the inherent roughness of the polymer surfaces. Only upon increasing the concentration to 5mg/ml could a pattern could be detected, as shown in Figure 2-8 . The dark regions are bare PDMS surface while the protein surrounding the regions is BSA. Fibrinogen was backfilled (1 mg/ml for 1 hour) to form a dual protein layer on PDMS. Figure 2-10 a and b shows a distinct decrease in both the height and the phase signal between the BSA pattern and adsorbing fibrinogen after delivering fibrinogen (1mg/ml) for 0.5 hour. After 1hour incubation of fibrinogen, the two proteins were indistinguishable from one another in the phase image thereby forming a uniform protein layer on PDMS substrate (Figs. 2-9c and 2-9d). The binary protein layer was incubated with conjugated nanogold solution similar to mica substrate described earlier. The antibody against fibrinogen binds to the fibrinogen in the circular pattern and is again identified using the phase lag produced by the hard gold labels with respect the surrounding protein. The dark holes represent fibrinogen adsorbed

on the PDMS substrate whereas the brighter regions represent the patterned BSA protein layer.

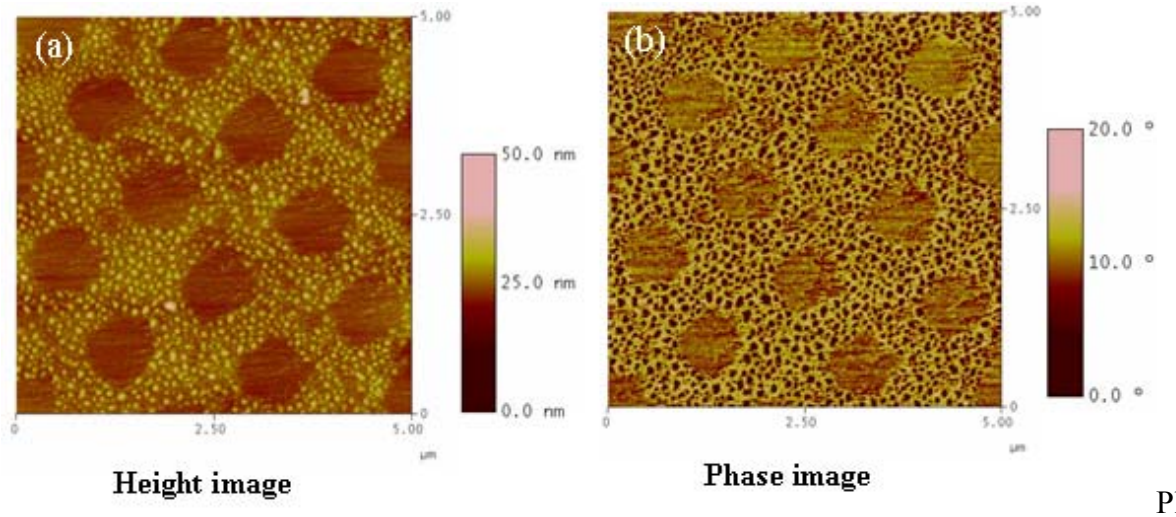

Place

Figure **2-8**: Tapping mode AFM images: BSA pattern stamped onto PDMS substrate imaged by height (a) and phase (b). The circular patterns (diameter ~800 nm) are PDMS substrate and the protein surrounding the holes is BSA.

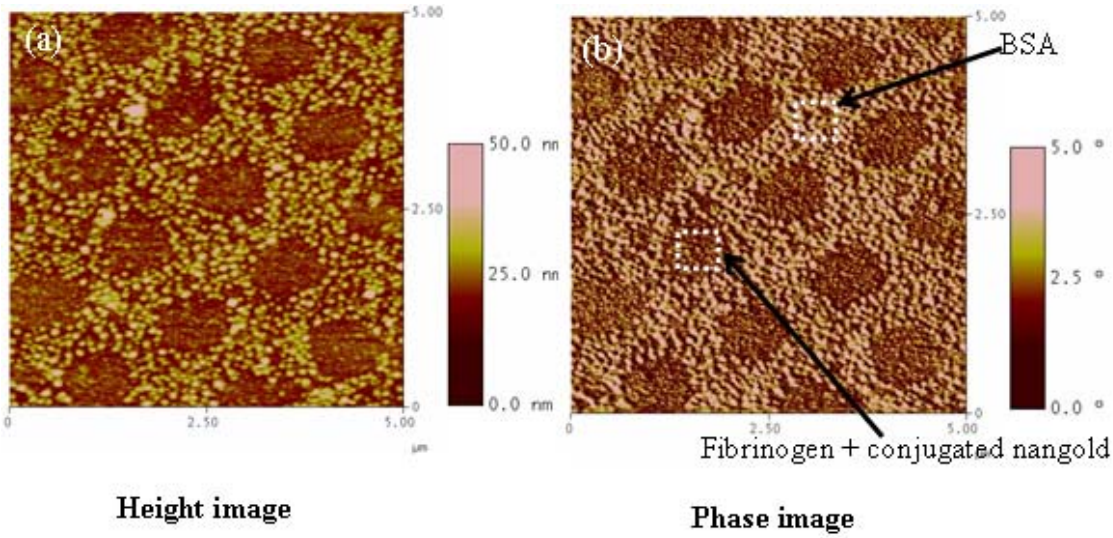

Figure **2-9**: Height (a) and phase (b) images after incubation with conjugated nanogold illustrate the fibrinogen pattern. The dotted squares in the figure highlight dark regions showing fibrinogen and the bright regions corresponding to BSA.

-

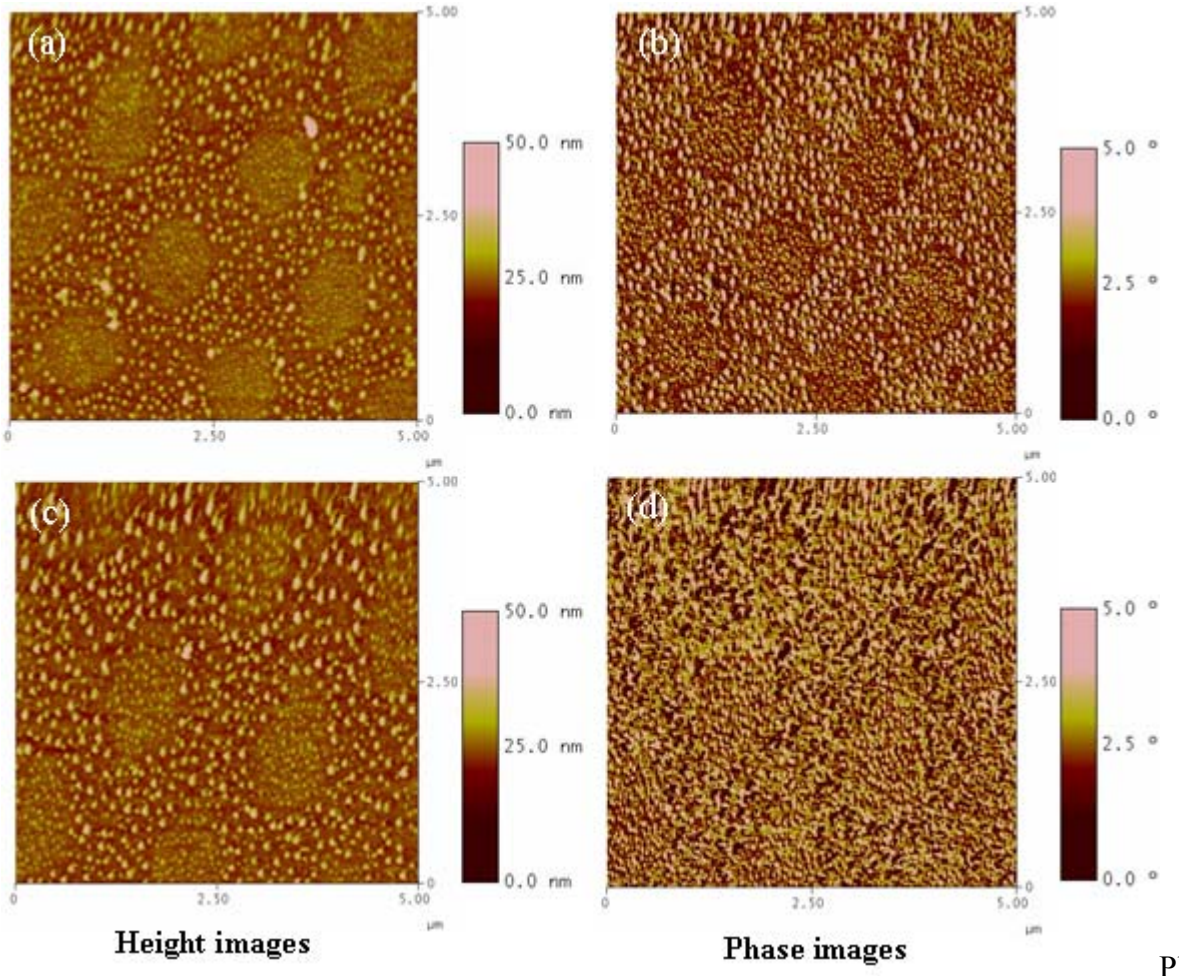

Place

Figure **2-10**: Height (a) and phase (b) images following fibrinogen adsorption for ½ hour demonstrate the filling of the circular pattern with fibrinogen. After 1 hour of fibrinogen adsorption, the pattern is still faintly seen in the height image (c) but undetectable in the phase image (d), demonstrating the formation of a uniform layer of two proteins

AFM methods typically utilize sub-monolayer distributions of a single protein type from dilute solutions onto model material surfaces. This situation lies far from the actual physiologic reality where all of the nearly 500 proteins present in plasma have the potential to adsorb onto rough polymeric biomaterial surfaces, and AFM identification of

protein types at the molecular level is nearly impossible in such a system. We previously described an adhesion mapping method for protein identification in a 2-component protein film that was based on measuring the interaction forces between antibodies coupled to the end of an AFM probe and adsorbed proteins on the surface (Agnihotri and Siedlecki 2005). Force curves obtained from the non-specific interactions between antibodies and BSA were distinctly different from the specific antibody-fibrinogen interactions and could be used to identify fibrinogen on mica substrate. While this adhesion mapping technique allowed for measurement of the distribution of one specific type of protein, the new method utilizing a gold-labeled antibody described in this work offers numerous advantages over the adhesion force technique used previously; data can be acquired at much higher resolution (512 x 512 pixels vs 32 x 32 pixels) and much faster acquisition times (≤ 8 minutes vs ~60 minutes for the adhesion technique) using standard AFM equipment. It is a direct imaging method and therefore it does not require the same complex statistical analyses that were necessary to interpret AFM force measurement images. Furthermore, using this technique in combination with various monoclonal antibodies could offer unique opportunities to address how the distribution of functionally active protein molecules affects subsequent biological functions, moving the field closer to single molecule immunochemistry techniques and providing much needed information on structure/function relationships in single proteins, contributing to our knowledge of protein-surface interactions that are important in the biological response to implanted biomaterials.

2.4 Conclusions

Gold nanoprobe labels were conjugated to an anti-fibrinogen polycolonal antibody to produce a marker that identified fibrinogen distributed in 2-component protein films by AFM phase imaging. A patterned sample consisting of circular regions of fibrinogen dispersed in BSA was prepared by micro-contact printing to test the specificity of the label. The data showed that the gold-conjugated labels identify the regions of the sample corresponding to fibrinogen with little-to-no nonspecific labeling seen. This labeling technique offers advantages over other single molecule AFM identification technique that are based on adhesion force measurements, including improved resolution and faster acquisition times, and could potentially be used to study competitive protein adsorption, to address conformation/functional changes in proteins on biomaterial surfaces and to study the composition and makeup of the adsorbed proteins layer in retrieved biomedical implants.

2.5 References

1. Agnihotri, A. Molecular level interactions between blood components and model biomaterials studied by atomic force microscopy. The Pennsylvania State University, Hershey, PA, 2005.

2. Agnihotri, A.; Garrett, J.; Runt, J.; Siedlecki, C., Atomic force microscopy visualization of poly(urethane urea) microphase rearrangements under aqueous environment. *Journal of Biomaterials Science Polymer Edition* **2006,** 17, (1-2), 227-238.

3. Agnihotri, A.; Siedlecki, C., Adhesion mode atomic force microscopy study of dual component protein films. *Ultramicroscopy* **2005,** 102, (4), 257-268.

4. Agnihotri, A.; Siedlecki, C., Time-dependent conformational changes in fibrinogen measured by atomic force microscopy. *Langmuir* **2004,** 20, 8846-8852.

5. Argaman, M.; Golan, R.; Thomson, N.; Hansma, H., Phase imaging of moving DNA molecules and DNA molecules replicated in the atomic force microscope. *Nucl. Acids Res.* **1997,** 25, (21), 4379-4384.

6. Balasubramanian, V.; Grusin, N.; Bucher, R.; Turitto, V.; Slack, S., Residence-time dependent changes in fibrinogen adsorbed to polymeric biomaterials. *J Biomed Mater Res A* **1999,** 44, 253-260.

7. Bar, G.; Thomann, Y.; Brandsch, R.; Cantow, H., Factors affecting the height and phase images in tapping mode atomic force microscopy: study of phase-separated polymer blends of poly(ethene-co-styrene) and poly (2,6-dimethyl-1-1,4-phenylene oxide). *Langmuir* **1997,** 13, 3807-3812.

8. Binnig, G.; Quate, C.; Gerber, C., Atomic force microscope. *Physical Review Letters* **1986,** 56, 930-933.

9. Eppell, S. J.; Simmons, S. R.; Albrecht, R. M.; Marchant, R. E., Cell-surface receptors and proteins on platelets imaged by scanning force microscopy using immunogold contrast enhancement. *Biophysical Journal* **1995,** 68, 671-680.

10. Gorbet, M.; Sefton, M., Biomaterial-associated thrombosis: roles of coagulation factors, complement, platelets and leukocytes. *Biomaterials* **2004,** 25, (26), 5681-5703.

11. Green, R.; Davies, J.; Davies, M.; Roberts, C.; Tendler, S., Surface plasmon resonance for real time in situ analysis of protein adsorption to polymer surfaces. *Biomaterials* **1997a,** 18, (5), 405-413.

12. Green, R. J.; Davies, J.; Davies, M. C.; Roberts, C. J.; Tendler, S. J. B., Surface plasmon resonance for real time in situ analysis of protein adsorption to polymer surfaces. *Biomaterials* **1997b,** 18, (5), 405-413.

13. Hainfeld, J. F.; Powell, R. D., Nanogold Technology: New frontiers in gold labeling. *Cell Vision* **1997,** 4, 408-432.

14. Hinterdorfer, P.; Baumgartner, W.; Gruber, H.; Schilcher, K.; Schindler, H., Detection and localization of individual antibody-antigen recognition events by atomic force microscopy. *PNAS* **1996,** 93, (8), 3477-3481.

15. Holland, N.; Marchant, R., Individual plasma proteins detected on rough biomaterials by phase imaging AFM. *Journal of Biomedical Materials Research* **2000,** 51, (3), 307-315.

16. Hussain, M.; Agnihotri, A.; Siedlecki, C., AFM imaging of ligand binding to platelets integrin alpha IIb ß3 receptors reconstituted into planar lipid bilayers. *Langmuir* **2005,** 21, 6979-6986.

17. Lin, H.; Lal, R.; Clegg, D., Imaging and mapping heparin-binding sites on single fibronectin molecules with atomic force microscopy. *Biochemistry* **2000,** 39, (12), 3192-3196.

18. Marchant, R.; Kang, I.; Sit, P.; Zhou, Y.; Todd, B.; Eppell, S.; Lee, I., Molecular views and measurements of hemostatic processes using atomic force microscopy. *Curr Protein Pept Sci* **2002,** 3, (3), 249-74.

19. Milner, K.; Snyder, A.; Siedlecki, C., Sub-micron texturing for reducing platelet adhesion to polyurethane biomaterials. *Journal of Biomedical Materials Research A* **2006,** 76A, (3), 561-570.

20. Montesano-Roditis, L.; Glitz, D. G.; Traut, R. R.; Stewart, P. L., Cryo-electron microscopic localization of protein L7/L12 within the Escherichia coli 70 S ribosome by difference mapping and Nanogold labeling. *J Biol Chem* **2001,** 276, (17), 14117-14123.

21. Osada, T.; Itoh, A.; Ikai, A., Mapping of the receptor-associated protein (RAP) binding proteins on living fibroblast cells using an atomic force microscope. *Ultramicroscopy* **2003,** 97, (1-4), 353-357.

22. Pickering, J.; Vancso, G., Apparent contrast reversal in tapping mode atomic force microscope images on films of polystyrene-b-polyisoprene-b-polystyrene. *Polymer Bulletin* **1998,** 40, 549-554.

23. Putnam, C. A. J.; de Grooth, B. G.; Hansma, P. K.; van Hulst, N. F.; Greve, J., Immunogold labels: Cell-surface markers in atomic force microscopy. *Ultramicroscopy* **1993,** 48, 177-182.

24. Radmacher, M., Measuring the elastic properties of biological samples with the AFM. *Engineering in Medicine and Biology Magazine, IEEE* **1997,** 16, (2), 47-57.

25. Raghavachari, M.; Kottke-Marchant, K.; Marchant, R., Determining intramolecular binding sites on surface-bound von Willebrand Factor under aqueous conditions. *Thrombosis Research* **2000,** 98, 351-358.

26. Reviakine, I.; Brisson, A., Formation of supported phospholipid bilayers from unilamellar vesicles investigated by atomic force microscopy. *Langmuir* **2000,** 16, 1806-1815.

27. Reviakine, I.; Simon, A.; Brisson, A., Effect of Ca2+ on the morphology of mixed DPPC-DOPS supported phospholipid bilayers. *Langmuir* **2000,** 16, 1473-1477.

28. Thibault, C.; Le Berre, V.; Casimirius, S.; Trevisiol, E.; Francois, J.; Vieu, C., Direct microcontact printing of oligonucleotides for biochip applications. *Journal of Nanobiotechnology* **2005,** 3, (1), 7.

29. Toscano, A.; Santore, M., Fibrinogen adsorption on three silica-based surfaces: conformation and kinetics. *Langmuir* **2006,** 22, (6), 2588-2597.

30. Touhami, A.; Nysten, B.; Dufrene, Y. F., Nanoscale mapping of the elasticity of microbial cells by atomic force microscopy. *Langmuir* **2003,** 19, (11), 4539-4543.

31. Truong, C.; Sykes, M.; McDermott, M., Real-time observation of plasma protein film formation on well-defined surfaces with scanning force microscopy. *Langmuir* **1998,** 14, 2435-2443.

32. Wakako, S.; Mime, K.; Hiroshi, S.; Kozo, H.; Touichiro, G.; Ichiro, F.; Keiichi, T.; Katsuhiko, M., Visualization of inositol 1,4,5-trisphosphate receptor by atomic force microscopy. *Neuroscience Letters* **2006,** 391, (3), 102-107.

33. Yang, R.; Tabata, S.; Crowley, H. H.; Margolskee, R. F.; Kinnamon, J. C., Ultrastructural localization of gustducin immunoreactivity in microvilli of type II taste cells in the rat. *J Comp Neurol* **2000,** 425, (1), 139-151.

Chapter 3
Measuring the Time-Dependent Functional Activity of Adsorbed Fibrinogen by Atomic Force Microscopy

Abstract

In this work, we measured time-dependent functional changes in adsorbed fibrinogen by measuring antigen-antibody debonding forces with atomic force microscopy (AFM). AFM probes were functionalized with monoclonal antibodies recognizing fibrinogen γ392-411, which includes the platelet binding dodecapeptide region. These probes were used to collect force measurements between the antibody and fibrinogen on mica substrates and the probability of antigen recognition was calculated. Statistical analysis showed that the probability of antibody-antigen recognition peaked at ~45 minutes post-adsorption and decreased with increasing residence time. Macroscale platelet adhesion measurements on these mica substrates were determined to be greatest at fibrinogen residence times of ~45 minutes, which correlated well with the functional activity of adsorbed fibrinogen as measured by the modified AFM probes. These results demonstrate the utility of this approach for measuring protein function at or near the molecular scale and offers new opportunities for improved insights into the molecular basis for the biological response to biomaterials.

3.1 Introduction

Surface-induced thrombosis has remained a major obstacle for the biocompatibility and eventual success of both implanted and peripheral medical devices.(Lamba, Woodhouse et al. 1998; Hirsh, Colman et al. 2001) One mechanism of surface-induced thrombosis involves the interaction of circulating blood platelets with proteins at the biomaterial surface. Circulating inactive platelets do not bind soluble fibrinogen, yet inactive platelets can adhere to surface-adsorbed fibrinogen via the platelet integrin receptor $\alpha_{IIb}\beta_3$ (GIIbIIIa).(Plow and Shattil 2001) Each fibrinogen molecule possesses a pair of dodecapeptide sequence (HHLGGAKQAGDV) in each of the γ chains, which is the primary ligand for platelet adhesion to adsorbed fibrinogen.(Farrell, Thiagarajan et al. 1992; Farrell and Thiagarajan 1994; Wei-Bor Tsai 2003) While the mechanisms of fibrinogen adsorption and subsequent generation of platelet binding activity are not fully understood, there is evidence in the literature that conformational changes following protein adsorption expose the otherwise-inaccessible platelet-binding epitopes. Many investigators have reported that the functional activity and availability of the dodecapeptide is related to the conformation and/or the orientation of adsorbed fibrinogen.(Shiba, Lindon et al. 1991; Balasubramanian, Grusin et al. 1999; Michel, Pasche et al. 2005; Chiumiento, Lamponi et al. 2007)

The analysis of adsorbed proteins relies heavily on surface analysis and spectroscopic techniques such as infrared spectroscopy,(Barbucci, Lamponi et al. 2003) circular dichroism,(Damodaran 2003) attenuated total reflection Fourier-transform infrared

(ATR-FTIR) spectroscopy,(Clarke, Wang et al. 2005; Roach, Farrar et al. 2005; Tunc, Maitz et al. 2005; Wang, Chen et al. 2006) vibrational sum frequency spectroscopy (VSFG),(Jung, Lim et al. 2003; Evans-Nguyen, Fuierer et al. 2006) quartz crystal microbalance (QCM),(Hemmersam, Foss et al. 2005; Roach, Farrar et al. 2005) and time of flight secondary ion mass spectrometry,(Michel, Pasche et al. 2005) among a multitude of other techniques(Horbett and Brash 1995). Although these techniques have provided indirect information about time dependent conformation and activity in proteins on surfaces (the residence time effects) the functional activity or molecular potency of absorbed proteins is still not well-understood.

Tunc et al. used a monoclonal antibody (mAb) clone to determine the functional changes in the carboxyl terminal region of the γ chain of fibrinogen.(Tunc, Maitz et al. 2005) However, the conformational changes were too small to be detected using an enzyme-linked immunosorption assay. Balasubramanian et al. used radiolabeling to study the effects of fibrinogen residence time on various biomaterials using a 400-411). γ-mAb directed against the C terminal dodecapeptide of the gamma chain ((Balasubramanian, Grusin et al. 1999) These studies also measured platelet adhesion but were unable to correlate the changes in platelet adhesion to changes in the mAb recognition of adsorbed fibrinogen. In a recent paper, Holmberg et al. showed that the radiolabeling so commonly used to determine the amounts of protein adsorbed on a surface can potentially lead to enhanced aggregation and fragmentation of proteins leading to potential misinterpretation of the results.(Holmberg, Stibius et al. 2007)

Atomic force microscopy (AFM) has been used extensively for studying biological molecules under physiologically relevant aqueous conditions with nanometer-scale resolution.(Binnig, Quate et al. 1986; Siediecki, Lestini et al. 1996; Argaman, Golan et al. 1997; Radmacher 1997; Reviakine and Brisson 2000; Marchant, Kang et al. 2002; Osada, Itoh et al. 2003; Touhami, Nysten et al. 2003; Hussain, Agnihotri et al. 2005; Toscano and Santore 2006) Our group as well as many others has directly studied the conformational changes and spreading of fibrinogen on hydrophobic, hydrophilic, and various charged surfaces.(Sit and Marchant 1999; Marchin and Berrie 2003; Agnihotri and Siedlecki 2004; Clarke, Wang et al. 2005; Tunc, Maitz et al. 2005; Toscano and Santore 2006) Most of these studies assess the conformational changes in fibrinogen based on the observed changes in the trinodular structure of the protein as seen by topography imaging and therefore require the use of ultrasmooth model surfaces to characterize nanometer scale protein features. Truong and McDermott used scanning force microscopy to map fibrinogen adsorption onto different functional groups.(Ta and McDermott 2000) Changes in frictional contrast were attributed to various conformations/ orientation of adsorbed fibrinogen on different functional domains, although other parameters have also been shown to affect this contrast. Because of the mechanism of contrast generation, AFM experiments can be quite limited in scope, particularly in complicated multi-protein adsorption experiments and are especially difficult on clinically relevant biomaterials that usually have rough topography.(Holland and Marchant 2000; Soman, Rice et al. In press) Moreover, information about the functional activity of adsorbed proteins cannot be obtained using conventional AFM techniques.

The force spectroscopy mode of the AFM uses the rupture force between the tip and the surface to detect interactions. The technique has been used to detect artificially patterned proteins,(Agnihotri and Siedlecki 2005) to distinguish different red blood cell populations,(Grandbois, Dettmann et al. 2000) to determine the elastic properties of biological samples(Radmacher 1997) and to characterize antibody-antigen interactions(Hinterdorfer, Baumgartner et al. 1996) as well a multitude of other applications. Our group previously used an AFM probe modified with polyclonal antibodies to detect fibrinogen in a dual protein layer of proteins.(Agnihotri and Siedlecki 2005) In this section, we extend these force spectroscopy studies to the study of protein activity changes and indirectly the putative conformational changes in fibrinogen on mica surfaces by measuring the time-dependent recognition between AFM probes modified with a monoclonal antibody recognizing fibrinogen -chain dodecapeptide that is γ392-411, a region that includes the fibrinogen critical for platelet adhesion.

3.2 Materials and methods

3.2.1 General

Phosphate buffered saline (PBS, 0.01 M sodium phosphate buffer, 150mM NaCl, pH 7.4, Sigma Inc.) was prepared using water from a Millipore Simplicity 185 system (18 MΩ) which utilizes two ultraviolet filters (185 and 254 nm) to reduce carbon contaminants. Human fibrinogen (90% clottable) was used as received from Calbiochem, La Jolla, CA.

Monoclonal mouse anti-fibrinogen gamma chain (γ 392 – 411; clone: 4 -2; Isotype: IgG1) was obtained from Accurate Chemicals and Scientific Corporation, NY. Bovine serum albumin (BSA) was obtained from Sigma Chemicals Co, St. Louis, MO. Coli S69 (IgG_1 isotype control) was obtained from the Washington State University Monoclonal Antibody Center (WSUMAC). All the proteins were dissolved in phosphate buffer and aliquots were stored at -20°C until use.

3.2.2 AFM probe modification

Silicon nitride AFM probes with integral pyramidal tips (NPS, Veeco, Santa Barbra, CA, nominal k = 0.06 N/m) were cleaned in 10 ml of acetone for 15 minutes and then treated in a glow-discharge plasma cleaner for 30 minutes at 100 W power. The tips were modified by placing into 10 ml of 1% (v/v) aminopropyltriethoxysilane in ethanol for 1 hr to provide a reactive amine group, and then rinsed 3 times using Millipore water. Tips were incubated in 15 ml of 10% gluteraldehyde for 1 hr to provide a reactive crosslinking site and again washed using Millipore water. The activated probes were incubated for 1 hr with either monoclonal antibodies (25 μg/ml) that recognize fibrinogen γ392-411, a region that includes the platelet binding dodecapeptide sequence γ402-411 or Coli S69A (25 μg/ml), an isotype control for IgG_1 antibodies. Modified tips were stored in PBS (10 mM, pH 7.4) at 4°C and used within 2 days. This linking mechanism provides sufficient mobility to the antibodies to bind to their target molecules on the surface.(Chowdhury and Luckham 1998; Agnihotri and Siedlecki 2005)

3.2.3 Force Spectroscopy Measurements

Freshly cleaved muscovite mica sheets (10 mm x 10 mm, Ted Pella, Inc) were used as substrates for protein adsorption experiments. Bovine serum albumin (BSA) (100 μg/ml) or fibrinogen (100 μg/ml) solutions in PBS were adsorbed onto mica substrates for 5 minutes in an external fluid cell. Remaining free protein was washed away for 3 minutes using a syringe pump that provides a steady flow of PBS at 0.3 ml/min. The channel geometry was circular with an inner diameter of 0.063 inches. All data was collected using a Nanoscope III Multimode AFM (Digital Instruments, CA) under buffer conditions in a fluid cell. The hydrated protein sample was loaded onto the microscope and data was collected using the monoclonal anti-fibrinogen-modified probes under buffer. The ramp size (500nm) and trigger threshold (100nm) were kept constant while the scan size (500nm-5000nm) and scan rate (0.3 Hz – 1 Hz) were varied. Images were collected as 16 x 16 and 32 x 32 force arrays with 256 data points per force curve.

3.2.4 AFM data analysis

In the force spectroscopy mode of the AFM, the deflection of cantilever (d, measured as a function of the vertical displacement of the AFM scanner) is translated into a force-distance curve using Hooke's law ($F_{rupture}$ = -k x d, where k is the cantilever spring constant). BSA adsorbed on mica substrates for 5 minutes was used as a negative control for non-specific interactions of the antibody. The non-specific force-distance data for each modified probe was extracted from the AFM files and analyzed off-line with tools

developed in MatLab™ (The Mathworks Inc., MA). Data was plotted as rupture-force histograms and mean rupture force values (μ) and standard deviations (σ) were established. A 95% confidence interval was determined for each tip as $\mu \pm 2\sigma$ and this force was subsequently used as a cut-off value for differentiating between non-specific and specific mAb-fibrinogen interactions.

Interactions between fibrinogen and the mAb probe were acquired at varying scan rates as a 32 x 32 array of individual force curves. The time corresponding to each individual force measurement was determined from the scan rate for that particular image. Non-specific versus specific interactions were characterized by using the cut-off value previously determined in the control BSA experiments as explained earlier. The force data was bundled into groups of 32 (corresponding to one across scan line of the rupture force map). The probability of detecting a positive binding event was calculated as follows:

Probability = number of specific binding events in each scan line / 32.

Time-dependent force data from multiple experiments ($n \geq 6$ for every time point) was converted to probability data. Probability data was pooled together and fibrinogen residence times were plotted from t = 15 minutes residence time with bins of 10 minute size ($t \pm 5$ minutes). The mean probability of detecting a specific event at varying fibrinogen residence time points (15, 25, 35 …195 minutes) was plotted as a function of fibrinogen residence time on mica substrate. In certain control experiments, fibrinogen was absorbed on mica substrate for 5 minutes, washed with PBS and initiation of rupture

force measurements was delayed for as long as 60 minutes fibrinogen residence time. Additionally, the same antibody modified tip was occasionally used for consecutive experiments to demonstrate that changes did not result from spoiling of the antibody-coupled probe.

3.2.5 Platelet adhesion

Salvaged human platelets (~50 cc) with citrate-phosphate-dextrose (CPD) anticoagulant were obtained from the Blood Bank at Hershey Medical Center. Platelets were characterized using flow cytometry and aggregation studies as described elsewhere(Michelson 1996; Kamath, Blann et al. 2001). Results strongly suggest that salvage platelets are biologically functional and can be fully activated. The platelets were centrifuged (5 minutes, 900g) to remove remaining red blood cells and platelet fractions, visually identified by turbidity, were separated. The supernatant was centrifuged (10 minutes, 900g) to separate platelets into a pellet. The platelet pellet was resuspended in 10 mL of PBS and centrifuged again (5 min, 900g). The final platelet pellet was resuspended in 5 ml of PBS and the platelet concentration was determined with a Sysmex XE 2100 (Sysmex, Kobe, Japan). This platelet rich plasma solution was diluted with PBS to a physiologically relevant platelet concentration (200×10^3). This stock platelet solution was then serially diluted in order to generate a Lactate Dehydrogenase (LDH) assay calibration curve for each experiment.

Freshly cleaved mica samples of diameter 9.9mm were incubated in 0.5 ml of fibrinogen solution (100 μg/mL in PBS) for 5 minutes in a 24 well plate at room temperature. Samples were subsequently rinsed with PBS (3 times with 0.5 mL PBS/well) and allowed to incubate in PBS for 15, 30, 45, 60, 75, 90, 105 and 120 minutes before exchanging for recalcified (2.5 mM $CaCl_2$) platelet solution. The platelet solution was aspirated after 10 minutes and samples were rinsed 5 times with 0.5 mL PBS each rinse. Samples were transferred to a fresh 24-well plate containing 0.5 mL Triton X-100 solution (1%) for 1 hour at room temperature. 50 μL aliquots from each well in the 24-well plate were added to a 96-well plate and incubated with 50 μL of the Reaction Mixture prepared from the Cytotoxicity Detection Kit (Roche Applied Science 11644793001) for 1 hour. The reaction was stopped by adding 50 μL of 1N HCl. The changes in the absorption at 492 nm were measured using a spectrophotometer (μQuant^{TM} Microplate Spectrophotometer, BioTek Instruments, Inc.) using a reference wavelength of 610nm ($O.D._{490} - O.D._{610}$). The calibration curve was generated in the same manner as described for the mica samples except platelet solutions (100μl) of different dilutions were directly lysed with 1% Triton X-100 solution.

3.2.6 Statistical analysis

A minimum of six independent experiments were performed for each measurement. Statistical differences were determined using One-way Analysis of Variance (ANOVA)

with post test (Tukey-Kramer Multiple Comparisons Test) with $p < 0.05$ being considered significant.

3.3 Results and Discussion

3.3.1 Functional activity of fibrinogen

A monoclonal antibody recognizing a region that includes the platelet binding epitope of the γ-chain dodecapeptide (γ400-411) was used to collect rupture force measurements as a function of fibrinogen residence times. The first step in the analysis of the data is to separate specific fibrinogen-mAb rupture forces from non-specific interactions. Force curves were obtained from control experiments to evaluate the interactions between (1) bare mica and bare probe, (2) bare mica and a mAb-modified probe, (3) BSA adsorbed on mica and a mAb-modified probe and (4) fibrinogen adsorbed on mica and an AFM probe functionalized with a generic IgG. Force spectroscopy recorded very little-to-no rupture forces between the bare AFM probe and bare mica substrate in the presence of PBS buffer (Data not shown). Figure **3-1a** shows the distribution of rupture forces between a mAb-modified AFM probe and bare mica substrates for one particular probe. Most of the rupture forces are found in the range of 400 to 700 pN with a maximum occurring at ~520 pN. Figure 3-1b shows force distributions between adsorbed BSA and the same mAb probe. There is a substantial shift in the force distribution, with most of the rupture forces in the range of 0 – 150 pN. The lack of overlap between force values

in Figures 3-1a and b suggests that the probe encounters little bare mica during the measurements. The mean and standard deviation of this distribution were used to establish a cut - off value for specific/nonspecific interactions (150 pN for this particular probe) based on a 95 % confidence interval. Note that this analysis method does not require that we know the actual spring constant

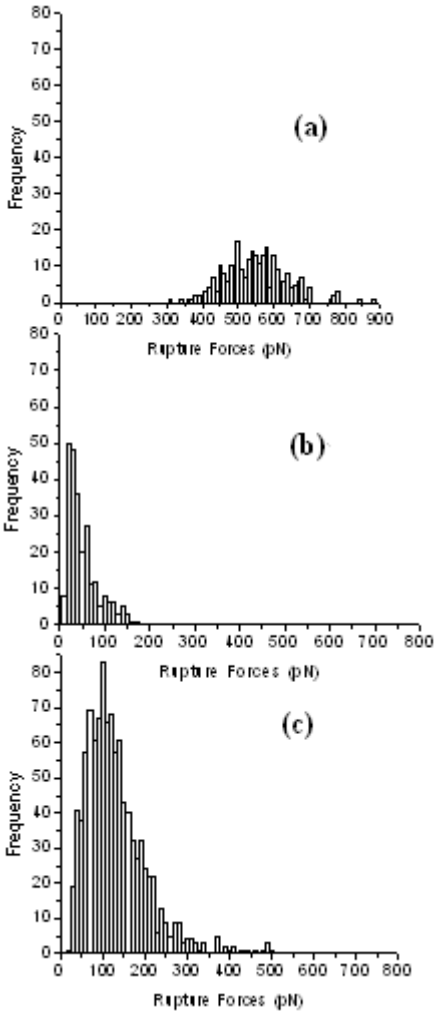

Figure **3-1**: Representative distributions of maximum rupture forces between monoclonal anti-fibrinogen (mAb) modified probe and (a) bare mica (b) BSA adsorbed on mica (100µg/ml) (c) fibrinogen adsorbed on mica (100µg/ml). Scan Rate = 1 Hz. The distributions in (b) & (c) suggest nearly complete coverage of the mica substrate with BSA and fibrinogen respectively

of the cantilever or even the number of antibodies on the probe tip as each probe is characterized for non-specific interactions independently. Before using the modified probes for specific recognition of dodecapeptide sequence, control experiments were carried out to determine non-specific recognition using generic mouse IgG modified AFM probes. Rupture forces between IgG probes and fibrinogen adsorbed on mica substrate were found in the range of 0 -70 pN, substantially lower than the non-specific BSA control in Figure 3.1b (Data not shown). Fibrinogen was adsorbed on mica substrates and the monoclonal antibody modified probes were used to obtain rupture force measurements. Histograms of these rupture forces were in the range of 0 – 400 pN. Figure 3.1b and c show that there are sufficient differences between the distributions to be confident that the coupled antibody specifically recognizes its antigen. Data obtained spatially was converted to the appropriate time of measurement and probability of antigen recognition at that time as described in the Methods section. Figure **3-2a** shows an example of a typical probability plot for antigen recognition measured against fibrinogen-adsorbed surfaces. Individual time points are shown by the data points and clearly demonstrate that the activity of fibrinogen is time dependent, with the maximum likelihood of recognition occurring in the time range around 45 minutes and then decreasing at longer adsorption times. The line represents a 5 point average used to simply guide the eye.

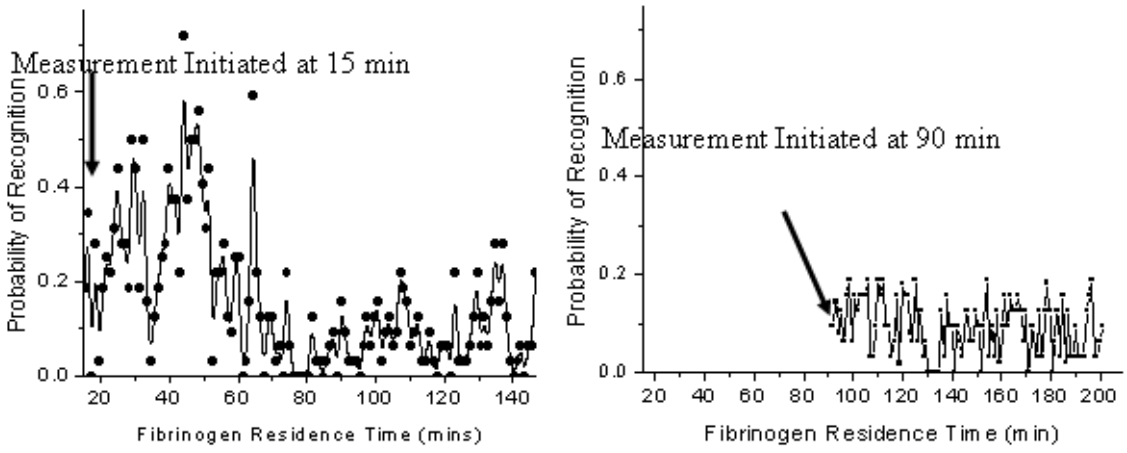

Figure Here

Figure **3-2**: (a) Time-dependent changes in the probability of recognition between an AFM probe 392-411, that recognizes fibrinogen region that includes the platelet binding dodecapeptide domain, and adsorbed fibrinogen (100μg/ml). The black line shows a running 5 point average to guide the eye. The probability of recognition is highest at ~ 45 minutes fibrinogen residence time and decreases at longer residence times. (b) Measurement was initiated at 90 minutes fibrinogen residence time. The probabilities of recognition are in the range of 0-0.18, similar to those in figure (a) after 90 minutes.

Control experiments were conducted to confirm that the activity of fibrinogen is a time-dependent process rather than an artifact of antibody degradation after prolonged periods of scanning. Fibrinogen was absorbed on mica substrates and probe scans were initiated after 90 minutes fibrinogen residence time (Figure 3.2b). In figure 2b, low probabilities of rupture forces (0-0.18) are seen similar to probabilities in figure 3.2a after 90min. In these experiments, identical recognition probabilities were seen at that particular fibrinogen residence times, regardless of measurement initiation times. Control experiments were carried out using the same mAb modified tip to scan several ($n \geq 4$) adsorbed fibrinogen samples. Results showed trends in rupture force values similar to the

general trends seen previously in figure 3.2a, demonstrating insignificant aging or degradation effects on the antibodies bound to the AFM probe.

Figure **3-3** shows pooled probability data from multiple experiments ($n \geq 6$ for each time point) as a function of fibrinogen residence time on mica substrate. The probability of antibody-antigen recognition (used as a measure of the functional activity of adsorbed fibrinogen) peaks at ~45 minutes post-adsorption and thereafter decreases with increasing adsorption time. Although, fibrinogen activity at 15, 25 and 35 minutes residence time is not statistically significant when compared to activity at 45 minutes, the recognition probability peak at ~45 minutes was consistently seen in all the experiments. Moreover, statistical analysis indicates that functional activity of adsorbed fibrinogen as measured by AFM force spectroscopy at the 45 minute time point is significantly greater than all time points ≥65 minutes ($P<0.001$).

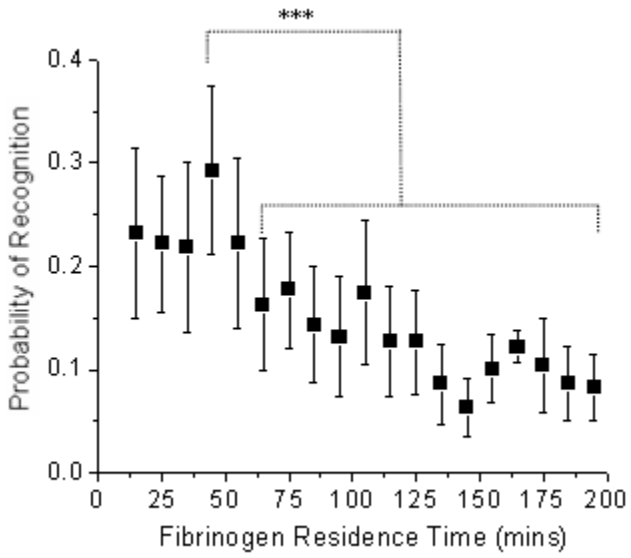

Figure **3-3**: Rupture force probability data from multiple experiments ($n \geq 6$ for each time point). The probability of antibody-antigen recognition (functional activity of adsorbed fibrinogen) peaks at ~45 minutes post-adsorption and thereafter decreases with increasing residence time. The activity of fibrinogen at 45 minutes fibrinogen residence time is significantly greater than all time points ≥65 minutes ($P<0.001$).

Although the exact mechanism behind the changes in epitope activity is not clear in the literature, there seems to be two potential mechanisms: either the activity of the exposed epitope changes with time due to changes in the degree of denaturation of adsorbed fibrinogen, or structural changes in fibrinogen following adsorption results in transient exposure of the functional domains. Hemmersam used monoclonal antibodies to study fibrinogen adsorption and found that differences seen in the recognition of antibodies could be due to different orientations and/or different degrees of denaturation of adsorbed fibrinogen.(Hemmersam, Foss et al. 2005) Shiba et al.(Shiba, Lindon et al. 1991) assessed nine monoclonal antibodies against various epitopes on fibrinogen and found that the differences in antibody binding on different polymers are more likely due to

differences in the degree of preservation of the epitopes of fibrinogen as opposed to differences in orientation of fibrinogen molecules. Grunkemeier et al. evaluated antibody binding affinity using the M1 antibody against γ402-411 and fibrinogen adsorbed from 1% plasma.(Grunkemeier, Wan et al. 1996) The study found that the Ka determined with the M1 antibody decreased with residence time but there was little change in maximal antibody binding. This suggests that the affinity of the dodecapeptide sequence towards platelets change with time, but the number of sites or number of exposed sequences remain constant with residence time.

Platelet adhesion using LDH assay

Macro-scale platelet adhesion measurements on mica substrates were carried out using a standard LDH assay to assess time dependence.(Tamada, Kulik et al. 1995; Grunkemeier, Tsai et al. 1998) Fibrinogen residence time or adsorption time is defined here as the time from the start of fibrinogen adsorption to the addition of platelets. This assay used Triton buffer for lysing adherent platelets and measured released lactate dehydrogenase (LDH) at varying residence times, as described in the Methods section. The absorbance of the samples measured by UV spectrometry corresponds to the LDH activity, which is proportional to the number of adherent platelets. A calibration experiment was performed alongside every platelet adhesion experiment. An example of one of these calibration curves is shown in Figure **3-4** and indicates a linear relationship between the concentration of platelets and the measured UV absorbance value. Curve fitting of the data gave a linear fit with an R^2 value of 0.9996. These curves were used to convert the absorbance values from the mica substrates into the number of adherent platelets.

Multiple experiments ($n \geq 6$) for each time point were carried out and the data was pooled according to the fibrinogen residence time on the substrate. Results in Figure **3-5** show that platelet adhesion reaches a peak at ~ 45 minutes fibrinogen residence time, which correlates well with the molecular scale AFM results. Statistical analysis indicate that platelet adhesion at 45 minutes fibrinogen residence time is significantly greater than platelet adhesion at 15 minutes ($P<0.001$) and at all times greater than or equal to 90 minutes ($P<0.01$).

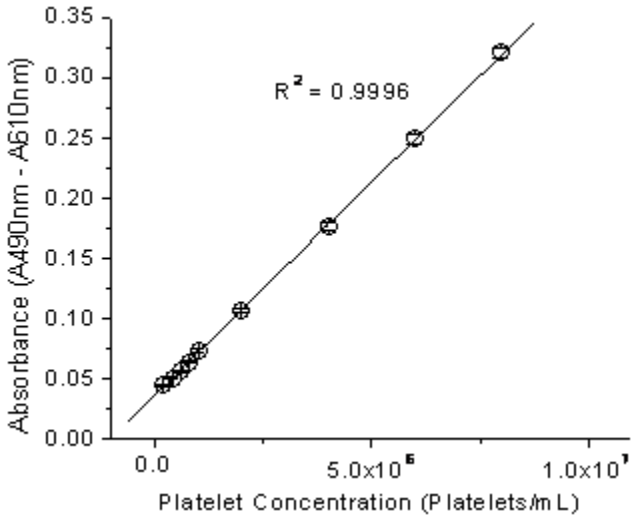

Figure **3-4**: Typical calibration curve for Lactate Dehydrogenase (LDH) assay. The figure indicates a linear relationship between the concentration of platelets and the measured UV absorbance value. Curve fitting of the data (linear fit, R2 value = 0.9996) converts the LDH activity (absorbance) to the number of adherent platelets.

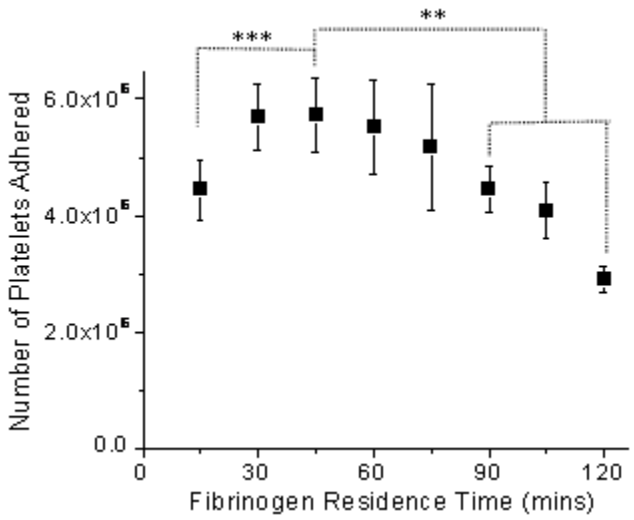

Figure **3-5**: Platelet adhesion data from multiple experiments ($n \geq 6$ for each time point) showing changes in platelet adhesion as a function of fibrinogen residence times on mica substrates. Platelet adhesion was found to reach the maximum value at a fibrinogen residence time of ~45 minutes, which corresponds well with the molecular scale AFM results. Statistical analysis indicate that platelet adhesion at 45 minutes fibrinogen residence time is significantly greater than at 15 minutes ($P<0.001$) and $t \geq 90$ minutes ($P<0.01$).

These data suggest that the exposure of the dodecapeptide epitope correlates well with platelet adhesion, and that platelet adhesion will peak at 45 minutes fibrinogen residence time on this hydrophilic mica substrate. However, the activity of fibrinogen (exposure of dodecapeptide sequence) decreases significantly after 65 minutes, while platelet adhesion shows a decrease only after 90 minutes. This apparent inconsistency can be explained by two possible mechanisms.

There has to be a critical number of available/exposed epitopes (in this case, dodecapeptide sequence) on adsorbed fibrinogen in order to attain maximum platelet adhesion. As seen in Figure 3.5, there are no significant changes in platelet adhesion at

residence times of 30, 45, 60 and 75 minutes, although the number of specific recognition events begins to decrease after 65 minutes. It seems likely that the number of available epitopes in the adsorbed fibrinogen is still above a critical number of epitopes necessary for maximal platelet adhesion. However, as the number of gamma-chain binding sites continues to fall, eventually there are too few sites available to support maximal platelet adhesion.

Another possible mechanism would include cooperative contributions from other putative platelet binding sites (RGDF and RGDS) of fibrinogen. There is some evidence in the literature that there is cooperation between the different RGD sites and -chain binding site which causes a cumulative increase in affinity of the platelet binding to adsorbed fibrinogen. Horbett et al. used mAbs against all three putative platelet binding sites on fibrinogen to provide a detailed study of changes in adsorbed fibrinogen with increasing residence time.(Horbett and Lew 1994) The binding of mAbs to the dodecapeptide sequence did not change with residence time, while binding to RGD near the N terminus of the Aα chain was very low initially but increased with residence time. This increase of binding in the RGDF sequence with increased residence time could be responsible for the prolonged platelet adhesion seen in Figure 5. Such an argument would suggest that the binding of platelets to the adsorbed fibrinogen may also be mediated by time-dependent cooperative changes in both epitopes which would be a highly complex phenomenon to address. While it is possible that the contributions from the two RGD sites of adsorbed fibrinogen might become important after 45 minutes fibrinogen residence time, our data is not yet sufficient to directly address this possibility at this time.

There is evidence in the literature that the dodecapeptide sequence is primarily responsible for platelet adhesion. Tsai et al. used 3 mAbs against platelet binding sites on fibrinogen domains to test the correlation of platelet adhesion and the exposure of the binding sites on various polystyrene based materials. This work showed strong correlation between binding of the M1 antibody against the dodecapeptide sequence of adsorbed fibrinogen and platelet adhesion, suggesting this sequence to be more important than the RGD sequences.(Tsai, Grunkemeier et al. 2003) Simonovsky el al. used ELISA to measure mAbs binding to adsorbed fibrinogen on 10 different types of polyurethane surfaces and also found good correlation between the dodecapeptide sequence detection and platelet adhesion, but poorer correlation with the other potential binding sites.(Wu, Simonovsky et al. 2005) Therefore, in this work, we used a monoclonal antibody recognizing -chain□fibrinogen γ392-411, a region that includes the fibrinogen dodecapeptide, to measure the activity of fibrinogen. Results indicate an excellent correlation between the functional activity of fibrinogen at the molecular scale and macroscale platelet adhesion, in line with the macroscale measurements made by others.

Chinn et al. found that fibrinogen adsorbed to a polymer surface undergoes conformational changes with residence time resulting in a decrease in elutability by SDS, anti-fibrinogen binding and ability to mediate platelet adhesion. In the study by Chinn however, the protein adsorption was allowed to proceed for 2 hours, which might not truly capture the post-adsorptive changes immediately after adsorption.(Chinn, Posso et al. 1991) In our work, we detect functional changes continuously from ~10 minutes to

~190 minutes post-adsorption of fibrinogen, thereby capturing the transitional changes in the activity of adsorbed fibrinogen on mica.

Several studies demonstrate the importance of fibrinogen orientation on the surface, emphasizing the necessity of considering both the total amount of adsorbed fibrinogen and its biological activity as modulated by the exposure of platelet binding epitopes.(Hemmersam, Foss et al. 2005; Massa, Yang et al. 2005; Chiumiento, Lamponi et al. 2007) In this paper, we developed a novel method of using monoclonal antibodies in conjunction with AFM to detect the functional activity of adsorbed fibrinogen on mica surface. The data suggest that the exposure of the dodecapeptide epitope as measured by an 392-411 correlates well with AFM probe immobilized monoclonal antibody against platelet adhesion. Peaks in both platelet adhesion and antibody binding occur at ~45 minutes residence time on the mica substrate, suggesting that the biological activity of fibrinogen or the availability of functional epitopes is critically responsible for platelet adhesion. This functional measurement technique can be applied to a variety of biomedical polymers having rough topographies and allows for the potential measurement of protein function at or near the single molecule level.

3.4 Conclusions

The molecular recognition capability of AFM developed in this work has extended the scope of the traditional AFM imaging studies to epitope recognition imaging in adsorbed proteins. This technique also has the potential to overcome the limitation of AFM

imaging that requires ultrasmooth model surfaces. An AFM probe 392-411 in fibrinogen, was modified with a monoclonal antibody that recognizes a region that includes the gamma chain dodecapeptide platelet binding site. The time to the peak in the probability of antibody binding correlated well to the residence time necessary for observing a peak in platelet adhesion, although the probability of antibody recognition was found to decrease faster than platelet adhesion. When the methodology described here is combined with the high resolution of the AFM, it offers a unique opportunity to begin to assess the biological activity of single adsorbed protein molecules.

3.5 References

Agnihotri, A. and C. Siedlecki (2004). "Time-dependent conformational changes in fibrinogen measured by atomic force microscopy." Langmuir **20**: 8846-8852.

Agnihotri, A. and C. Siedlecki (2005). "Adhesion mode atomic force microscopy study of dual component protein films." Ultramicroscopy **102**(4): 257-268.

Argaman, M., R. Golan, et al. (1997). "Phase imaging of moving DNA molecules and DNA molecules replicated in the atomic force microscope." Nucl. Acids Res. **25**(21): 4379-4384.

Balasubramanian, V., N. Grusin, et al. (1999). "Residence-time dependent changes in fibrinogen adsorbed to polymeric biomaterials." J Biomed Mater Res A **44**: 253-260.

Barbucci, R., S. Lamponi, et al. (2003). "Fibrinogen conformation and platelet reactivity in relation to material-blood interaction: effect of stress hormones." Biomacromolecules **4**(6): 1506-1513.

Binnig, G., C. Quate, et al. (1986). "Atomic force microscope." Physical Review Letters **56**: 930-933.

Chinn, J., S. Posso, et al. (1991). "Postadsorptive transitions in fibrinogen adsorbed to Biomer: Changes in baboon platelet adhesion, antibody binding, and sodium dodecyl sulfate elutability." Journal of Biomedical Materials Research **25**(4): 535-555.

Chiumiento, A., S. Lamponi, et al. (2007). "Role of fibrinogen conformation in platelet activation." Biomacromolecules **8**(2): 523-531.

Chowdhury, P. and P. Luckham (1998). "Probing recognition process between an antibody and an antigen using atomic force microscopy." Colloids and Surfaces A: Physicochemical and engineering aspects **143**: 53-57.

Clarke, M. L., J. Wang, et al. (2005). "Conformational Changes of Fibrinogen after Adsorption." J. Phys. Chem. B **109**(46): 22027-22035.

Damodaran, S. (2003). "In situ measurement of conformational changes in proteins at liquid interfaces by circular dichroism spectroscopy." Analytical and Bioanalytical Chemistry **376**(2): 182-188.

Evans-Nguyen, K. M., R. R. Fuierer, et al. (2006). "Changes in adsorbed fibrinogen upon conversion to fibrin." Langmuir **22**(11): 5115-5121.

Farrell, D. and P. Thiagarajan (1994). "Binding of recombinant fibrinogen mutants to platelets." J. Biol. Chem. **269**(1): 226-231.

Farrell, D., P. Thiagarajan, et al. (1992). "Role of fibrinogen alpha and gamma chain sites in platelet aggregation." PNAS **89**(22): 10729-10732.

Grandbois, M., W. Dettmann, et al. (2000). "Affinity imaging of red blood cells using an atomic force microscope." J. Histochem. Cytochem. **48**(5): 719-724.

Grunkemeier, J., W. Tsai, et al. (1998). "Hemocompatibility of treated polystyrene substrates: contact activation, platelet adhesion, and procoagulant activity of adherent platelets." Journal of Biomedical Materials Research **41**(4): 657-670.

Grunkemeier, J., C. Wan, et al. (1996). "Changes in binding affinity of a monoclonal antibody to a platelet binding domain of fibrinogen adsorbed to biomaterials." J. Biomater. Sci. Polymer Edn **8**(3): 189-209.

Hemmersam, A. G., M. Foss, et al. (2005). "Adsorption of fibrinogen on tantalum oxide, titanium oxide and gold studied by the QCM-D technique." Colloids and Surfaces B: Biointerfaces **43**(3-4): 208-215.

Hinterdorfer, P., W. Baumgartner, et al. (1996). "Detection and localization of individual antibody-antigen recognition events by atomic force microscopy." PNAS **93**(8): 3477-3481.

Hirsh, J., R. Colman, et al. (2001). Overview of thrombosis and its treatment. Philadelphia, Lippincott Williams and Wilkins.

Holland, N. and R. Marchant (2000). "Individual plasma proteins detected on rough biomaterials by phase imaging AFM." Journal of Biomedical Materials Research **51**(3): 307-315.

Holmberg, M., K. Stibius, et al. (2007). "Protein aggregation and degradation during iodine labeling and its consequences for protein adsorption to biomaterials." Analytical Biochemistry **361**(1): 120-125.

Horbett, T. and J. Brash (1995). Proteins at interfaces II : fundamentals and applications. Washington, DC, American Chemical Society, 1995.

Horbett, T. A. and K. R. Lew (1994). "Residence time effects of monoclonal antibody binding to adsorbed fibrinogen." J. Biomater. Sci. Polymer Edn **6**(1): 15-33.

Hussain, M., A. Agnihotri, et al. (2005). "AFM imaging of ligand binding to platelets integrin alpha IIb ß3 receptors reconstituted into planar lipid bilayers." Langmuir **21**: 6979-6986.

Jung, S.-Y., S.-M. Lim, et al. (2003). "The vroman effect: a molecular level description of fibrinogen displacement." J. Am. Chem. Soc. **125**(42): 12782-12786.

Kamath, S., A. D. Blann, et al. (2001). "Platelet activation: assessment and quantification." European Heart Journal **22**: 1561-1571.

Lamba, N., K. Woodhouse, et al. (1998). Polyurethanes in biomedical applications. Boca Raton, CRC Press.

Marchant, R., I. Kang, et al. (2002). "Molecular views and measurements of hemostatic processes using atomic force microscopy." Curr Protein Pept Sci **3**(3): 249-74.

Marchin, K. L. and C. L. Berrie (2003). "Conformational Changes in the Plasma Protein Fibrinogen upon Adsorption to Graphite and Mica Investigated by Atomic Force Microscopy." Langmuir **19**(23): 9883-9888.

Massa, T. M., M. L. Yang, et al. (2005). "Fibrinogen surface distribution correlates to platelet adhesion pattern on fluorinated surface-modified polyetherurethane." Biomaterials

Dedicated to Canadian Biomaterials Research **26**(35): 7367-7376.

Michel, R., S. Pasche, et al. (2005). "Influence of PEG architecture on protein adsorption and conformation." Langmuir **21**(26): 12327-12332.

Michelson, A. D. (1996). "Flow cytometry: a clinical test of platelet function." Blood **87**(12): 4925-4936.

Osada, T., A. Itoh, et al. (2003). "Mapping of the receptor-associated protein (RAP) binding proteins on living fibroblast cells using an atomic force microscope." Ultramicroscopy **97**(1-4): 353-357.

Plow, E. and S. Shattil (2001). Integrin alpha IIb ß3 and platelet aggregation. Philadelphia, Lippincott Williams and Wilkins.

Radmacher, M. (1997). "Measuring the elastic properties of biological samples with the AFM." Engineering in Medicine and Biology Magazine, IEEE **16**(2): 47-57.

Reviakine, I. and A. Brisson (2000). "Formation of supported phospholipid bilayers from unilamellar vesicles investigated by atomic force microscopy." Langmuir **16**: 1806-1815.

Roach, P., D. Farrar, et al. (2005). "Interpretation of protein adsorption: surface-induced conformational changes." J. Am. Chem. Soc. **127**(22): 8168-8173.

Shiba, E., J. N. Lindon, et al. (1991). "Antibody-detectable changes in fibrinogen adsorption affecting platelet activation on polymer surfaces." Am J Physiol Cell Physiol **260**(5): C965-974.

Siediecki, C., B. Lestini, et al. (1996). "Shear-dependent changes in the three-dimensional structure of human von Willebrand factor." Blood **88**(8): 2939-2950.

Sit, P. and R. Marchant (1999). "Surface-dependent conformations of human fibrinogen observed by atomic force microscopy under aqueous conditions." Thromb Haemost **82**: 1053–60.

Soman, P., Z. Rice, et al. (In press). "Immunological identification of fibrinogen in dual-component protein films by AFM imaging." Micron.

Ta, T. C. and M. T. McDermott (2000). "Mapping interfacial chemistry induced variations in protein adsorption with scanning force microscopy." Anal. Chem. **72**(11): 2627-2634.

Tamada, Y., E. Kulik, et al. (1995). "Simple method for platelet counting." Biomaterials **16**: 259-261.

Toscano, A. and M. Santore (2006). "Fibrinogen adsorption on three silica-based surfaces: conformation and kinetics." Langmuir **22**(6): 2588-2597.

Touhami, A., B. Nysten, et al. (2003). "Nanoscale mapping of the elasticity of microbial cells by atomic force microscopy." Langmuir **19**(11): 4539-4543.

Tsai, W., J. Grunkemeier, et al. (2003). "Variations in the ability of adsorbed fibrinogen to mediate platelet adhesion to polystyrene-based materials: A multivariate statistical analysis of antibody binding to the platelet binding sites of fibrinogen." Journal of Biomedical Materials Research Part A **67A**(4): 1255-1268.

Tunc, S., M. F. Maitz, et al. (2005). "In situ conformational analysis of fibrinogen adsorbed on Si surfaces." Colloids and Surfaces B: Biointerfaces **42**(3-4): 219-225.

Wang, J., X. Chen, et al. (2006). "Vibrational spectroscopic studies on fibrinogen adsorption at polystyrene/protein solution interfaces: hydrophobic side chain and secondary structure changes." J. Phys. Chem. B **110**(10): 5017-5024.

Wei-Bor Tsai, J. M. G., Thomas A. Horbett, (2003). "Variations in the ability of adsorbed fibrinogen to mediate platelet adhesion to polystyrene-based materials: A multivariate statistical analysis of antibody binding to the platelet binding sites of fibrinogen." Journal of Biomedical Materials Research Part A **67A**(4): 1255-1268.

Wu, Y., F. Simonovsky, et al. (2005). "The role of adsorbed fibrinogen in platelet adhesion to polyurethane surfaces: A comparison of surface hydrophobicity, protein adsorption, monoclonal antibody binding, and platelet adhesion." Journal of Biomedical Materials Research Part A **74A**(4): 722-738.

Chapter 4

Effects of Competitive Protein Adsorption on Functional Activity of Adsorbed Fibrinogen

4.1 Introduction

Competitive adsorption of proteins is important in the many interfacial phenomena that occur in the presence of mixture of proteins. These phenomena include blood and tissue compatibility of biomaterials(Lassen et al. 1996; Zhuo et al. 2007), cell culture on solid supports(McFarland et al. 2000), bacterial adhesion to implanted materials(Liu et al. 2008), protein fouling during food processing (Santos et al. 2006). In context of blood-biomaterial interactions, the general consensus is that upon contact with any protein-rich media such as plasma, surface becomes associated or adsorbed with a layer of multi-proteins, and subsequent cellular responses are largely mediated by the bioactivity and the total amount of proteins.

In case of plasma adsorption studies on biomaterials, more than 500 different proteins are involved. This constitutes an intricate case of competitive adsorption which is a result of a complex interplay between transports of various molecules to the surface region. Moreover, it is also necessary to take into account the effects of protein displacement by other proteins, an effect first observed by Vroman and collegues while investigating the response of surfaces to blood plasma nearly 35 years ago. Fibrinogen, an abundant protein playing a central role in blood coagulation, was found to adsorb onto

surfaces, only to be displaced by higher molecular weight plasma proteins (HMWK) and this effect is widely known in the literature as the 'Vroman effect'. Early explanations were sought from biochemical mechanisms such as higher affinity of HMWK for surface as compared to fibrinogen. However over the years such mechanisms alone are not adequate to explain certain aberrations, for example the relative resistance of human serum albumin (HSA) to displacement at hydrophobic surfaces. Vogler and associates demonstrated that a protein-size discrimination results in selective adsorption of smaller proteins from a mixture of larger-and-smaller proteins.(Krishnan et al. 2004; Noh et al. 2007) Vogler used mass-balance equations to propose that the so-called Vroman's effect is the result of selective pressure imposed by a fixed interfacial-concentration capacity specific to surface properties and suggested that this effect, atleast in part, is due to a purely physical process unrelated to protein biochemistry or protein-adsorption kinetics.

Several groups have investigated protein adsorption from much simpler single, binary and tertiary protein mixtures on a variety of surfaces using several orders of dilution. Lassen and Malmsten investigated single, binary, and ternary protein solutions of human serum albumin (HSA), IgG, and fibrinogen (Fgn) and found that adsorbed HSA is not displaced by IgG and/or Fgn to any large extent. IgG and HSA dominate the adsorption from the ternary protein mixture, although fibrinogen is also present in the adsorbed layer to a smaller extent.(Lassen and Malmsten 1996) Ying et al. used atomic force microscopy (AFM) and imaging ellipsometry to study competitive adsorption of collagen and bovine serum albumin (BSA) on model hydrophilic and hydrophobic substrates(Ying et al. 2002). The competitive adsorption between collagen and BSA showed that serum albumin preferentially adsorbed onto a hydrophobic surface, while

collagen adsorbed on a hydrophilic surface. In the binary solution of BSA (1 mg/ml BSA) and collagen (0.1 mg/ml), nearly 100% of the protein adsorbed onto the hydrophobic surface was BSA, but on the hydrophilic surface only about 6% was BSA. Ta et al. used Scanning force microscopy (SFM) to examine bovine serum albumin (BSA) films adsorbed on highly oriented pyrolytic graphite (HOPG) and observed no displacement of the BSA during the time-scale of the experiment.(Ta et al. 2003)

Biological activity of proteins has been studied on various surfaces using competitive protein adsorption. The biomaterial literature describes protein activity as a function of the total amount of adsorbed proteins, the conformational/orientation state of protein and the properties of surface. Steele describes the ability of the proteins to express/expose specific epitopes as 'molecular potency'(Steele et al. 1993). There is evidence in the literature that conformational changes in the γ chain dodecapeptide sequence (HHLGGAKQAGDV) of adsorbed fibrinogen exposes the otherwise-inaccessible platelet-binding epitopes(Shiba et al. 1991; Balasubramanian et al. 1999; Michel et al. 2005; Chiumiento et al. 2007). Molecular potency or biological/functional activity in our experiment can be defined as the ability of an adsorbed fibrinogen molecule to expose dodecapeptide epitopes necessary for subsequent platelet interactions.

There are several papers showing that, predicting cellular response by considering only the total amount of adhesive protein on the surface is insufficient. Surface properties have enormous effects on the biological activity of proteins by variations in the degree of retention of native structure upon adsorption. Perhaps the broadest, most widely accepted generalization regarding surface properties concerns hydrophobicity and holds that the more the hydrophobicity, greater is the extent of adsorption. There is abundant evidence

showing that the biological activity or molecular potency of adsorbed proteins strongly depends on the type of surface to which it adsorbed. Grainger's lab used monoclonal antibody against RGD cell binding domain to study biological activity of fibronectin on carboxyl and methyl terminated SAMs. The fraction of fibronectin on methyl-terminated SAM able to bind the mAb was much lower (10% mol/mol) as compared to carboxyl-terminated SAM (25% mol/mol). When albumin was coadsorbed, the ratios increased to 21 and 39% on methyl and carboxyl SAMs respectively.(Mcclary et al. 2000). Similar studies by Garcia found that antibody-binding affinity is much higher for fibrinectin adsorbed on the OH SAM than on the other surfaces(Benjamin G. Keselowsky 2003). Concentration of the adsorbing protein also has influence on the exposure of various epitopes. Garcia and his collaborators carried out studies using either untreated or tissue culture polystyrene(García et al. 1999). They found that some mAbs bind better to tissue culture polystyrene than to plain polystyrene while some other antibodies show the contrary results. In these experiments, concentration played a vital part since this effect was only observed at lower amounts of adsorbed fibronectin. This difference is probably observed as a result of conformational changes in fibronectin as a function of concentration.

Biological activity of adsorbed proteins is also affected by the residence time or the time elapsed after adsorption of a protein at a particular site on a surface. Upon adsorption, with increase in residence time, the molecule tends to undergo conformational changes. The effects of these changes for single protein solution are different than that of complicated multiprotein or even binary protein solutions. Studies by Horbett using fibrinogen found that antibody binding was a function of residence time

and vary greatly with the target mAb used for these experiments. Horbett observed both an increase and decrease in binding of some antibodies while some other antibodies remaining unchanged with residence time on the surface. (Horbett et al. 1994). Several studies using similar approach have shown formation/exposure of previously unexposed sites after adsorption of fibrinogen. Plow showed that excess fibrinogen addition to the antibody solution did not prevent the binding of the antibody to adsorbed fibrinogen or fibrinogen on the surface. (Zamarron et al. 1990). Similar studies, confirmed that fibrinogen undergoes some conformational changes thereby exposing neoepitopes that are only exposed after adsorption.

Variations in conformation or in exposure of specific epitopes of adsorbed adhesion proteins affect cellular response due to surface properties like hydrophilicity, concentration of the adsorbing proteins and the residence time of certain proteins on substrates. It's been observed that chemically different surfaces with similar amounts of adsorbed proteins exhibit differences in cell adhesion. Kiaei et al. demonstrated that fibrinogen adsorbed to CF3 rich plasma treated surface does not support platelet adhesion as well as fibrinogen adsorbed to tetrafluoroethylene (TFE), even though similar amounts of fibrinogen on both substrates(Kiaei et al. 1995). Tang's group also used P1 and P2, antibodies against specific sequence of the gamma chain of fibrinogen to study phagocyte adhesion on five different polymers(Tang et al. 1996). There was a rough linier correlation between phagocyte adhesion and exposure of P1/P2 sites which are previously hidden in the molecule. Garcia and his colleagues showed that myoblast proliferation and differentiation was affected by the state of the adsorbed fibronectin. (García, Vega et al. 1999). His studies demonstrated that for carboxyl-terminated SAM,

high levels of fibronectin cell binding domain accessibility detected by several mAbs correlate with high degree of cell attachment, spreading and growth. Additionally, for methyl-terminated SAM, lower amounts of cell-binding domain availability correlates with lower fibroblast interactions. The authors found that coadsorbed albumin enhanced the ability of fibronectin to bind to antibody specific to cell domain on both surfaces. However, on methyl-terminated SAM, this enhancement of the fibronectin ability or functional activity was not enough to overcome the accompanying decrease in the total amount of adsorbed fibronectin.

Our lab has reported a good correlation between the functional activity of adsorbed fibrinogen (molecular potency) and the subsequent cellular response (platelet adhesion) using atomic force microscopy(Soman et al. 2008). It is very well possible that any cellular response depends only upon the number of functional moieties exposed/available for interactions with cellular elements. Factors like concentration, competitive protein adsorption, residence time and surface properties affect subsequent cellular events (platelet adhesion) ONLY by changing the functional activity of adsorbed proteins. For example, in this chapter, increase in fibrinogen concentration results in an increase in platelet adhesion ONLY by an increase in the number of dodecapeptide sequences on the surface. Any increase or decrease in fibrinogen activity is ONLY due to corresponding increase or decrease in the number of active epitopes. The AFM technique developed in chapter 3 provides a new tool to investigate the complex process of protein adsorption. This chapter will quantify the effects of competitive protein adsorption and concentration on the biological activity at a molecular scale on mica substrate and correlate to macroscale platelet adhesion results under similar conditions.

4.2 Materials and methods

4.2.1 General

Phosphate buffered saline (PBS, 0.01 M sodium phosphate buffer, 150mM NaCl, pH 7.4, Sigma Inc.) was prepared using water from a Millipore Simplicity 185 system (18 MΩ) which utilizes two ultraviolet filters (185 and 254 nm) to reduce carbon contaminants. Human fibrinogen (90% clottable) was used as received from Calbiochem, La Jolla, CA. Monoclonal mouse anti-fibrinogen gamma chain (γ 392 – 411; clone: 4 -2; Isotype: IgG1) was obtained from Accurate Chemicals and Scientific Corporation, NY. Bovine serum albumin (BSA) was obtained from Sigma Chemicals Co, St. Louis, MO. Coli S69 (IgG_1 isotype control) was obtained from the Washington State University Monoclonal Antibody Center (WSUMAC). All the proteins were dissolved in phosphate buffer and aliquots were stored at -20°C until use.

4.2.2 AFM Imaging

All images were acquired in tapping mode (intermittent contact mode) with a Nanoscope IIIa Multimode® AFM (Digital Instruments, CA) under aqueous PBS buffer using short thick cantilever silicon nitride probes (NP – S; spring constant ~ 0.6 N/m^2, Digital Instruments, CA). Topographic images and phase images were captured at 256 x 256 pixels resolution with scan size of 2 x 2 μm^2, which is the same scan size used for all the AFM force spectroscopy experiments on adsorbed protein layer. All imaging was carried out at a scan rate of 1 Hz with a resonant frequency of ~9.37 kHz. The AFM probe free

amplitude of oscillation and r_{sp} values were fixed at 20 nm and 0.75, respectively, for all images. AFM images were flattened using a first order line fit and low pass filtered to remove high frequency noise spikes from the images.

4.2.3 Force Spectroscopy Measurements

Probe was modified with either monoclonal antibody (25 μg/ml) that recognize fibrinogen γ392-411, a region that includes the platelet binding dodecapeptide sequence γ402-411 as described in chapter 3. Modified tips were stored in PBS (10 mM, pH 7.4) at 4°C and used within 2 days. Freshly cleaved muscovite mica sheets (10 mm x 10 mm, Ted Pella, Inc) were used as substrates for protein adsorption experiments. Bovine serum albumin or fibrinogen solutions in PBS with two different concentrations (100 and 1000 μg/ml) were adsorbed onto mica substrates in various ratios (100:0, 90:10, 50:50, 10:90 and 0:100) for 5 minutes in an external fluid cell. Remaining free protein was washed away for 3 minutes using a syringe pump that provides a steady flow of PBS at 0.3 ml/min. All data was collected using a Nanoscope III Multimode AFM (Digital Instruments, CA) under buffer conditions in a fluid cell. The hydrated protein sample was loaded onto the microscope and data was collected using the monoclonal anti-fibrinogen-modified probes under buffer. The ramp size (500nm) and trigger threshold (100nm) were kept constant while the scan size (500nm-5000nm) and scan rate (0.3 Hz – 0.75 Hz) were varied. Images were collected as 16 x 16 and 32 x 32 force arrays with 256 data points per force curve.

4.2.4 AFM data analysis

Data was analyzed as explained in chapter 3. Briefly, the deflection of cantilever is translated into a force value with tools developed in MatLab™ (The Mathworks Inc., MA). BSA adsorbed on mica substrates for 5 minutes was used as a negative control for non-specific interactions of the antibody. The non-specific force-distance data for each modified probe was extracted from the AFM files and analyzed off-line and a 95% confidence interval was determined for each tip as $\mu \pm 2\sigma$ and this force was subsequently used as a cut-off value for differentiating between non-specific and specific mAb-fibrinogen interactions. Time-dependent force data from multiple experiments ($n \geq 3$ for every time point) was converted to probability data. The mean probability of detecting a specific event on mica substrate was plotted as a function of protein residence time.

4.2.5 Platelet adhesion

Previous concerns about functionality of salvaged platelets from the blood bank were taken under consideration and fresh human platelets were used for all experiments. Whole blood was drawn slowly by venipuncture from healthy human donors into a syringe containing EDTA anticoagulant (BD; K2 EDTA spray-dried, #366643) at a facility in Hershey Medical Center. The protocols approved by Institutional Review Board were followed and all subjects enrolled in this research signed an informed consent form. The donor denied taking any medications, including aspirin, during the preceding 2 weeks. Platelet-rich plasma (PRP) was harvested by centrifugation at 180g for 20 min at room temperature. The PRP was centrifuged at 400g for 20 min at room temperature to

get a pellet of platelets. The supernatant was discarded and the platelet pellets were gently resuspended in PBS. The platelet washing procedure was repeated three times and platelet concentration was determined with a Sysmex XE 2100 (Sysmex, Kobe, Japan). . Washed platelets were mixed to give a final suspension of a physiologically relevant platelet concentration (250 x 10^3 /µL).

4.2.6 Mixed protein experiments

Freshly cleaved mica samples of diameter 9.9mm were incubated in 0.5 ml of fibrinogen solution in varying concentration (1mg/ml and 100 µg/mL in PBS) and ratios with bovine serum albumin (Fib:BSA(w/w)= 100:0; 90:10; 50:50; 10:90 and 0:100) for 5 minutes in a 24 well plate at room temperature. Samples were subsequently rinsed with PBS (3 times with 0.5 ml/well) and allowed to incubate in PBS for 15, 30, 45, 60, 75, 90, 105 and 120 minutes. Platelet solution (~0.5 ml) recalcified with 2.5 mM $CaCl_2$ was added to the well plates and incubated for 10 min at room temperature, such that the mica samples are completely immersed in the platelet solution. The platelet solution was aspirated and samples were rinsed 5x with PBS (0.5 ml/rinse). PBS was replaced by adding 1 % PFA (~0.5ml) and was incubated for 60min at room temperature. The PFA was replaced by adding PBS making sure that the sample is always submerged in solution. A primary antibody solution was prepared by combining 1.5ml of 6 % normal serum (Jackson ImmunoResearch Lab,Inc.) and 1.24µl mouse anti-human $\alpha_{IIb}\beta_3$ antibody (ab662; Abcam Inc). This monoclonal antibody labels all the platelets adhered to the mica samples. Primary antibody solution was added to each sample (0.5ml for each well)

and incubated overnight at 4°C. The samples are washed with PBS (5x) to remove the primary antibody solution ensuring that the mica surface remains submerged. A secondary antibody solution is prepared by combining 1ml of 6 % normal goat serum (Jackson ImmunoResearch Lab, Inc) and 10µl alexa fluoro 555 goat anti-mouse IgG (Invitrogen) which labels the CAPP2A antibody. Secondary antibody was added to all the samples and incubated in dark at room temperature for 60 min. All the samples were rinsed with PBS (0.5 ml, 3x) and placed on a microscope slide with 50 µl anti-fade solution (Biomeda). Labeled platelets were imaged and counted at 40x resolution (actual size = 220µm x 170µm) counted and normalized using fluorescent microscopy (Eclipse 80i, Nikon). A minimum of 3 samples were analyzed for each condition with a minimum of 3 images per sample.

4.2.7 Statistical analysis

A minimum of 3 independent experiments were performed for each measurement. Statistical differences were determined using One-way Analysis of Variance (ANOVA) with post test (Tukey-Kramer Multiple Comparisons Test) with atleast $P<0.05$ being considered significant.

4.3 Results

4.3.1 AFM Imaging

A series of experiment with binary solutions with varying ratios were performed. Typical AFM images of 2 concentrations and 3 different ratios are shown in Figure **4-1**. The RMS roughness changes as the ratio of fibrinogen is increased from 90% to 10% for both the concentrations. The roughness also increases with an increase in concentration from 100μg/ml to 1mg/ml (RMS roughness range = 1.3nm to 5.76nm). AFM topographical images provide no information about the total amount or the biological activity of fibrinogen on mica. This illustrates a critical limitation of the AFM when it is used for studying protein adsorption especially mixed protein experiment with concentrations close to physiological concentrations. No identifiable protein shape or size (either BSA or fibrinogen) was identified in these images.

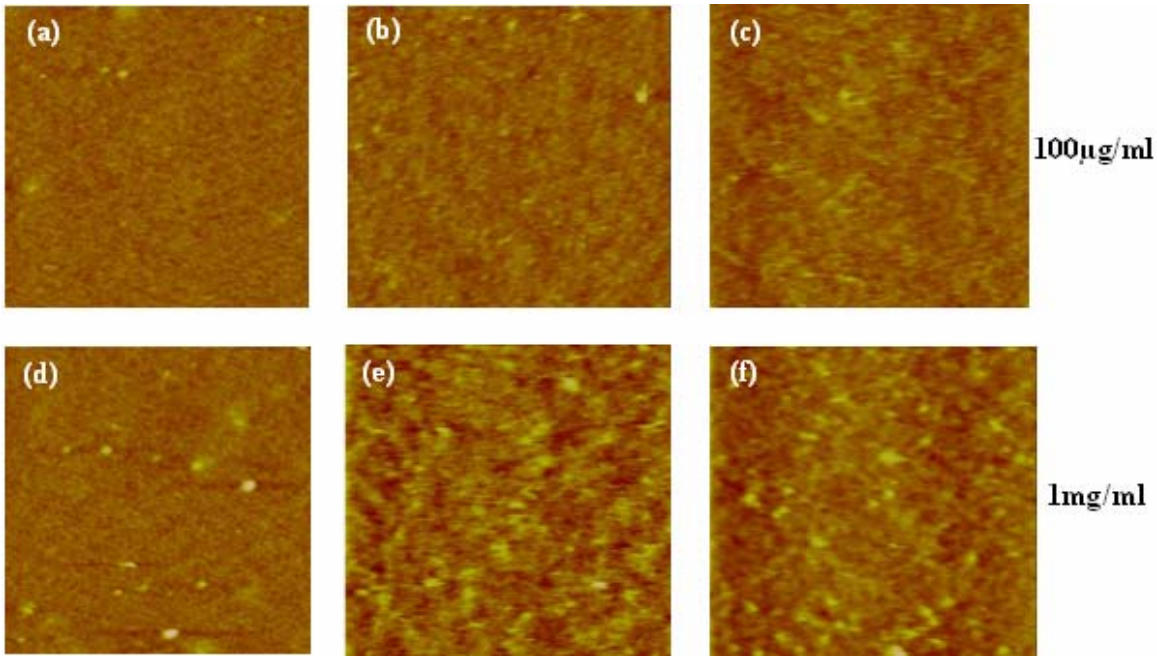

Figure **4-1**: AFM tapping mode images in PBS buffer with varying concentration and albumin co-adsorption ratios by weight: (a) 1mg/ml with Fib:BSA=10:90 (b) 1mg/ml with Fib:BSA=50:50 (c) 1mg/ml with Fib:BSA=90:10 (d) 100µg/ml with Fib:BSA=10:90 (e) 100µg/ml with Fib:BSA=50:50 and (f) 100µg/ml with Fib:BSA=90:10

4.3.2 Functional activity of fibrinogen

A monoclonal antibody recognizing a region that includes the platelet binding epitope of the γ-chain dodecapeptide (γ 400-411) was used to collect rupture force measurements as a function of fibrinogen residence times. As described in the methods section, for every AFM probe, a control experiment was carried out which is used to separate specific fibrinogen-mAb rupture forces from non-specific interactions. Force curves were obtained from control experiments to evaluate the interactions between BSA adsorbed on mica and a mAb-modified probe. Albumin is one of the most abundant proteins in serum or plasma and is often used as a passivating agent to prevent the adhesion of cells.(Ying

et al. 2002) Many investigators have tried to develop biomaterials that would adsorb layers enriched in passivating proteins like albumin and depleted of activation proteins like fibrinogen. In this project, fibrinogen was adsorbed on mica substrates in different concentrations and co-adsorbed with BSA and the monoclonal antibody modified probes were used to obtain rupture force and length measurements. Data obtained spatially was converted to the appropriate time of measurement and probability of antigen recognition at that time as described in the methods section.

Figure **4-2** illustrates recognition probabilities of detection of dodecapeptide sequence in 3 different conditions using 1mg/ml as the total protein concentration. As we increase the ratio of BSA in the binary protein solution, the functional activity peak shifts towards earlier residence times. Co-adsorption with BSA does not improve biological activity of fibrinogen, but merely shift the maximal activity at earlier time-points. For 100% fibrinogen concentration, we observe a peak in biological activity at ~45min post-adsorption time, similar to one discussed in chapter 3. For 50% fibrinogen ratio, a peak in activity can still be observed however this peak occurs at 40min instead of 45min with 100% fibrinogen. With 10% fibrinogen, we see a drastic shift in the activity of fibrinogen. Since it's not trivial to get AFM reading in time-points in the range of 0-10mins, we cannot confirm the existence of a functional activity peak in that range. The activity of fibrinogen is highest at 20min post-adsorption time or residence time and drastically decreases with increasing residence time. It is very well possible, that there is no activity peak for 10% fibrinogen, but it is also possible that the peak shift to an earlier residence time (0-10min), and therefore we are not able to detect it due to experimental limitations.

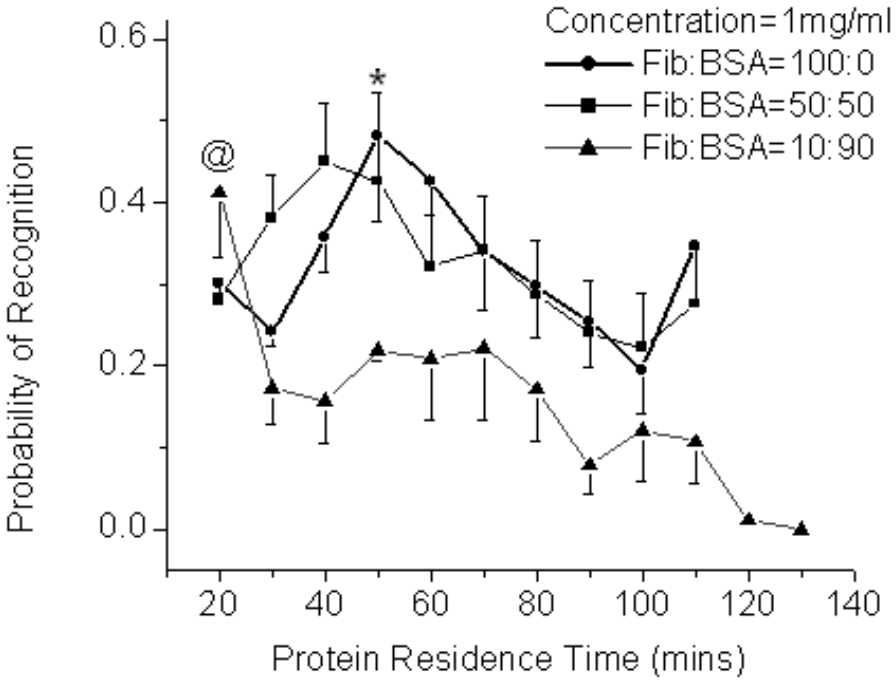

Figure **4-2**: Pooled data from multiple experiments ($n \geq 3$ for each time-range) showing the functional activity of adsorbed fibrinogen on mica substrate when co-adsorbed with BSA at varying ratios: Note: For statistical analysis, data from specific time-range (10-20, 30-40, 60-70 and 100-110min) was pooled to calculate recognition probability at 15, 45, 75 and 105min time-points. (*) - For 100% fibrinogen, recognition probability peaks at ~45 minutes post-adsorption and thereafter decreases with increasing residence time and is statically significant. Similar trend is observed for 50% fibrinogen. (@) - For 10% fibrinogen, the activity peaks at 15mins and drastically decreases with residence time. Activity at 15min is statistically significant that all other time points.

Figure **4-3** illustrates recognition probabilities of detection of dodecapeptide sequence in 3 different conditions using 100µg/ml as the protein concentration. For 100% fibrinogen in the binary protein layer on mica, we observe that the biological activity increases with residence time, reaches a peak at 45mins post-adsorption and then decreases with increase in residence time. With 50% fibrinogen, there is a drastic shift in the activity of fibrinogen. The maximum activity is detected at 15min residence time and steadily decreases with residence time. The rate of decrease is drastic from 15 min to 30 min and

then follows a noisy trend albeit still decreasing in residence time. With 10% fibrinogen, we are not able to detect any distinct peak in its activity and the functional activity remains steady in the probability range of 0-0.1.

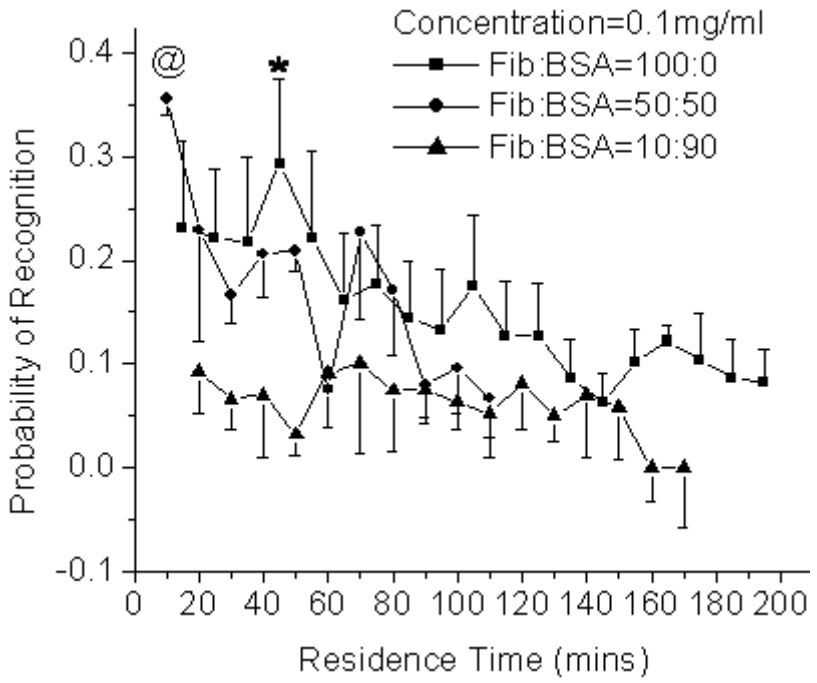

Figure **4-3**: Pooled data from multiple experiments (n ≥ 3 for each time-range) showing the functional activity of adsorbed fibrinogen on mica substrate when co-adsorbed with BSA at varying ratios: Note: For statistical analysis, data from specific time-range (10-20, 30-40, 60-70 and 100-110min) was pooled to calculate recognition probability at 15, 45, 75 and 105min time-points. (*) – For 100% fibrinogen, the activity at 45 minutes fibrinogen residence time is significantly greater than all time points ≥65 minutes ($P<0.001$). (@) - Fibrinogen activity at 15min was significantly greater than 75 and 105min time-point ($P<0.0245$)

Control experiments similar to experiments explained in chapter 3 were conducted to confirm that the activity of fibrinogen is a time-dependent process rather than an artifact of antibody/probe degradation after prolonged periods of scanning. A major factor which governs competitive protein adsorption is the relative concentration of the competing

proteins. For example, increase in concentration of fibrinogen in plasma results in increase in the amount of fibrinogen adsorbed to surfaces. Similarly, it has been shown that the adsorption of fibrinogen from binary mixtures decreases as the concentration of the competing species increases. However, in the presence of an inert protein like BSA, there have been conflicting results about the biological activity of fibrinogen when researchers tried to correlate protein adsorption data with cellular events data including platelet adhesion.

4.3.3 Platelet Adhesion

Platelet adhesion studies were carried out in an attempt to correlate macroscale cellular event like platelet adhesion to molecular functional activity in the presence of binary protein layer on mica.

Fluorescence microscopy was used to determine platelet adhesion (number of platelets per unit area - μm^2). Figure **4-4** shows characteristic images of platelet on mica substrate with varying ratios of Fibrinogen and BSA at 1mg/ml concentration. The number of platelets increases with an increase in the ratio of fibrinogen in the binary mixture. At 90% fibrinogen, some of the platelets are activated, whereas for 10% fibrinogen, we see minimal activation.

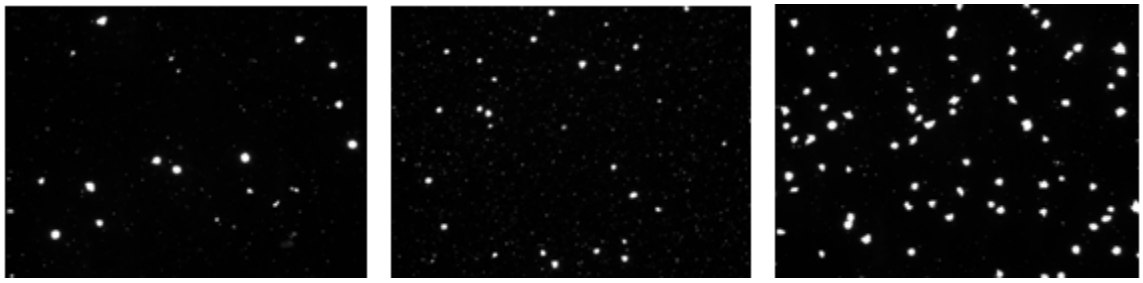

Figure **4-4**: Characteristic fluorescence microscopy images of platelets at residence time 45min post-adsorption at 1mg/ml concentration with varying ratios: (a) Fib:BSA = 10:90 (b) Fib:BSA = 50:50 and (c) Fib:BSA = 90:10. Platelets were labeled with ab662 mouse anti-human $\alpha_{IIb}\beta_3$ primary antibody and alexa fluoro 555 goat anti-mouse IgG which labels the ab662 antibody.

Care should be taken while handling/separating platelets from human blood. There is always a problem of platelet activation as shown in figure **4-5** . We have tried different techniques mainly platelet separation by centrifugation at various speeds or by Sepharose separating gel (Sigma-Aldrich). Figure 4-5 shows characteristic images with different conditions of concentration, ratio and residence time. There are no differences in platelet adhesion and activation in any of these conditions. Upon platelet activation, they become sticky and probably adhere to all surfaces and no longer are a function of concentration, residence time or concentration. For the result discussed in this chapter, both the centrifugation speed and blood handling procedure has been optimized to cause minimal platelet activation.

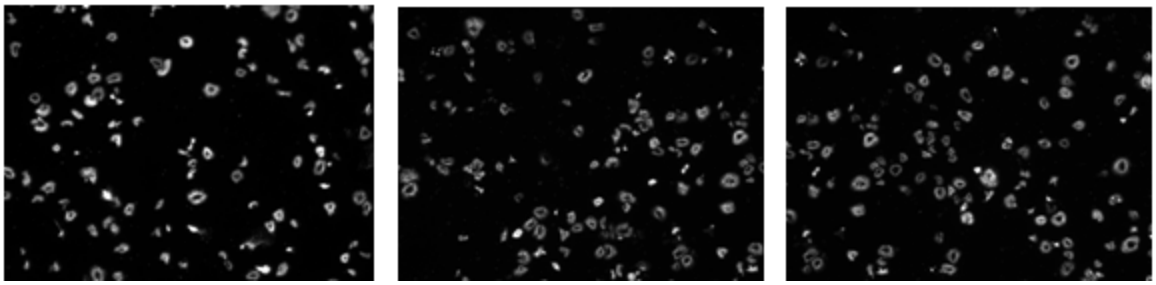

Figure **4-5**: Typical fluorescence microscopy images of platelet adhesion/activation due to presence of some plasma proteins in the pure platelet solution used for adsorption studies: (a) 1mg/ml; Fib:BSA = 90:10; residence time=45min, (b) 1mg/ml; Fib:BSA = 10:90; residence time=15min and (c)100µg/ml; Fib:BSA = 50:50; residence time=15min. Following platelet activation, the number of adhered platelets do not depend on concentration of the protein solution or residence time or the ratio by weight of binary proteins.

In a previous study, our lab has shown that for 100µg/ml fibrinogen concentration, platelet adhesion correlates very well with functional activity of fibrinogen at a molecular scale(Soman, Rice et al. 2008). The introduction of BSA changes fibrinogen activity towards earlier time-points, an effect also seen in the AFM experiments (Fig **4-6**). For both 90% and 50% fibrinogen, we see activity peak at 15min and then a steady decrease with increasing residence times. At 10% and 0% fibrinogen, we observe no changes in the platelet adhesion with mean platelet count of 5 and 1 platelets respectively. For 50% fibrinogen, the data correlates very well with the AFM data which also peaks at 15mins residence time and decreases with increase in residence times. For 10% fibrinogen, the AFM data records very low fibrinogen activity with no change with residence time, also correlating very well with platelet adhesion data. In summary, when coadsorbed with BSA, the activity peak shifts dramatically to the earlier time points suggesting that the

dodecapeptide sequence are most active or exposed for binding ~15min and decrease with increasing residence time.

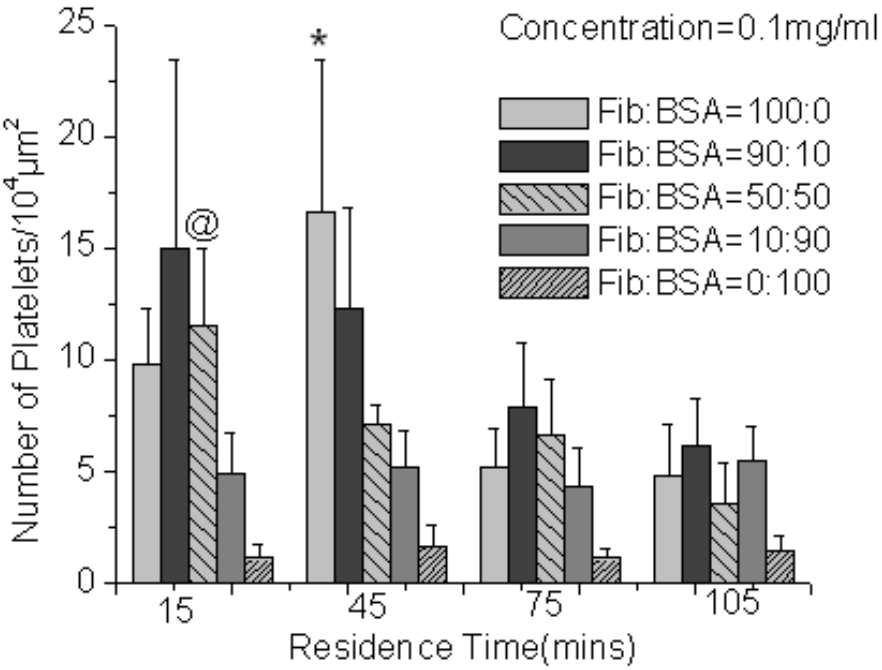

Figure **4-6**: Pooled data from multiple experiments ($n \geq 3$ for each time point) showing Platelet adhesion as a function of protein residence time on mica substrate: Protein concentration = 100μg/ml and varying ratios by weight of human fibrinogen and bovine serum albumin. For 100% fibrinogen or a pure fibrinogen solution, (*) platelet adhesion at 45min residence time is not significantly greater than 45min, however is greater ($P<0.05$) than both 75 and 105min. Maximal platelet adhesion at 45min correlate well with AFM data. For 90% fibrinogen, there is no statiscal significance, however the trend suggest a shift of platelet adhesion toward 15min residence times and steadily decreases with residence times. For 50% fibrinogen, (@) platelet adhesion at 15min was significantly greater than 105min ($P<0.01$). For both 10% and 0% fibrinogen, there is no change in platelet adhesion as a function of residence time.

For 1mg/ml concentration on mica substrate, we observe similar trend with peak activity occurring at 45min residence time (Figure **4-7**). For pure fibrinogen solution or 100% fibrinogen, the platelet adhesion increases from 22 at 15min residence time to 50 at

45min residence time and then decreases with further increase in residence time. As we go on decreasing the concentration from 100% fibrinogen to 90% fibrinogen, the overall platelet adhesion trend remains the same, with maximal platelet adhesion occurring at 45min residence time. However, we see a shift in the platelet adhesion peak at increasing BSA concentrations (50%, 10% and 0% fibrinogen). At 50% fibrinogen, the platelet adhesion is maximal (33) at 15min residence time and steadily goes on decreasing with residence time. This does not correlate with the molecular AFM data for recognition probability seen in figure 4-2. The net shift in the maximum activity of fibrinogen in fig 4-2 is very small (from ~45min to ~40min, when fibrinogen ratio is changed from 100% to 50%) as compared to the macroscale platelet adhesion results where the shift in the peak is significant (from ~45 min to ~15min, for similar conditions).At 10% fibrinogen, the maximum platelet adhesion occurs at 15min, albeit not statistically different. However, the general trend correlates with the molecular data in fig 4-2a. For 0% fibrinogen or pure BSA solution, there is no change in platelet adhesion with residence time and is in the range of ~5 platelets per unit area. This demonstrates some non-specific adhesion of platelets. AFM experiments with mixed protein demonstrate that coadsorption of BSA with fibrinogen leads to a shift in the probability recognition peak (Refer Fig 4-2 and 4-3). Most of the platelet adhesion results correlate very well with the AFM data (Refer Fig 4-6 and 4-7).

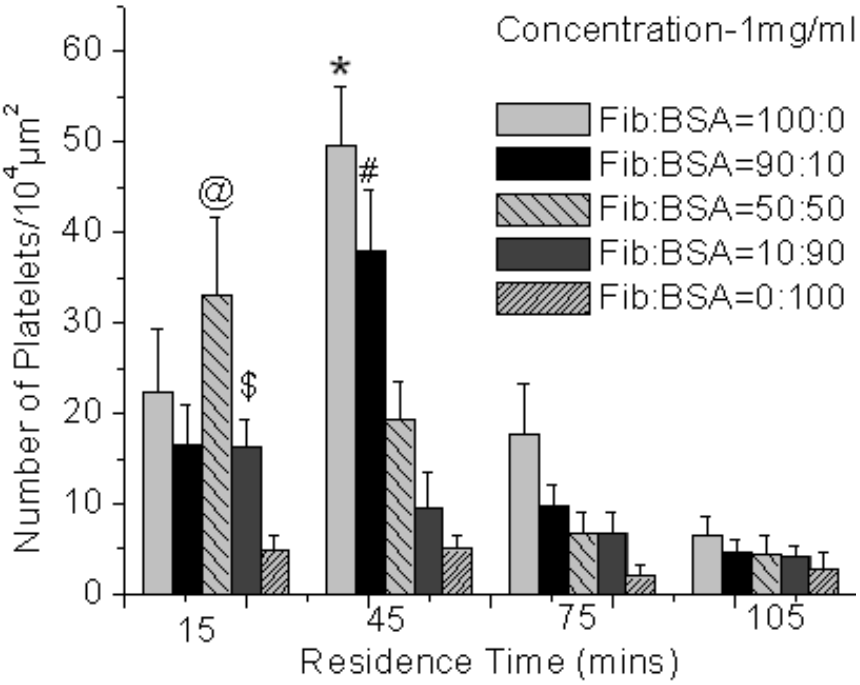

Figure **4-7**: Pooled data from multiple experiments ($n \geq 3$ for each time point) showing platelet adhesion as a function of protein residence time on mica substrate: Protein concentration = 1mg/ml and varing ratios by weight of human fibrinogen and bovine serum albumin. For 100% fibrinogen or a pure fibrinogen solution, (*) platelet adhesion at 45min residence time is significantly greater ($P<0.001$) than 45, 75 and 105min. For 90% fibrinogen, (#) platelet adhesion at 45min was not significantly greater that 15min time point but was greater ($P<0.001$) than 75 and 105min. For 50% fibrinogen, (@) platelet adhesion at 15min was significantly greater that 45min ($P<0.01$) and 75/105min ($P<0.001$). For 10% fibrinogen, ($) platelet adhesion at 15min was not significantly greater that 45min but is significantly greater than 75 ($P<0.01$) and 105 ($P<0.001$) time points. For 0% fibrinogen or basically a pure BSA solution.

4.4 Discussion

Competitive protein adsorption is a very complicated process. A rigorous description of the process of competitive of proteins will have to include both a complete molecularly based model as well as the inclusion of the rate of transport of the various species. In this

project, we have taken a more functional approach to find the exposure of specific epitope responsible for subsequent cellular events. Because of the complex and time-dependent nature of protein adsorption, the only reliable way to characterize the competitive adsorption effectiveness of different proteins is to compare them under identical conditions on a given surface. In this project, mica substrate is used for all experiments and the effects of the residence time, concentration and competitive protein adsorption of fibrinogen and BSA on the functional activity of fibrinogen are investigated.

When proteins such as BSA and fibrinogen arrive at the biomaterial interface, they undergo some kind of conformational changes/relaxation in a time dependent manner, which may lead to exposure of certain epitopes as a function of residence time. In some cases if the change is rapid occurring in the time scale of seconds to few minutes, this experimental procedure won't be able to detect any changes as a function of residence times. In the results, for example, any changes in activity of fibrinogen in the time-range of 0-10mins residence time cannot be captured.

In the AFM data, we observe several functional activity peaks as measured by the probability of recognition of the dodecapeptide sequence as a function of time. The finite time required for reaching the activity peak and the duration of time it stays at this highly active state is a key point, because it allows for maximal platelet adhesion. Competitive protein adsorption with BSA might prevent fibrinogen from ever achieving the active state. Co-adsorption with BSA affects the conformational changes of fibrinogen at the surface either by steric hinderances which might either subjugate or accentuate fibrinogen activity by either preventing or assisting the molecule to achieve its most active state. For

example, at residence time of 15min, an increase in the activity is observed when fibrinogen ratio decreases from 100% to 50% (Refer fig 4-3). At residence time of 15min, recognition probability for 50% fibrinogen is ~3.5 as opposed to ~0.3 in case of 100% fibrinogen. In the case of 1mg/ml concentration, there are no changes in the maximum activity when fibrinogen ratios are varied; however, a distinct shift in the occurrence of activity peak is clearly seen.

4.5 References

Balasubramanian, V., N. Grusin, et al. (1999). "Residence-time dependent changes in fibrinogen adsorbed to polymeric biomaterials." J Biomed Mater Res A **44**: 253-260.

Benjamin G. Keselowsky, D. M. C. A. J. G. (2003). "Surface chemistry modulates fibronectin conformation and directs integrin binding and specificity to control cell adhesion." Journal of Biomedical Materials Research Part A **66A**(2): 247-259.

Chiumiento, A., S. Lamponi, et al. (2007). "Role of fibrinogen conformation in platelet activation." Biomacromolecules **8**(2): 523-531.

García, A., M. Vega, et al. (1999). "Modulation of cell proliferation and differentiation through substrate-dependent changes in fibronectin conformation." Mol Biol Cell **10**(Mar): 785-98.

Horbett, T. A. and K. R. Lew (1994). "Residence time effects of monoclonal antibody binding to adsorbed fibrinogen." J. Biomater. Sci. Polymer Edn **6**(1): 15-33.

Kiaei, D., A. Hoffman, et al. (1995). "Platelet and monoclonal antibody binding to fibrinogen adsorbed on glow-discharge-deposited polymers." Journal of biomedical materials research **29**(6): 729-739.

Krishnan, A., C. A. Siedlecki, et al. (2004). "Mixology of Protein Solutions and the Vroman Effect." Langmuir **20**(12): 5071-5078.

Lassen, B. and M. Malmsten (1996). "Competitive Protein Adsorption Studied with TIRF and Ellipsometry." Journal of Colloid and Interface Science **179**: 470-477.

Liu, Y., J. Strauss, et al. (2008). "Adhesion forces between Staphylococcus epidermidis and surfaces bearing self-assembled monolayers in the presence of model proteins." Biomaterials **29**(33): 4374-4382.

Mcclary, K., T. Ugarova, et al. (2000). "Modulating fibroblast adhesion, spreading, and proliferation using self-assembled monolayer films of alkylthiolates on gold." Journal of biomedical materials research **50**(no3): 428-439.

McFarland, C., C. Thomas, et al. (2000). "Protein adsorption and cell attachment to patterned surfaces." Journal of Biomedical Materials Research **49**(2): 200-210.

Michel, R., S. Pasche, et al. (2005). "Influence of PEG architecture on protein adsorption and conformation." Langmuir **21**(26): 12327-12332.

Noh, H. and E. A. Vogler (2007). "Volumetric interpretation of protein adsorption: Competition from mixtures and the Vroman effect." Biomaterials **28**(3): 405-422.

Santos, O., T. Nylander, et al. (2006). "Whey protein adsorption onto steel surfaces--effect of temperature, flow rate, residence time and aggregation." Journal of Food Engineering **74**(4): 468-483.

Shiba, E., J. N. Lindon, et al. (1991). "Antibody-detectable changes in fibrinogen adsorption affecting platelet activation on polymer surfaces." Am J Physiol Cell Physiol **260**(5): C965-974.

Soman, P., Z. Rice, et al. (2008). "Measuring the Time-Dependent Functional Activity of Adsorbed Fibrinogen by Atomic Force Microscopy." Langmuir **24**(16): 8801-8806.

Steele, J., B. Ann Dalton, et al. (1993). "Polystyrene chemistry affects vitronectin activity: An explanation for cell attachment to tissue culture polystyrene but not to unmodified polystyrene." Journal of Biomedical Materials Research **27**(7): 927-940.

Ta, T. and M. McDermott (2003). "Investigation of dual component protein films on graphite with scanning force microscopy." Colloids and Surfaces B: Biointerfaces **32**: 191-202.

Tang, L., T. Ugarova, et al. (1996). "Molecular determinants of acute inflammatory responses to biomaterials." J. Clin. Invest. **97**(5): 1329-1334.

Ying, P., Y. Yong, et al. (2002). "Competitive protein adsorption studied with atomic force microscopy and imaging ellipsometry." Colloids and Surfaces B **15 July**.

Ying, P., Y. Yu, et al. (2002). "Competitive protein adsorption studied with atomic force microscopy and imaging ellipsometry." Colloids and Surfaces B **15 July**.

Zamarron, C., M. Ginsberg, et al. (1990). "Monoclonal antibodies specific for a conformationally altered state of fibrinogen." Thromb Haemost **Aug 13**(64(1)): 41-6.

Zhuo, R., C. A. Siedlecki, et al. (2007). "Competitive-protein adsorption in contact activation of blood factor XII." Biomaterials **28**(30): 4355-4369.

Chapter 5

Functional Activity of Fibrinogen using AFM Probe Modified with Polyethylene Glycol linker

5.1 Introduction

Many molecular recognition interactions occurring between immobilized entities, for example a platelet receptor binding to fibrinogen on a biomaterial surface, are important events in biology. The so-called lock-and-key mechanism between the ligand and the receptor has to withstand some tensile force for a required amount of time. Optimum binding between a ligand and a receptor depends not only on surmounting the activation barrier, but also on the ability of the partners to reorient (rotational diffusion) themselves for proper coupling. Force spectroscopy has recently emerged as a powerful technique for investigating protein-protein and ligand-receptor interactions at the single molecule level (Hinterdorfer et al. 1996; Chen et al. 2002; Hinterdorfer 2004). Functionalization of AFM probes with bioligands transform them into sensing devices which can capture the interaction between complimentary receptors on the sample surface.

A silicon nitride probe is usually functionalized with an antibody against protein of interest via a linker. This linker gives the attached protein the flexibility needed for interacting with the receptor on the sample surface with various conformations so as to

create a tight coupling between the antibody on the AFM tip and the receptor of the adsorbed protein, which translates to better accuracy. In previous chapters, glutaraldehyde linker was used for investigating functional activity of fibrinogen and the effects of various aspects on its activity. One of the major problems facing such studies is that of non-specific interactions between the AFM probe and the substrate. This problem of distinguishing between specific ligand-receptor and non-specific probe-substrate interactions has persistently hampered accuracy in AFM experiments(Stuart and Hlandy 1999, Soman, et al. 2008). One methodology to overcome molecular mobility and non-specific tip–probe adhesion forces obscuring specific interactions is the use of flexible spacer molecules like polyethylene glycol (PEG), first reported by Hinterdorfer(Hinterdorfer, et al. 1996). Several advantages of PEG spacer include (1) allowing the probe molecule to freely reorient for unconstrained receptor–ligand recognition, (2) probe molecule can scan a large surface for target molecules during a tip–substrate encounter depending on the length of the linker (3) probe molecule can escape the danger of being crushed between the tip and substrate during hard contact and most importantly (4) PEG linker creates a water buffer zone around itself due to its affinity towards water molecules, thereby minimizing non-specific adhesion by creating a buffer between the AFM probe and protein on the surface.

Commercially available AFM probes consist of microfabricated pyramids of silicon (Si) or silicon nitride (Si_3N_4). Coating methods consist of altering the surface composition of the tip to improve its properties, and to enhance force measurement capabilities. The first step however is cleaning of the AFM probes. Many contaminants can become

physisorbed to AFM probes during manufacture, shipping, storage, or handling especially silicone oil from packing material. It appears that harsh treatment like cleaning with stronger acids like H_2SO_4 or piranha (Hinterdorfer, et al. 1998) reduces the optical reflectivity of cantilevers thereby affecting its deflection sensitivity. Therefore gentler cleaning methods including rinsing in acetone and/or plasma-cleaning are recommended.

Several chemical strategies to functionalized AFM probe can be found in any recent reviews(Barattin and Voyer 2008). Over the years, the AFM probe have been functionalization with (1) biotinylated BSA(Florin, et al. 1994), (2) electrografting of polymer on gold probes(Jérôme, et al. 2004), (3) various types of SAM including mixed SAMs(Li, et al. 2005) (4) selective electro-oxidation of OEG-coated tips (Yam, et al. 2003) (5) carbon nanotubes or CNT (Hafner, et al. 1999) and (7) polyethylene glycol as a spacer molecule (Hinterdorfer, Baumgartner, Gruber, Schilcher and Schindler 1996). In this chapter we will be only concentrating on funtionalization of AFM probes with commercially available PEG spacer molecules.

Monofunctional PEGs are activated at one end and bifunctional PEGs carry a reactive group at both ends. Either these groups are identical (homo-bifunctional) or the PEG is synthesized with different reactive groups (hetero-bifunctional). Heterobifunctional PEG spacers are especially useful for the immobilization of biomolecules. The spacer can be coupled to the surface with one reactive group. The free reactive group can be used to couple the biomolecule in the next step. Several homofunctional PEG linkers and heterofunctional probes have been designed. Protein molecules have also been anchored directly to AFM probes by homobifunctional NHS-PEG-NHS linkers(Ratto, et al. 2004),

Cystine-terminated peptides and proteins(Hinterdorfer, Schilcher, Baumgartner and Schindler 1998) as well as sulfhydryl-modified oligonucleotides(Lin, et al. 2006) can be linked directly to PEG-PDP ((pyridyldithio)propionate) and PEG-maleimide linkers.

It is worthwhile to mention some of the most common strategies to functionalize the AFM probe with functional PEGs. As mentioned previously, Hinterdorfer et al. used various types of PEG cross-linker functionalization to measure single molecular unbinding forces for typical systems: (a)biotin–avidin system, (b) antibody–antigen recognition system and the NTA–histidine complex (Fig 1). The biotin-avidin sytem using 8nm PEG length demonstrated a binding probability of 29% while a longer PEG chain (35 nm) seems to decrease the binding probability to 20% (fig **5-1**a)(Gabai, et al. 2005). Antibody-antigen system was studied by using Anti-human serum albumin (HSA) antibody. The antibody was first pre-derivatized by activating its lysine residues with the short linker N-succinimidyl-3(S-acethylthio)propionate (SATP) which resulted in a thiol group which was coupled to the PEG cross-linker previously anchored to the tip (fig 5-1b). This functionalization technique used an 8nm long PEG tether and demonstrated the flexibility and effectiveness for fast recognition of antigens with relatively short time(Hinterdorfer, Baumgartner, Gruber, Schilcher and Schindler 1996). Kienberger et al. demonstrated that the specific binding between ligand–receptor pairs was substantially greater using the nitrilo-triacetate (NTA)–Ni2+–His6 system (fig 5-1c)(Kienberger, et al. 2000). The problem with most of these techniques is that since antibodies contain no free thiol residues, prederivatization with N-succinimidyl 3-(acetylthio)propionate (SATP) is needed which causes a relatively high demand for antibody. Recently Ebner et al.

demonstrated another convenient alternative with minimal protein consumption and no prederivatization, using a new heterobifunctional cross-linker having two different amino-reactive functions(Ebner, et al. 2007).

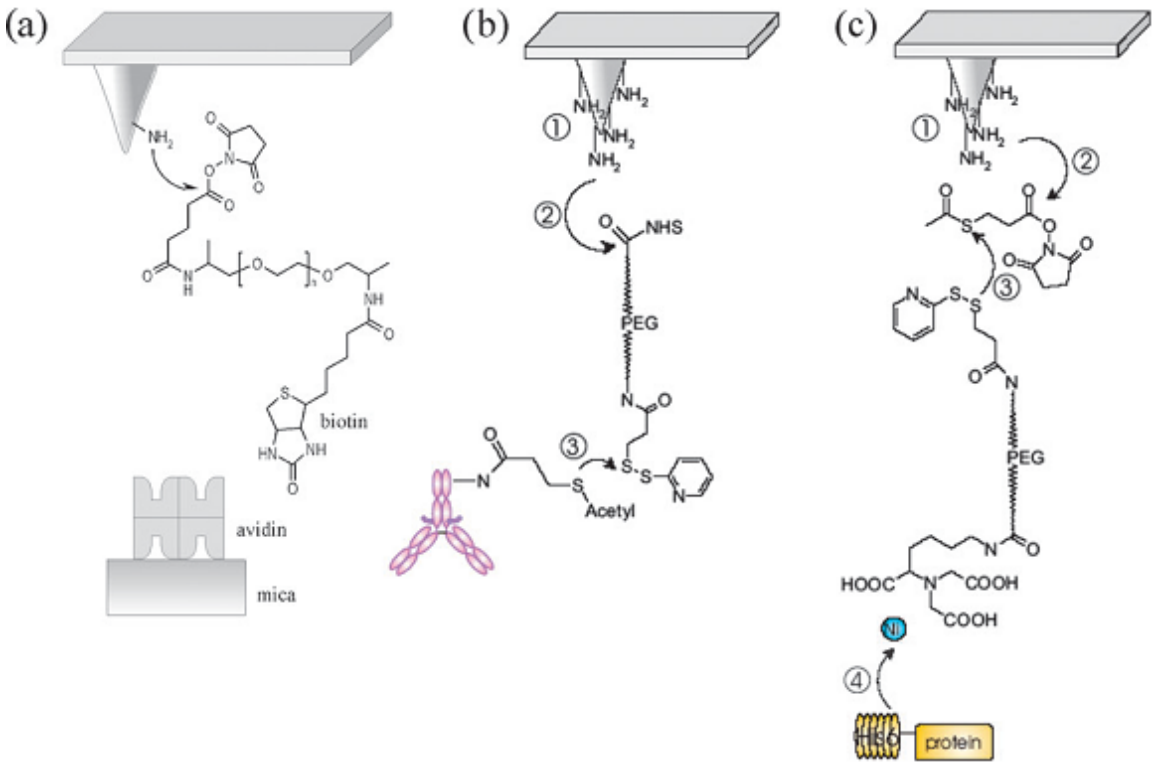

Figure **5-1**: Schematic representation of various probe functionalization with polyethylene glycol for investigating (a) biotin-avidin system (b) antibody-avidin system and (c) NTA-His complex. Reprinted from (Barattin and Voyer 2008), (Riener, et al. 2003) and (Kienberger, et al. 2006).

A virtually endless list of biological molecules can be attached to AFM probes via PEG tethers in order to map out molecular interactions with AFM. Native sulfhydryl groups on proteins, peptides, and other compounds can often be utilized to link them to PEG-maleimide or PEG-PDP tethers that have been anchored to aminated AFM probes.

The linker shown in the figure **5-2** is a heterobifunctional PEG derivative of 18 units, corresponding to an 8 nm extended length. The amino-terminated tip is coupled with a N-hydroxysuccinimide (NHS) ester function(Hinterdorfer, Schilcher, Baumgartner and Schindler 1998). On the other end, a thiol-reactive end group (2-(pyridyldithio)propionyl; PDP) can be coupled with the thiol-containing molecule of interest. Most of the biomolecules don't have a thiol group and therefore the molecules have to be thioloated. Since free sulfhydryl groups are not available near the surface of the molecules of interest, the molecule must be activated with a thiolating reagent or reduced with a reagent such as DTT in order to prepare them for bioconjugation. Unfortunately, reduction of disulfides with DTT also runs a risk of protein inactivation (Raab, et al. 1999) This kind of functionalization enables the anchoring of a ligand of interest as the last step by coupling of its thiol function to the thiol-reactive end of the PEG derivative and therefore, is applicable to a wide range of biologically-relevant probes.

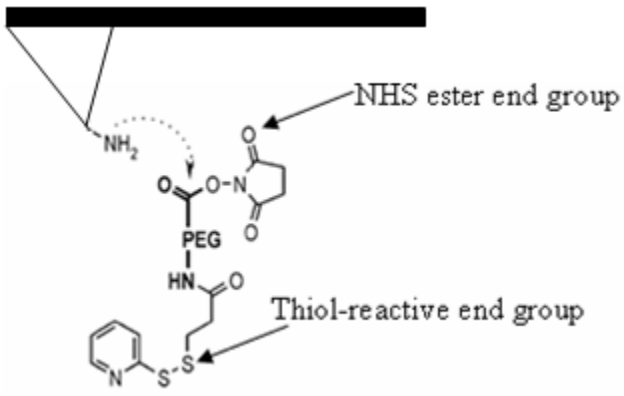

Figure **5-2**: Heterobifunctional PEG derivative that allows the fixation onto an amino-modified tip via its NHS ester function and the coupling of thiol-containing probe molecule via its thiol-reactive end group. Modified and reprinted from (Barattin and Voyer 2008)

A single-tethered system, i.e., tethering a molecule on the AFM probe, helps decrease nonspecific binding by moving the specific interaction away from the surface of the probe depending on the tether length. In this chapter, we are investigating the conformational changes in dodecapeptide sequence in physio-adsorbed fibrinogen using a mAb antibody conjugated to an AFM probe via a PEG tether. One end of the hetero-bifunctional NHS-PEO-maleimide linker is coupled to the AFM probe while the other end is conjugated with a mAb recognizes a sequence γ392-411, which includes the γ-chain dodecapeptide of fibrinogen. PEG tether instead of the glularaldehyde linker is used in this study in an attempt to reduce the non-specific interactions and increase accuracy and realiability of AFM measurements.

5.2 Materials and Methods

5.2.1 General

Phosphate buffered saline (PBS, 0.01 M sodium phosphate buffer, 150mM NaCl, pH 7.4, Sigma Inc.) was prepared using water from a Millipore Simplicity 185 system (18 MΩ) which utilizes two ultraviolet filters (185 and 254 nm) to reduce carbon contaminants. Human fibrinogen (90% clottable) was used as received from Calbiochem, La Jolla, CA. Monoclonal mouse anti-fibrinogen gamma chain (γ 392 – 411; clone: 4 -2; Isotype: IgG1) was obtained from Accurate Chemicals and Scientific Corporation, NY. Bovine serum albumin (BSA) was obtained from Sigma Chemicals Co, St. Louis, MO. Chloroform (99.9% purity) was obtained from Sigma-Aldrich, Inc.

(St. Louis, MO). All the proteins were dissolved in phosphate buffer and aliquots were stored at -20°C until use.

5.2.2 AFM probe activation

Silicon nitride AFM probes (k = 0.06N/m) were rinsed in acetone (10ml for 20 min). Probes were then glow discharge plasma cleaned for 45min in a glow-discharge plasma cleaner (Harrick Scientific Products, Inc., Ossining, NY) (Power – 100W). Silicon nitride probes surfaces when exposed to air oxidize and are covered with numerous reactive SiOH entities which can be used for grafting amine groups. One common method of amination of silanol-containing surfaces is silanization with 3-aminopropyltriethoxysilane (APTES). AFM probes were incubated in 1% APTES in ethanol for 1 hour at room temperature. Studies on low APTES concentration (1%) have shown that such films were essentially smooth, having low RMS roughness (less than 3-nm thick) and did not show strong temperature dependence (Wang and Vaughn 2008).

5.2.3 PEGylation of activated probes

NHS-PEO-Maleimide reagents are viscous pale liquids that are difficult to weigh and dispense. To facilitate handling, a stock solution was made before first use by dissolving the crosslinker in dry (anhydrous grade) dimethylsulfoxide (DMSO). A 250

mM PEG crosslinker stock solution was made by dissolving 100mg of NHS-PEO_{12}-Maleimide (approximately 100µl) in 360µl of dry DMSO. The NHS-ester reactive group is susceptible to hydrolysis and therefore stored in a moisture-free condition (capped under nitrogen) at -20°C. Before starting a new experiment, the stored vials were equilibrated to room temperature to avoid moisture condensation inside the container. Exposure to air was minimized by keeping the stock solution capped by a septum through which aliquots were obtained with a syringe. Phosphate buffered saline (PBS, pH 7.2) buffer was prepared and EDTA (5mM) was added to chelate divalent metals which would prevent metal-catalyzed disulfide formation. Aminated AFM probes were placed in a 24 well plate and 4 µl of the 250 mM PEG stock solution was added and incubated for 2 hours at 4°C (Fig **5-3**). Excess PEG was removed by thoroughly rinsing the probes by PBS buffer.

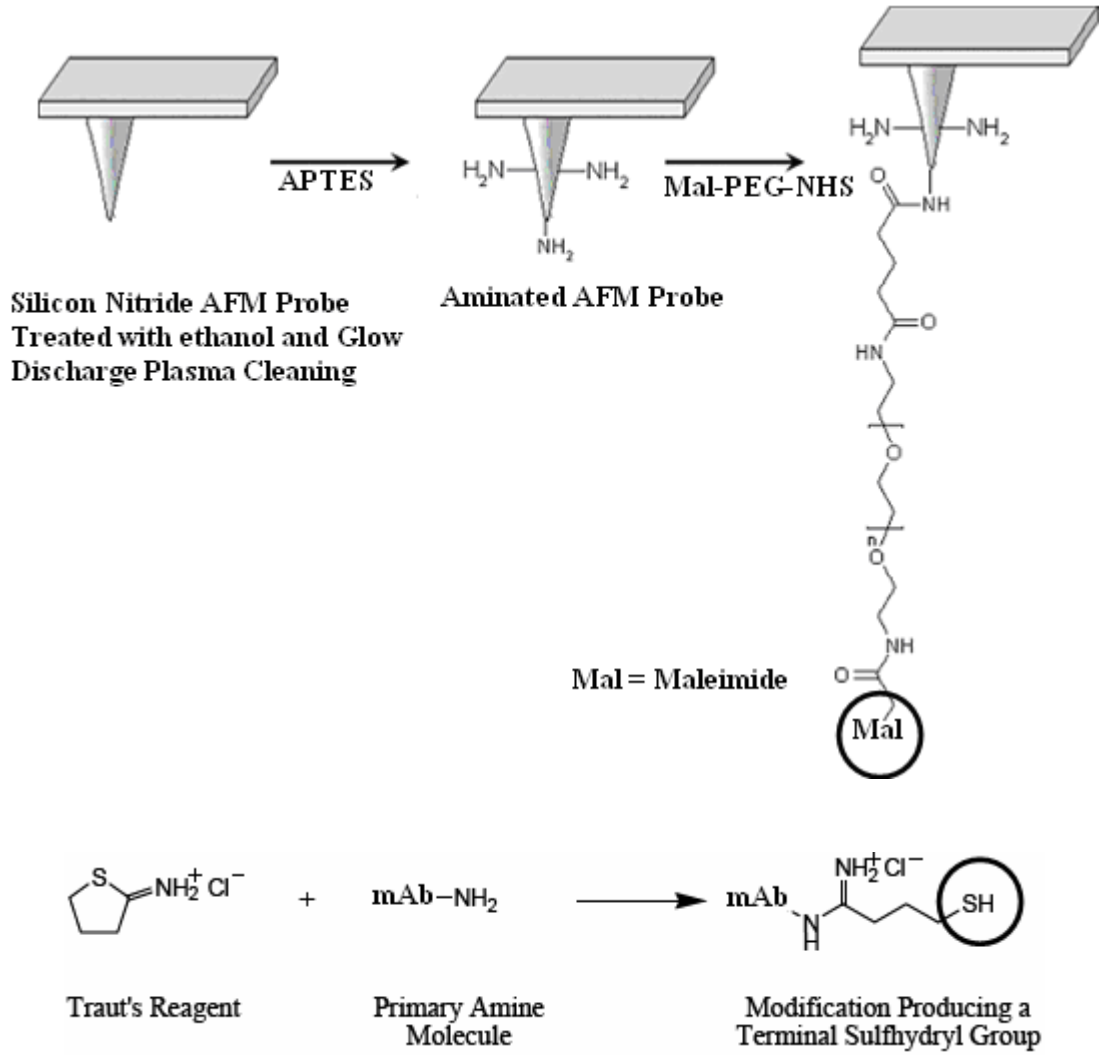

Figure **5-3**: Immobilization of a mAb on a surface using NHS-PEG-maleimide: The NHS-PEO_{12}-Maleimide (Thermo Scientific, Mol.Wt=865.92) are heterobifunctional crosslinkers with *N*-hydroxysuccinimide (NHS) ester and maleimide groups that allow covalent conjugation of amine- and sulfhydryl-containing molecules. NHS ester react with primary amines at pH 7-9 to form amide bonds, while maleimides react with sulfhydryl groups at pH 6.5-7.5 to form stable thioether bonds. (a) The NHS-group reacts with an amino-modified surface on the AFM probe. The maleimide group is not involved in this coupling reaction. (b) Traut's reagent is used to thiolate the mAb by producing a terminal sulfhydryl group which reacts with the maleimide end group of the PEG linker. Note: This figure is modified and redrawn from the application notes from Agilent technologies and Thermo-Scientific.

5.2.4 Bioconjugation with mAb

Traut's Reagent (2-Iminothiolane) is a cyclic thioimidate compound for thiolation (sulfhydryl addition). Traut's Reagent reacts with primary amines ($-NH_2$) of the monoclonal antibody to introduce sulfhydryl (-SH) groups while maintaining charge properties similar to the original amino group (Fig 5-3). Monoclonal antibody (100µg/ml) was dissolved in a non-amine buffer (phosphate buffer, pH 8.0 + 5 mM EDTA to chelate divalent metals in the solution, which helps to prevent oxidation of formation of disulfide bonds). A 20-fold molar excess of Traut's Reagent was added to the solution and incubated for 1 hour at room temperature in a rotating mixer. Desalting column (Zeba™ Desalt Spin Column) was equilibrated with buffer and was used to separate thiolated antibodies from excess Traut's Reagent. Thiolated antibody solution was added to the PEGylated AFM probes at room temperature for 30 minutes or 2 hours at 4°C. Probes were rinsed with PBS and immediately used for experiments. Functionalized probes were not used more than 2 days.

5.2.5 OTS SAM on glass cover-slips

n-Octadecyltrichlorosilane (OTS, 95% purity) was purchased from Gelest, Inc. (Morrisville, PA). Glass coverslips (12 mm diameter, Fisher Scientific International Inc., Hampton, NH) were cleaned by sonicating in chloroform for 30 min. Coverslips were plasma etched with a glow-discharge plasma cleaner (Harrick Scientific Products, Inc., Ossining, NY) at 100 W for 10 min per side. Silane solutions were prepared by adding

OTS (1% by volume) to chloroform. Complete films on coverslips were formed by a 30 min reaction of OTS at room temperature. Both beads and coverslips were sonicated in chloroform for 30 min and dried under a stream of N_2 as the final step in preparation.

5.2.6 Contact angle measurements

The water wettability of each substrate was determined by sessile drop measurements of the advancing water contact angle (θ) using a Krüss contact angle goniometer. All measurements were made using PBS as a probe liquid. Advancing contact angles were measured by a minimum of nine independent measurements and are presented as mean±standard deviation.

5.2.7 Force spectroscopy measurements

AFM probe was modified with monoclonal antibody (25 μg/ml) that recognize fibrinogen γ392-411, a region that includes the platelet binding dodecapeptide sequence γ402-411 as described in the methods section. Freshly cleaved muscovite mica sheets (10 mm x 10 mm, Ted Pella, Inc), HOPG substrates (grade II, Structure Probe Inc., PA) and OTS SAMs on glass cover-slips were used as substrates for protein adsorption experiments. Bovine serum albumin or fibrinogen solutions in PBS (100μg/ml) were adsorbed onto various substrates for 5 minutes in an external fluid cell. Remaining free protein was washed away for 3 minutes using a syringe pump that provides a steady flow

of PBS at 0.3 ml/min. All data was collected using a Nanoscope III Multimode AFM (Digital Instruments, CA) under buffer conditions in a fluid cell. The hydrated protein sample was loaded onto the microscope and data was collected using the monoclonal anti-fibrinogen-modified probes under buffer. The ramp size (500nm) and trigger threshold (100nm) were kept constant while the scan size (500nm-5000nm) and scan rate (0.3 Hz – 0.75 Hz) were varied. Images were collected as 16 x 16 and 32 x 32 force arrays with 256 data points per force curve. Data was analyzed as explained in chapter 3. Time-dependent force data from multiple experiments ($n \geq 3$ for every time point) was converted to probability data and was plotted as a function of protein residence time.

Human platelets (250×10^3 /μL) were used for adhesion studies as described in chapter 4. Labeled platelets were imaged and counted and normalized using fluorescent microscopy (Eclipse 80i, Nikon). A minimum of 3 samples were analyzed for each condition with a minimum of 3 images per sample.

5.2.8 Statistical analysis

A minimum of 3 independent experiments were performed for each measurement. Statistical differences were determined using One-way Analysis of Variance (ANOVA) with post test (Tukey-Kramer Multiple Comparisons Test) with atleast $P<0.05$ being considered significant.

5.3 Results and Discussion

5.3.1 Fibrinogen activity on mica substrates

Fibrinogen solution (100μg/ml) and BSA solution was adsorbed onto mica substrates (contact angle=8±2°) and PEG modified AFM probes were used to characterize interactions between the mAb attached onto the PEG probe and fibrinogen on the surface. BSA was used as the non-specific control for all the recognition experiments. A cut-off parameter based on either rupture force or length was selected to differentiate between specific and non-specific interactions. Fig **5-4** illustrates characteristic rupture or adhesion force for fibrinogen on mica substrates using both the glualdehyde linker used in previous work and the newly developed PEG linker. Glutaraldehyde linker-modified probe demonstrate that the rupture force was found to be in the range of 0-800pN, while for the PEG-linker AFM probe, more than 95% of the forces were in the range from 0-400pN.

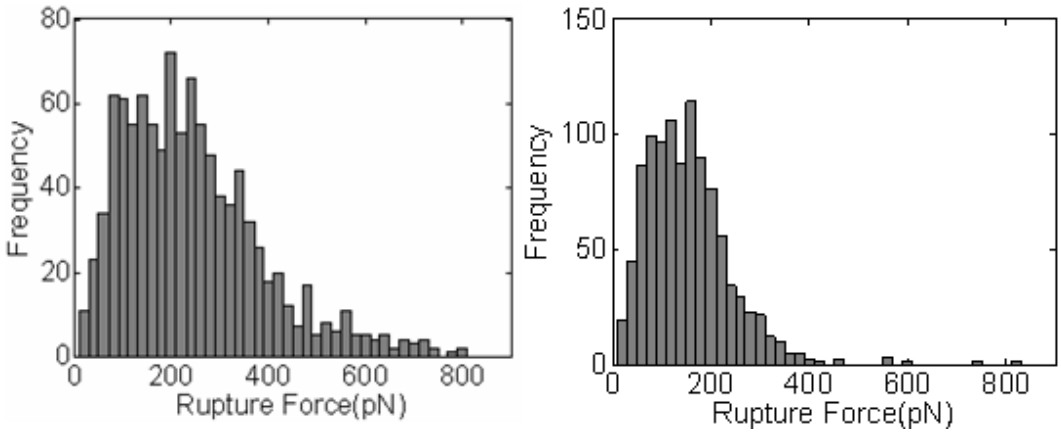

Figure **5-4**: Comparison of maximum adhesion (rupture) force distribution between AFM probe modified with mAb (that recognizes fibrinogen γ392-411, which including the γ-chain dodecapeptide sequence) and adsorbed fibrinogen on mica samples using 2 different types of linkers: (a) Glutaldhehyde linker and (b) Heterobifunctional PEG (polyethylene glycol) tether

Similar analysis with rupture length is illustrated in fig **5-5**. For BSA control, with the glutaraldehyde-linker tip, the range was from 0-200nm while similar BSA control experiment with PEG-linker tip lead to a drastic decrease in the non-specific rupture length (0-30nm). For the glutaraldehyde-linker probe, BSA cut-off is ~200nm. Therefore fibrinogen data (fig 5-5b) only greater than 200nm can be used (usable range for recognition studies=200nm-400nm). However in case of PEG-linker tips, since the BSA control data is ~30nm, the usable range for probability recognition studies is from ~30nm to ~400nm, thereby increasing the accuracy of AFM measurements. From fig 5-5a and 5-5d, we find a 10 fold decrease in the rupture length for non-specific BSA control experiments with the PEGylated probes. Since we see a significant decrease in the non-specific interactions, rupture length was selected to be the parameter to distinguish specific vs non-specific recognition for calculation of recognition probability of the

monoclonal antibody. Results for fibrinogen activity on mica substrates were obtained by both glutaraldehyde and PEG modified probes. In both fig 5-5c and 5-5f, the activity peaks at ~45min post-adsorption or residence time and then decreases with increase in residence time. This demonstrates the ability of PEGylated probes to obtain reliable and accurate AFM measurements with significant decrease in non-specific interactions.

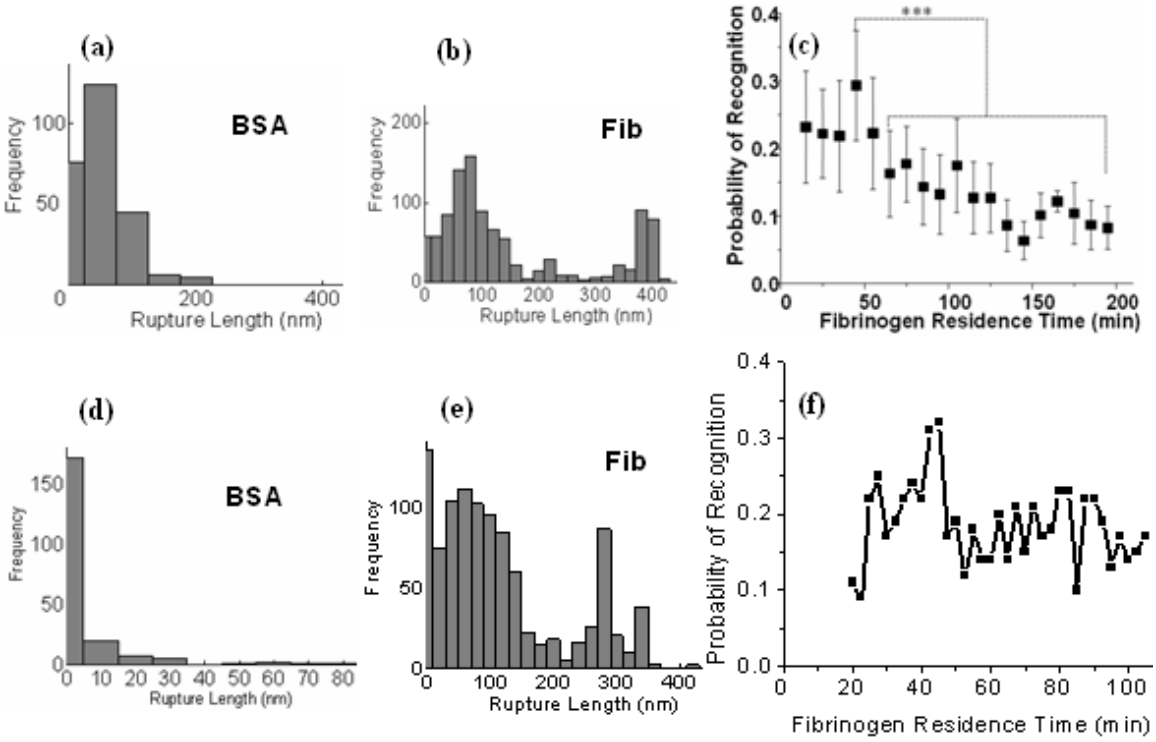

Figure 5-5: Functional activity of fibrinogen on mica substrates by functionalized AFM probes using rupture length parameter to obtain cut-off values for non-specific interactions: (a) Control experiment for glutaldehyde modified probe shows rupture length from 0-200nm (b) Interactions between adsorbed fibrinogen and glutaldehyde modified probe shows rupture length range from 0-400nm (c) Probability of recognition data from chapter 3 shows an activity peak at ~45min fibrinogen residence time (d) Control experiment for PEG-modified probe shows rupture length from 0-30nm. This is a substantial decrease in the non-specific interactions when compared to 0-200nm rupture length range in (a). (e) Interactions between adsorbed fibrinogen and AFM probe modified with PEG-linker shows rupture length range from 0-350nm and (f) Probability of recognition or fibrinogen activity peaks at ~45min fibrinogen residence time and decreases with increase in residence time. PEG-linker AFM probes demonstrates similar trend as compared to the glutaldehyde modified probe activity peak in (c). Since the non-specific interactions with PEG-AFM probes are less than 30nm as illustrated in (d), all the interactions in the range of 30nm-350nm are used to obtain recognition probability or fibrinogen activity thereby increasing the accuracy of AFM measurements.

5.3.2 Fibrinogen activity on OTS SAMs

OTS self-assembled monolayer (SAMs) on glass cover-slips (contact angle=94.8±4.05°) were prepared as explained in the methods section. PEG-linker tips were used to measure the activity of fibrinogen on these hydrophobic substrates. From fig **5-6** , we don't observe any temporal dependence of fibrinogen activity on these substrates. The recognition probability illustrated in fig 6a lies in the range of 0.05-0.15, which is less than what we observe on hydrophilic mica substrates (refer fig 5-5f). Hydrophobicity alters the conformation of fibrinogen leading to a decrease in the biological activity of dodecapeptide sequence. Macroscale platelet adhesion data illustrated in fig 5-6b demonstrate low platelet adhesion comparable to non-specific labeling in case of BSA in chapter 4. Platelet adhesion results also don't demonstrate any dependence of fibrinogen activity with fibrinogen residence time which correlate well with the AFM results.

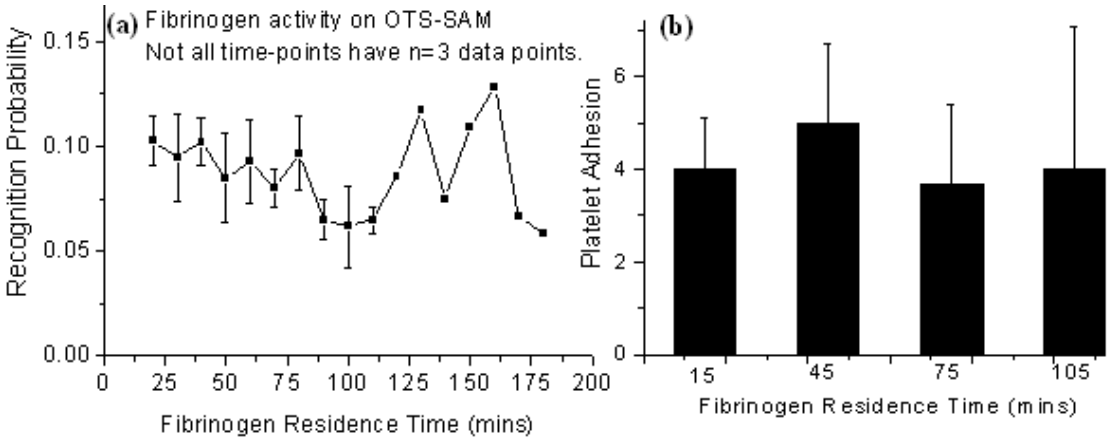

Figure **5-6**: Fibrinogen activity on OTS-SAM glass cover-slips using PEGylated AFM probes and macroscale platelet adhesion: (a) Fibrinogen activity or probability of recognition of the dodecapeptide sequence varies in the range of 0.05-0.15 and demonstrate no dependence on fibrinogen residence time. Time-points in the range 20min-110min are obtained from n=3 individual experiments, whereas time-points after 110min only represent one experiment (b) Platelet adhesion data also demonstrates no dependence on fibrinogen residence time correlating well with AFM data. Platelet adhesion values are lower than similar experiments on hydrophilic mica substrate in chapter 4.

5.3.3 Fibrinogen activity on HOPG substrate

Experiments were carried out with PEG-linker AFM probes using HOPG substrate (contact angle=84.11±2.26°). Results form Fig **5-7** illustrates that the recognition probability or fibrinogen activity on HOPG varies from 0-0.175, similar to OTS SAM substrate in fig 5-6a. Fibrinogen activity on HOPG substrate does not seem to be dependent on fibrinogen residence time, although only 2 independent experiments were carried out.

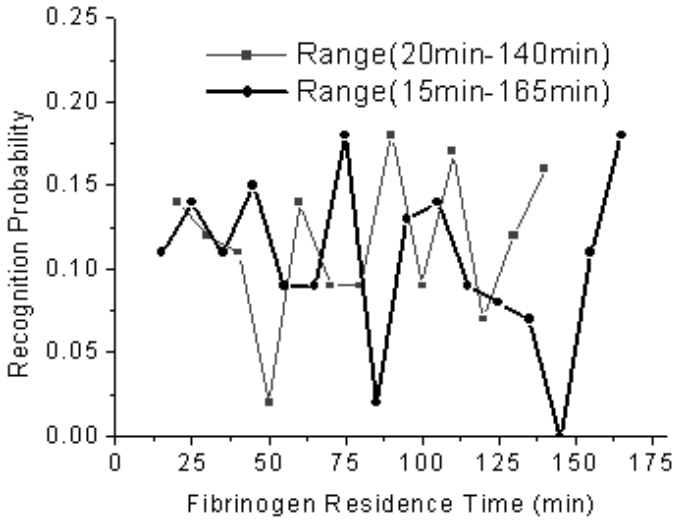

Figure **5-7**: Recognition probability of the dodecapeptide sequence (fibrinogen activity) using PEGylated AFM probes on HOPG substrates. Recognition probability is in the range of 0-0.175 (n=2).

To summarize, bioconjugation chemistry and surface immobilization chemistry enhance the power and utility of AFM as an immunodetection tool. PEG linkers attached to AFM probes promote receptor-ligand recognition by providing the necessary rotational freedom. Moreover, the ability of PEG to bind to water molecules provides a buffer against probe-substrate non-specific interactions thereby increasing the accuracy of AFM measurements. PEG linker conjugated to AFM probes can be used to investigate specific biomolecular interactions between a variety of biological molecules of scientific interest and physiological importance on a variety of biomaterial surfaces.

5.4 References

1. Barattin, R.; Voyer, N., Chemical modifications of AFM tips for the study of molecular recognition events. *Chem. Commun.,* **2008**, 1543-1532.

2. Ebner, A.; Wildling, L.; Kamruzzahan, A.; Rankl, C.; Wruss, J.; Hahn, C.; Holzl, M.; Zhu, R.; Kienberger, F.; Blaas, D.; Hinterdorfer, P.; Gruber, H., A new, simple method for linking of antibodies to atomic force microscopy tips. *Bioconjugate Chem.* **2007,** 18, (4), 1176 - 1184.

3. Florin, E. L.; Moy, V. T.; Gaub, H. E., Adhesion forces between individual ligand-receptor pairs. *Science* **1994,** 264, (5157), 415-417.

4. Gabai, R.; Segev, L.; Joselevich, E., Single polymer chains as specific transducers of molecular recognition in scanning probe microscopy. *Journal of the American Chemical Society* **2005,** 127, (32), 11390-11398.

5. Hafner, J.; Cheung, C.; Lieber, C., Direct growth of single-walled carbon nanotube scanning probe microscopy tips. *Journal of the American Chemical Society* **1999,** 121, (41), 9750-9751.

6. Hinterdorfer, P.; Baumgartner, W.; Gruber, H.; Schilcher, K.; Schindler, H., Detection and localization of individual antibody-antigen recognition events by atomic force microscopy. *PNAS* **1996,** 93, (8), 3477-3481.

7. Hinterdorfer, P.; Schilcher, K.; Baumgartner, W. G., HJ; Schindler, H., A mechanistic study of the dissociation of individual antibody-antigen pairs by atomic force microscopy. *Nanobiology* **1998,** 4, 177-188.

8. Jérôme, C.; Willet, N.; Jérôme, R. D., AS, Electrografting of polymers onto AFM Tips: A novel approach for chemical force microscopy and force spectroscopy. *ChemPhysChem* **2004,** 5, (1), 147-149.

9. Kienberger, F.; Ebner, A.; Gruber, H.; Hinterdorfer, P., Molecular Recognition Imaging and Force Spectroscopy of Single Biomolecules. *Accounts Chem. Res.* **2006,** 39, 29-36.

10. Kienberger, F.; Kada, G.; Gruber, H.; Pastushenko, P.; Riener, C.; Trieb, M.; Knaus, H.; Schindler, H.; Hinterdorfer, P., Recognition Force Spectroscopy Studies of the NTA-His6 Bond. Single Molecule. *Single Molecules* **2000,** 1, 25-31.

11. Li, G.; Xi, N.; Wang, D., Investigation of angiotensin II type 1 receptor by atomic force microscopy with functionalized tip. *Nanomedicine: Nanotechnology, Biology and Medicine* **2005,** 1, (4), 306 - 312.

12. Lin, L.; Wang, H.; Liu, Y.; Yan, H.; Lindsay, S., Recognition imaging with a DNA aptamer. *Biophys. J.* **2006,** 90, (11), 4236-4238.

13. Raab, A.; Han, W.; Badt, D.; Smith-Gill, S.; Lindsay, S.; Schindler, H.; Hinterdorfer, P., Antibody recognition imaging by force microscopy. *Nature Biotechnology* **1999,** 17, (September).

14. Ratto, T.; Langry, K.; Rudd, R.; Balhorn, R.; Allen, M.; McElfresh, M., Force spectroscopy of the double-tethered concanavalin-A mannose bond. *Biophys. J.* **2004,** 86, (4), 2430-2437.

15. Riener, C.; Kienberger, F.; Hahn, C.; Buchinger, G.; Egwim, I.; Haselgrübler, T.; Ebner, A.; Romanin, C.; Klampfl, C.; Lackner, B.; Prinz, H.; Blaas, D.; Hinterdorfer, P.;

Gruber, H., Heterobifuctional crosslinkers for linking of single ligand molecules to scanning probes. *Anal. Chim. Acta* **2003,** 497, 101-114.

16. Soman, P.; Rice, Z.; Siedlecki, C., Measuring the time-dependent functional activity of adsorbed fibrinogen by atomic force microscopy. *Langmuir* **2008,** 24, (16), 8801-8806.

17. Stuart, J.; Hlandy, V., Feasibility of measuring antigen-antibody interaction forces using a scanning force microscope. *Colloids and Surfaces B: Biointerfaces* **1999,** 15, 37-55.

18. Wang, W.; Vaughn, M., Morphology and amine accessibility of (3-Aminopropyl) triethoxysilane films on glass surfaces. *Scanning* **2008,** 30, (2), 65-77.

19. Yam, C.; Xiao, Z.; Gu, J.; Boutet, S.; Cai, C., Modification of silicon AFM cantilever tips with an oligo(ethylene glycol) derivative for resisting proteins and maintaining a small tip size for high-resolution imaging. *J. Am. Chem. Soc.* **2003,** 125, (25), 7498-7499.

VITA

Pranav Soman

EDUCATION:

- **Ph.D. (Bioengineering), The Pennsylvania State University**, Hershey, PA
  May 2009
- **Dissertation Title:** Characterization of protein films by novel atomic force microscopy techniques **Advisor:** Dr. Christopher A. Siedlecki
- **B.E. (Mechanical Engineering), Pune University, India**
  August 1997-2001
  Dissertation Title: Design and Fabrication of Lapping Machine.

PUBLICATIONS:

- L.C. Xu, **P. Soman,** J. Runt and C.A. Siedlecki: Characterization of surface microphase structure of poly(urethane urea) biomaterials by nanoscale indentation with AFM. **Journal of Biomaterial Science Polymer Edition** 2007, 18:4:353-368.
- **P. Soman,** Z. Rice and C.A. Siedlecki: Immunological identification of fibrinogen in multi-component protein films by AFM imaging. 2008 Oct. **Micron** 39(7):832-42
- **P. Soman**, Z. Rice and C.A. Siedlecki: Measuring the Time-Dependent Functional Activity of Adsorbed Fibrinogen by Atomic Force Microscopy. 2008 Aug 19. **Langmuir.** 24(16):8801-6
- L. Xu, **P. Soman**, A. Agnihotri, C.A. Siedlecki: *AFM Methods for Characterizing Protein Interactions with Microphase-Separated Polyurethane Biomaterials*: Biological Interactions on Materials Surfaces: Understanding and Controlling Protein, Cell and Tissue Responses. Springer Publishing Company **Submitted**
- A. Agnihotri, **P. Soman** and C.A. Siedlecki: Interactions of the Platelet Integrin Receptor GPIIbIIIa with Surface-Adsorbed Fibrinogen. **Submitted.**
- **P.Soman** and C. A. Siedlecki: Effect of competitive protein adsorption on functional activity of fibrinogen on mica substrates. **In preparation.**

Journal Reviewer: Colloids and Surfaces B: Biointerfaces

AWARDS:

- "Penn State 2008 Alumini Scholarship"